

# Anti-tumoral activity of axitinib in preclinical models of lung carcinoids: Chronicle of a Death Foretold.

Alessandra Dicitore (1), Maria Celeste Cantone (1), Davide Saronni (1), Germano Gaudenzi (2), Silvia Carra (3), Alice Plebani (2), Maria Orietta Borghi (4, 5), Luca Persani (1, 3), Giovanni Vitale (1, 2)

(1) Department of Medical Biotechnology and Translational Medicine (BIOMETRA), University of Milan, Milan, Italy

(2) Istituto Auxologico Italiano, IRCCS, Laboratory of Geriatric and Oncologic Neuroendocrinology Research, Cusano Milanino (MI), Italy

(3) Istituto Auxologico Italiano, IRCCS, Laboratory of Endocrine and Metabolic Diseases, Cusano Milanino (MI), Italy

(4) Istituto Auxologico Italiano, IRCCS, Experimental Laboratory of Immuno-rheumatology, Milan, Italy

(5) Department of Clinical Sciences and Community Health (DISCCO), University of Milan, Milan, Italy

## Background/Significance to NETs

Lung carcinoids are a rare type of tumor, accounting for only 1-2% of all lung cancers. They are divided in two types: typical carcinoids (TC) and atypical carcinoids (AC). Although these tumors usually grow slowly, lung carcinoids develop distant metastases in 25-30% of cases [1]. In these patients the treatment strategy is not curative and is directed at controlling symptoms from the tumor burden or hormonal production and slowing tumor growth. Therefore, new treatment options are urgently needed. In carcinoid tumors, overexpression of the vascular endothelial growth factor (VEGF), together with the VEGF receptor (VEGFR) subtypes, have been observed [2]. Axitinib, a small molecule tyrosine kinase inhibitor, is a potent and selective inhibitor of VEGFR 1, 2, and 3 approved by FDA in 2012 for the treatment of patients with metastatic renal cell carcinoma [3,4]. Beyond its effects on angiogenesis, axitinib showed anti-tumoral activity through modulation of cell cycle and cell death processes in some in vitro and in vivo tumor models [5,6]. In this preclinical study, we investigated the antitumor activity of axitinib in human lung carcinoid cell lines (NCI-H727, UMC-11 and NCI-H835) and in zebrafish xenografts implanted with these NET cells.

## b. Materials and Methods/Experimental Approach

In order to measure the cellular metabolic activity, as an indicator of cell viability, we performed a colorimetric assay, such as 3-(4,5-dimethylthiazol-2-yl)-2,5-diphenyltetrazolium bromide (MTT). Lung carcinoid cells were treated with medium containing vehicle (control), or different concentrations of axitinib. For experiments of long-term incubation, medium was replaced with new one containing vehicle or drugs after 3 days of incubation. Flow cytometry techniques for analysis of cell cycle and apoptosis were applied after staining of tumor cells with propidium iodide (PI) and Annexin-V-fluorescein isothiocyanate/PI, respectively. Cell cycle distribution was expressed as percentage of cells in G0/G1, S, and G2/M phases compared to control. By staining cells with a combination of Annexin-V-fluorescein isothiocyanate and PI, we identified viable cells (Annexin-V-/PI-), early apoptotic cells (Annexin-V+/PI-) and late apoptotic, necrotic cells (Annexin-V-/PI+).

Moreover, we analysed the changes in nuclear morphology using Hoechst fluorescence staining in order to identify multinucleated cells suggestive of mitotic catastrophe. We performed western blot analyses of protein extracts from cell lysates in order to evaluate expressions of key mediators of cell death pathways (full and cleaved caspase 3 and PARP, pH2AX, Chk1). Finally, we evaluated tumor-induced angiogenesis of NET lung grafted cells in zebrafish embryos. Briefly, tumor cells were labeled with a red fluorescent viable dye and grafted into the subperidermal space of *Tg(fli1a:EGFP)<sup>y1</sup>* embryos, close to the sub-intestinal vessels (SIV) plexus. As control of the implantation, we considered embryos injected with only PBS, the cell resuspension solution. This transplantable platform was used to test axitinib effect on tumor-induced angiogenesis.

#### c. Results (key findings to report at this meeting)

*In vitro* cell viability analysis showed that axitinib treatment significantly decreased the growth of NCI-H727, UMC-11, and NCI-H835 cells in a dose-dependent manner with a more prominent effect in UMC-11 cells. In NCI-H727 and UMC-11, axitinib significantly decreased cells in G0/G1 and S phases with a concomitant increase of cells in G2/M phase, whereas a significant decrease of NCI-835 cells in S phase was observed compared to control. Interestingly, we observed a significant increase of cells in G2/M phase (+93% vs control,  $p < 0.001$ ) and a concomitant increase of DNA content  $>4N$  in NCI-H727 after 6 days treatment with axitinib. This poliploidy occurs when cells in G2/M do not separate after DNA synthesis, becoming particularly sensitive to the induction of mitotic catastrophe. Thus, we decided to investigate this cell death process in lung carcinoid cell lines, by assessing the changes in nuclear morphology. Through Hoechst fluorescence staining, we observed that the nuclei became significantly larger after axitinib compared to control, and some cells contained several nuclei of unequal sizes in NCI-H727 cell line. Moreover, we found an increase of  $\gamma$ -H2AX and Chk1 kinase phosphorylation, key proteins of DNA damage response leading to G2/M cell cycle arrest and mitotic catastrophe in NCI-H727 cells. No significant induction of apoptosis after axitinib was found in NCI-H727 cells. After 6 days of axitinib treatment, we found an increased percentage of UMC-11 and NCI-H835 cells positive for Annexin V and PI, suggestive for apoptosis, and of NCI-H835 cells PI positive and annexin V negative, indicative of necrosis. The induction of apoptosis after axitinib was confirmed by an increase of caspase 3 activation and PARP cleavage in UMC-11 and NCI-H835 cells. Additionally, we evaluated the *in vivo* effects of axitinib on tumor-induced angiogenesis, in *Tg(fli1a:EGFP)<sup>y1</sup>* zebrafish embryos implanted with lung carcinoid cell lines. After 24 hours, axitinib significantly inhibited tumor-induced angiogenesis in embryos injected with all tumor cell lines with a more relevant effect in zebrafish grafted with UMC-11 cells.

#### d. Conclusions/next steps

In conclusion, we highlighted for the first time that axitinib exerted a prominent antitumor activity modulated by cell cycle arrest, induction of selective cell death mechanisms and inhibition in tumor-induced angiogenesis in lung carcinoid preclinical models, suggesting its potential therapeutic application in lung NET carcinoids.

#### References

- [1] Iyoda A et al. 2020
- [2] Telega A et al. 2012
- [3] Kelly RJ et al. 2009
- [4] Parekh H et al. 2016
- [5] Morelli MB et al. 2015
- [6] Morelli MB et al. 2017



# Neuroendocrine tumors of the lung: clinicopathological and molecular features

Akira Iyoda<sup>1</sup> · Yoko Azuma<sup>1</sup> · Atsushi Sano<sup>1</sup>

Received: 3 December 2019 / Accepted: 28 January 2020 / Published online: 19 March 2020  
© Springer Nature Singapore Pte Ltd. 2020

## Abstract

In 1970, neuroendocrine tumors of the lung were classified into three categories: typical carcinoid (TC), atypical carcinoid (AC), and small cell lung carcinoma (SCLC). The third edition of the World Health Organization (WHO) classification in 1999 defined large cell neuroendocrine carcinoma (LCNEC) as a variant of large cell carcinomas, whereas the fourth edition of the WHO classification redefined LCNEC as a neuroendocrine tumor. Currently, neuroendocrine tumors of the lung are classified into four main categories: TC, AC, LCNEC, and SCLC. Although the treatments for TC, AC, and SCLC have not changed remarkably, the treatment strategy for LCNEC is not yet established because of its reclassification from a variant of “large cell carcinoma” to a new category of “neuroendocrine tumor”. In this review article, we discuss the pathological findings, biological behavior, and treatment of neuroendocrine tumors of the lung.

**Keywords** Neuroendocrine tumor · Lung · Surgery

## Introduction

Currently, neuroendocrine tumors of the lung are classified into four main categories: typical carcinoid (TC), atypical carcinoid (AC), large cell neuroendocrine carcinoma (LCNEC), and small cell lung carcinoma (SCLC). This is based on the three classifications of 1970 of TC, AC, and SCLC [1, 2], and the fourth edition of the World Health Organization (WHO) redefinition of LCNEC as a neuroendocrine tumor, subsequent to its third edition in 1999, which defined LCNEC as a variant of large cell carcinomas ([3, 4]; Table 1). However, the terms, criteria, and clinical features of neuroendocrine tumors of the lung are different from those of gastrointestinal neuroendocrine tumors. We discuss the pathological findings, biological behavior, and treatment of neuroendocrine tumors of the lung.

## Carcinoids

Carcinoids have characteristic neuroendocrine morphology and growth patterns, including organoid, trabecular, palisading, rosette-like, and other arrangements [3]. The WHO classification of 1999 defined TCs as tumors with less than two mitoses per 2 mm<sup>2</sup> (ten high-power fields). This tumor type lacks necrosis and is 0.5 cm in size or larger [3]. On the other hand, ACs have 2–10 mitoses per 2 mm<sup>2</sup> (ten high-power fields) and/or necrosis in addition to a neuroendocrine morphology similar to TCs ([4]; Table 1). Tumors smaller than 0.5 cm are classified as “tumorlets”. TC-like tumors that exhibit necrosis or 2–10 mitoses are classified as ACs.

## Typical carcinoids: low-grade neuroendocrine tumors

Patients with TCs are typically younger than those with high-grade neuroendocrine tumors, including LCNEC or SCLC, there is no sex bias, and TCs appear not to be related to smoking [5, 6]. Although these tumors are classified as malignant epithelial tumors, the overall survival rate is better than that associated with ACs or high-grade neuroendocrine tumors [5]. Travis et al. reported that 13 of 20 patients with TCs had Cushing’s syndrome and one patient had

✉ Akira Iyoda  
aiyoda@med.toho-u.ac.jp

<sup>1</sup> Division of Chest Surgery, Department of Surgery, School of Medicine, Toho University, 6-11-1, Omori-Nishi, Ota-ku, Tokyo 143-8541, Japan

**Table 1** Classification and criteria for the diagnosis of neuroendocrine tumors of the lung

Tumor type	Grade	Criteria for diagnosis
Typical carcinoid	Low	A tumor with a carcinoid morphology Less than two mitosis per 2 mm <sup>2</sup> (ten high-power fields) and lack of necrosis 0.5 cm in size or larger
Atypical carcinoid	Intermediate	A tumor with a carcinoid morphology 2–10 mitosis per 2 mm <sup>2</sup> (ten high-power fields) and/or necrosis or both 0.5 cm in size or larger
Large cell neuroendocrine carcinoma	High	A tumor with a neuroendocrine morphology > 10 mitosis per 2 mm <sup>2</sup> and necrosis Cytological features of a non-small cell carcinoma: large cell size low nuclear-to-cytoplasmic ratio, vesicular coarse or fine chromatin, and/or frequent nucleoli Positive immunohistochemical staining for one or more neuroendocrine markers Neuroendocrine granules by electron microscopy
Small cell lung carcinoma	High	Small size and scant cytoplasm Finely granular nuclear chromatin, absent or faint nucleoli > 10 mitosis per 2 mm <sup>2</sup> and frequent necrosis

type one multiple endocrine neoplasia [7]. Although Travis et al. revealed high rates of paraneoplastic syndrome among patients with TCs, Soga et al. reported carcinoid syndrome in 135 (8.7%) of 1595 TC cases [6].

Regarding the molecular features of TCs, Rusch et al. found that these tumors do not express p53 and that they stain normally for Rb [8]. Onuki revealed that the genetic alterations of TC differed from those of AC and high-grade neuroendocrine tumors and neuroendocrine tumors exhibited a spectrum of genetic alterations from TC and AC to high-grade neuroendocrine tumors [9]. Walch used comparative genomic hybridization to show loss of chromosome 11q in TC but not in high-grade neuroendocrine tumors ([10]; Table 2).

The standard surgical procedure for TCs is lobectomy with lymph-node dissection. Many patients with TCs have tumor tissues located in the central airway and must undergo tracheobronchial-plasty to preserve residual lung function during surgery. Lymph-node metastases develop in fewer than 20% of patients with TCs [5, 6, 11–13]. Thus, TC is associated with significantly better survival than AC [11, 12, 15]. A significant difference in survival between patients

with carcinoids and those with high-grade neuroendocrine tumors has also been reported [5]. Based on the favorable prognoses of patients with TCs, some authors have advocated sublobar resection as suitable treatment [15, 16]. However, several guidelines recommend standard lobectomy with lymph node dissection for TCs because lymph-node metastases and multicentric forms may develop, even in patients with TCs and it is difficult to differentiate ACs from TCs preoperatively or by intraoperative frozen sections due to the presence of small amounts of necrosis or few mitoses [13, 17].

### Atypical carcinoids: intermediate-grade neuroendocrine tumors

ACs are differentiated from TCs by the presence of mitoses or necrosis and from LCNECs by the presence of mitoses. Patients with ACs have similar clinical characteristics to those with TCs, including age, sex, and smoking status [5]. Regarding the molecular features of ACs, Onuki reported that genetic alterations occur at a higher frequency in ACs

**Table 2** Molecular features of neuroendocrine tumors of the lung

Tumor type	Site of loss of heterozygosity	Ki-67 proliferation index
Typical carcinoid	11q	Up to 5%
Atypical carcinoid		Up to 20%
Large cell neuroendocrine carcinoma	3p and 5q	40–80%
Small cell lung carcinoma	3p, 4q, 5q, 13q and 15q	50–100%

than in TCs and at a lower frequency than in high-grade neuroendocrine tumors [9]. Like TCs, ACs reveal frequent loss of chromosome 11q, which encompasses the *MEN1* locus, representing a characteristic genetic alteration of this tumor ([10]; Table 2). Costes reported that ACs account for 2.43% of Ki-67-positive cells, a significantly higher rate than that for TCs [18]. Because patients with ACs have more frequent lymph node metastases and a poorer prognosis than those with TCs [5, 7, 14, 15], standard lobectomy with systematic lymph node dissection is recommended. The National Comprehensive Cancer Network (NCCN) guidelines recommend adjuvant chemotherapy for advanced-stage AC tumors [19]. The European Neuroendocrine Tumor Society (ENETS) also suggests that AC with a high proliferative index is an indication for adjuvant therapy, although there is currently no consensus on adjuvant therapy for pulmonary carcinoids after complete resection [20]. Preoperatively, it is difficult to differentiate TC from AC in patients with lung cancer because preoperative small biopsy specimens cannot reveal the characteristics of an entire tumor or identify small areas of necrosis or low numbers of mitoses.

Based on the NCCN guidelines, lobectomy or another type of anatomic resection with mediastinal node dissection or sampling is recommended for resectable tumors. For unresectable tumors, platinum-based chemotherapy with or without radiotherapy, or octreotide/lanreotide/everolimus/platinum-based chemotherapy, is recommended [19]. The ENETS guidelines recommend somatostatin analogues (octreotide or lanreotide) for advanced unresectable TC/ACs with fewer than 10% Ki-67-positive cells, strong positivity for somatostatin receptor (SSTR) expression, and slow growth. Everolimus is recommended for TC/ACs with progressive growth [20, 21]. If somatostatin analogues are not effective for ACs with more than 15% Ki-67-positive cells, chemotherapy is recommended [20, 21]. Everolimus was the first targeted agent to show robust anti-tumor activity with acceptable tolerability for neuroendocrine tumors, including those in the pancreas, lung, and gastrointestinal tract, in a randomized, double-blind, placebo-controlled phase 3 RADIANT-4 trial [22]. Programmed death-ligand 1 (PD-L1) is not expressed in TC/ACs [23].

### Large-cell neuroendocrine carcinomas: high-grade neuroendocrine tumors

Travis et al. proposed large cell neuroendocrine carcinomas as the fourth category of neuroendocrine tumors of the lung [1, 7]. The third edition of the World Health Organization (WHO) classification in 1999 categorized LCNEC as a variant of large cell carcinomas [3]. However, many studies since have found that the clinical and biological features of LCNEC are very similar to those of SCLC in many aspects

but very different from those of classic large cell carcinomas [1]. Thus, in 2015, the WHO reclassified LCNEC as a neuroendocrine tumor, together with carcinoids and SCLC [4].

Almost all previous studies have been retrospective because it is very difficult to perform preoperative diagnoses using small biopsy specimens, and most cases are diagnosed based on resected surgical specimens [1]. Patients with LCNEC are predominantly males, smokers, and older in age [24].

The cytological findings of LCNEC are very different from those of classic large-cell carcinoma [25]. Immunohistochemical staining analyses indicated different expression patterns between LCNEC and classic large cell carcinoma [26]. According to staining of Ki-67, LCNEC also exhibits greater proliferative activity and higher expression of Bcl-2 than classic large cell carcinomas [27]. In comparison with other neuroendocrine tumors of the lung, genetic alterations are more frequent in LCNEC than in TCs or ACs and less frequent in LCNEC than in SCLC according to microsatellite marker analyses [9]. LCNEC showed different expression patterns of Ki-67/P53/Rb [8] and Bcl-2 [28] to carcinoids, and higher proliferative activity [29]. The expression levels of p53, K-ras-2, and C-raf-1 were similar in LCNEC and SCLC [30], although those of p53 and Rb in LCNEC and SCLC differed from those in carcinoid tumors [31]. LCNEC revealed high telomerase activity, comparable with that in SCLC [32]. Comparative genomic hybridization [33], array-based comparative genomic hybridization analysis [34], and immunohistochemical staining analysis [35] all revealed both common and differential expression patterns in LCNEC and SCLC. A previous microarray analysis failed to distinguish LCNEC from SCLC in terms of gene expression profiles [36]. Analyses of microsatellite markers on chromosome 3p and methylation of p16 in LCNEC indicated features of both SCLC and classic large-cell carcinoma [37]. Frequent loss of heterozygosity on chromosome 5q has also been detected in LCNEC ([4, 38]; Table 2).

LCNEC, like SCLC, is classified as a high-grade neuroendocrine tumor [5, 39]. Radical surgical resection for SCLC is only performed in patients with stages I–IIA disease; however, curative surgical resection may be indicated for patients with more advanced LCNEC because a complete response cannot be achieved by chemoradiotherapy despite similar response rates of SCLC to SCLC-based chemotherapies [40, 41]. Many studies have reported good response rates to SCLC-based chemotherapies in patients with advanced or unresectable LCNEC, comparable to those in patients with SCLC [42–45]. The ASCO guideline-update suggested that a platinum plus etoposide combination might provide optimal efficacy for patients with LCNEC [46], despite an inferior response in patients with SCLC [47, 48]. After surgical resection, patients with LCNEC of the lung, even early-stage LCNEC [39, 50, 51], may have a poor prognosis [49],

according to a report of significantly poorer prognosis in patients with stage IA LCNEC than in patients with adenocarcinoma or squamous cell carcinoma [52]. LCNEC has a high rate of recurrence, mainly distant metastases [53], and many studies have shown the efficacy of adjuvant chemotherapy even for patients with stage I LCNEC, similar to SCLC ([54–63]; Table 3), although one study showed negative results [64].

Regarding molecular targeted therapies for LCNEC, EGFR mutations in exons 18 [65], 19 [66, 67], and 21 [68, 69] have been reported in this tumor, although they occur infrequently [65, 68, 70]. Neuroendocrine tumors of the lung exhibit overactivation of the mTOR pathway [71], and an analysis of genetic alterations in PI3K/AKT/mTOR in LCNEC revealed a similar genomic profile to that in SCLC [72]; thus, mTOR inhibitors may be effective against LCNEC [71]. A PD-L1 expression rate of 10.4% has been reported in LCNEC [23], and an immune checkpoint inhibitor was effective even in a PD-L1-negative case [73]. Tropomyosin-related kinase B (TrkB) [74], brain-derived neurotrophic factor (BDNF) [74], VEGF [65], c-kit [65], and HER2 [65] may also play roles in the treatment of LCNEC, although the role of c-kit is controversial [75–77]. One case report documented successful treatment of LCNEC metastasis to the iris by the intravitreal injection of anti-VEGF [78]. Because the response of LCNEC to chemotherapy varies, predictive markers of LCNEC or LCNEC subtypes have been examined. Molecular tumor subtypes according to RB1 expression might predict the outcome of patients with LCNEC after chemotherapy [79]. Genomic analyses have identified small-cell carcinoma-like, non-small-cell carcinoma (predominantly adenocarcinoma)-like, and carcinoid-like subtypes of LCNEC [80, 81], and the results of those analyses suggest that LCNEC exhibits the clinicopathological and biological characteristics of both SCLC and non-SCLC. The immunohistochemical staining patterns of

neuroendocrine markers may be predictive of the prognoses of patients with this tumor [82, 83]. The treatments for LCNEC of other organs are based on those for LCNEC of the lung [84–90].

### Small-cell lung carcinomas: high-grade neuroendocrine tumors

SCLCs are composed of small cells with scant cytoplasm and nuclei containing finely granular nuclear chromatin and absent/faint nucleoli. Histologically, SCLC tissues reveal a high mitotic rate with more than ten mitoses per 2 mm<sup>2</sup> and frequent necrosis. The size of small-cell carcinoma cells is less than the diameter of three small resting lymphocytes. When SCLC and non-small cell carcinomas, such as adenocarcinoma, squamous cell carcinoma, large cell neuroendocrine carcinoma, spindle cell carcinoma, and giant cell carcinoma, are combined, those tumors are called combined SCLC [4].

Patients with SCLC are predominantly male, smokers, and older, and their clinical characteristics are similar to those of patients with LCNEC [51]. Genetic alterations in SCLC were found to be most frequent among all four types of neuroendocrine tumors according to microsatellite marker analyses ([9]; Table 2). SCLC is classified as a high-grade neuroendocrine tumor because patients have a very poor prognosis [3], with a 5-years overall survival rate of only 16.4% [5]. Patients with clinical stage I–IIA SCLC usually undergo surgical resection, despite which the prognosis is still poor. Although the indications for surgery are broader in patients with LCNEC than in those with SCLC, curative surgical resection is possible only for patients with stage 1–IIA SCLC because SCLC is more often associated with lymph node metastases, rapid growth, and poorer prognosis than LCNEC [51]. Adjuvant chemotherapy using cisplatin/carboplatin and etoposide is recommended after surgical resection [91]. The main treatment option for SCLC is chemotherapy and irinotecan/cisplatin is effective for extensive disease (ED)–SCLC [92–94]. Atezolizumab plus chemotherapy was also demonstrated to be effective for extensive-stage SCLC [95]. Only about 2% of patients with SCLCs are never smokers. Of patients with de novo SCLCs who are never smokers, 25% have EGFR mutations [96]. To improve the prognosis, it is necessary to increase the treatment options for patients with SCLC.

### Conclusions

The current four types of neuroendocrine tumors have been more clearly defined by the reclassification of LCNEC as a neuroendocrine tumor, but the treatment strategies for patients with TC, AC, and SCLC have not changed

**Table 3** Published reports on adjuvant chemotherapy for patients with large cell neuroendocrine carcinoma

Author	Design	Result	Year	Journal
Dresler CM	Retrospective	Negative	1997	Ann Thorac Surg
Iyoda A	Retrospective	Positive	2001	Cancer
Rossi G	Retrospective	Positive	2005	J Clin Oncol
Iyoda A	Prospective	Positive	2006	Ann Thorac Surg
Veronesi G	Retrospective	Positive?	2006	Lung Cancer
Saji H	Retrospective	Positive	2010	Anti-Cancer Drugs
Sarkaria IS	Retrospective	Positive	2011	Ann Thorac Surg
Incekara F	Retrospective	Positive	2016	Turk J Med Sci
Kim KM	Retrospective	Positive	2017	World J Surg
Filosso PL	Retrospective	Positive	2017	Eur J Cardiothorac Surg
Wakeam E	Retrospective	Positive	2019	J Thorac Cardiovasc Surg

remarkably since the revised classification. On the other hand, despite the reclassification of LCNEC from a large cell carcinoma variant to a neuroendocrine tumor, the treatment strategy for LCNEC has not been established. Further research on neuroendocrine tumors of the lung is necessary to improve the prognosis.

**Funding** We received no funding for this manuscript.

## Compliance with ethical standards

**Conflict of interest** We have no conflict of interest to declare.

## References

- Iyoda A. Biological and clinicopathological features of pulmonary large-cell neuroendocrine carcinoma—a new era of research. *Toho J Med.* 2018;4:35–42.
- Arrigoni MG, Woolner LB, Bernatz PE. Atypical carcinoid tumors of the lung. *J Thorac Cardiovasc Surg.* 1972;64:413–21.
- World Health Organization. *Histological typing of lung and pleural tumours.* 3rd ed. Germany: Springer; 1999.
- Travis WD, Brambilla E, Burke AP, Marx A, Nicholson AG, editors. *WHO classification of tumours of the lung, pleural, thymus and heart.* 4th ed. Lyon: IARC; 2015.
- Iyoda A, Hiroshima K, Baba M, Saitoh Y, Ohwada H, Fujisawa T. Pulmonary large cell carcinomas with neuroendocrine features are high grade neuroendocrine tumors. *Ann Thorac Surg.* 2002;73:1049–54.
- Soga J, Yakuwa Y. Bronchopulmonary carcinoids: an analysis of 1,875 reported cases with special reference to a comparison between typical carcinoids and atypical varieties. *Ann Thorac Cardiovasc Surg.* 1999;5:211–9.
- Travis WD, Linnoila RI, Tsokos MG, Hitchcock CL, Cutler GB Jr, Nieman L, et al. Neuroendocrine tumors of the lung with proposed criteria for large-cell neuroendocrine carcinoma. *Am J Surg Pathol.* 1991;15:529–53.
- Rusch VW, Klimstra DS, Venkatraman ES. Molecular markers help characterize neuroendocrine lung tumors. *Ann Thorac Surg.* 1996;62:798–810.
- Onuki N, Wistuba II, Travis WD, Virmani AK, Yashima K, Brambilla E, et al. Genetic changes in the spectrum of neuroendocrine lung tumors. *Cancer.* 1999;85:600–7.
- Walch AK, Zitzelsberger HF, Aubele MM, Mattis AE, Bauchinger M, Candidus S, et al. Typical and atypical carcinoid tumors of the lung are characterized by 11q deletions as detected by comparative genomic hybridization. *Am J Pathol.* 1998;153:1089–98.
- Fink G, Krelbaum T, Yellin A, Bendayan D, Saute M, Glazer M, et al. Pulmonary carcinoid: presentation, diagnosis, and outcome in 142 cases in Israel and review of 640 cases from the literature. *Chest.* 2001;119:1647–51.
- Rea F, Rizzardi G, Zuin A, Marulli G, Nicotra S, Bulf R, et al. Outcome and surgical strategy in bronchial carcinoid tumors: single institution experience with 252 patients. *Eur J Cardiothorac Surg.* 2007;31:186–91.
- Daddi N, Ferolla P, Urbani M, Semeraro A, Avenia N, Ribacchi R, et al. Surgical treatment of neuroendocrine tumors of the lung. *Eur J Cardiothorac Surg.* 2004;26:813–7.
- Travis WD, Rush W, Flieder DB, Falk R, Fleming MV, Gal AA, et al. Survival analysis of 200 pulmonary neuroendocrine tumors with clarification of criteria for atypical carcinoid and its separation from typical carcinoid. *Am J Surg Pathol.* 1998;22:934–44.
- Ferguson MK, Landreneau RJ, Hazelrigg SR, Altorki NK, Naunheim KS, Zwischenberger JB, et al. Long-term outcome after resection for bronchial carcinoid tumors. *Eur J Cardiothorac Surg.* 2000;18:156–61.
- Fox M, Van Berkel V, Bousamra M 2nd, Sloan S, Martin RC 2nd. Surgical management of pulmonary carcinoid tumors: sublobar resection versus lobectomy. *Am J Surg.* 2013;205:200–8.
- Chen F, Sato T, Fujinaga T, Sakai H, Miyahara R, Bando T, et al. Surgical management of bronchopulmonary typical carcinoid tumors: an institutional experience. *Interact Cardiovasc Thorac Surg.* 2010;11:737–9.
- Costes V, Marty-Ané C, Picot MC, Serre I, Pujol JL, Mary H, et al. Typical and atypical bronchopulmonary carcinoid tumors: a clinicopathologic and KI-67-labeling study. *Hum Pathol.* 1995;26:740–5.
- National Comprehensive Cancer Network. Neuroendocrine and adrenal tumors. NCCN Guidelines, version 2.2018: NET-6-NET-9. NCCN Clinical Practice Guidelines in Oncology. [https://www.nccn.org/professionals/physician\\_gls/default.aspx](https://www.nccn.org/professionals/physician_gls/default.aspx).
- Caplin ME, Baudin E, Ferolla P, Filosso P, Garcia-Yuste M, Lim E, et al. Pulmonary neuroendocrine (carcinoid) tumors: European Neuroendocrine Tumor Society expert consensus and recommendations for best practice for typical and atypical pulmonary carcinoids. *Ann Oncol.* 2015;26:1604–20.
- Wolin EM. Advances in the diagnosis and management of well-differentiated and intermediate-differentiated neuroendocrine tumors of the lung. *Chest.* 2017;151:1141–6.
- Yao JC, Fazio N, Singh S, Buzzoni R, Carnaghi C, Wolin E, et al. Everolimus for the treatment of advanced, nonfunctional neuroendocrine tumours of the lung or gastrointestinal tract (RADIANT-4): a randomised, placebo-controlled, phase 3 study. *Lancet.* 2016;387:968–77.
- Tsuruoka K, Horinouchi H, Goto Y, Kanda S, Fujiwara Y, Nohhara H, et al. PD-L1 expression in neuroendocrine tumors of the lung. *Lung Cancer.* 2017;108:115–20.
- Iyoda A, Hiroshima K, Toyozaki T, Haga Y, Fujisawa T, Ohwada H. Clinical characterization of pulmonary large cell neuroendocrine carcinoma and large cell carcinoma with neuroendocrine morphology. *Cancer.* 2001;91:1992–2000.
- Iyoda A, Baba M, Hiroshima K, Saitoh H, Moriya Y, Shibuya K, et al. Imprint cytologic features of pulmonary large cell neuroendocrine carcinoma: comparison with classic large cell carcinoma. *Oncol Rep.* 2004;11:285–8.
- Nitadori J, Ishii G, Tsuta K, Yokose T, Murata Y, Kodama T, et al. Immunohistochemical differential diagnosis between large cell neuroendocrine carcinoma and small cell carcinoma by tissue microarray analysis with a large antibody panel. *Am J Clin Pathol.* 2006;125:682–92.
- Iyoda A, Hiroshima K, Moriya Y, Mizobuchi T, Otsuji M, Sekine Y, et al. Pulmonary large cell neuroendocrine carcinoma demonstrates high proliferative activity. *Ann Thorac Surg.* 2004;77:1891–5.
- Jiang SX, Kameya T, Sato Y, Yanase N, Yoshimura H, Kodama T. Bcl-2 protein expression in lung cancer and close correlation with neuroendocrine differentiation. *Am J Pathol.* 1996;148:837–46.
- Arbiser ZK, Arbiser JL, Cohen C, Gal AA. Neuroendocrine lung tumors: grade correlates with proliferation but not angiogenesis. *Mod Pathol.* 2001;14:1195–9.
- Przygodzki RM, Finkelstein SD, Langer JC. Analysis of p53, K-ras-2, and C-raf-1 in pulmonary neuroendocrine tumors. Correlation with histological subtype and clinical outcome. *Am J Pathol.* 1996;148:1531–41.
- Gugger M, Burckhardt E, Kappeler A, Hirsiger H, Laissue JA, Mazzucchelli L. Quantitative expansion of structural genomic

- alterations in the spectrum of neuroendocrine lung carcinomas. *J Pathol.* 2002;196:408–15.
32. Zaffaroni N, De Polo D, Villa R, Della Porta C, Collini P, Fabbrì A, et al. Differential expression of telomerase activity in neuroendocrine lung tumours: correlation with gene product immunophenotyping. *J Pathol.* 2003;201:127–33.
  33. Ullmann R, Petzmann S, Sharma A, Cagle PT, Popper HH. Chromosomal aberrations in a series of large-cell neuroendocrine carcinomas: unexpected divergence from small-cell carcinoma of the lung. *Hum Pathol.* 2001;32:1059–63.
  34. Peng WX, Shibata T, Katoh H, Kokubu A, Matsuno Y, Asamura H, et al. Array-based comparative genomic hybridization analysis of high-grade neuroendocrine tumors of the lung. *Cancer Sci.* 2005;96:661–7.
  35. Hiroshima K, Iyoda A, Shida T, Shibuya K, Iizasa T, Kishi H, et al. Distinction of pulmonary large cell neuroendocrine carcinoma from small cell lung carcinoma: a morphological, immunohistochemical, and molecular analysis. *Mod Pathol.* 2006;19:1358–68.
  36. Jones MH, Virtanen C, Honjoh D, Miyoshi T, Satoh Y, Okumura S, et al. Two prognostically significant subtypes of high-grade lung neuroendocrine tumours independent of small-cell and large-cell neuroendocrine carcinomas identified by gene expression profiles. *Lancet.* 2004;363:775–81.
  37. Hiroshima K, Iyoda A, Shibuya K, Haga Y, Toyozaki T, Iizasa T, et al. Genetic alterations in early-stage pulmonary large cell neuroendocrine carcinoma. *Cancer.* 2004;100:1190–8.
  38. Shin JH, Kang SM, Kim YS, Shin DH, Chang J, Kim SK, et al. Identification of tumor suppressor loci on the long arm of chromosome 5 in pulmonary large cell neuroendocrine carcinoma. *Chest.* 2005;128:2999–3003.
  39. Iyoda A, Jiang SX, Travis WD, Kurouzu N, Ogawa F, Amano H, et al. Clinicopathological features and the impact of the new TNM classification of malignant tumors in patients with pulmonary large cell neuroendocrine carcinoma. *Mol Clin Oncol.* 2013;1:437–43.
  40. Igawa S, Watanabe R, Ito I, Murakami H, Takahashi T, Nakamura Y, et al. Comparison of chemotherapy for unresectable pulmonary high-grade non-small cell neuroendocrine carcinoma and small-cell lung cancer. *Lung Cancer.* 2010;68:438–45.
  41. Tokito T, Kenmotsu H, Watanabe R, Ito I, Shukuya T, Ono A, et al. Comparison of chemotherapeutic efficacy between LCNEC diagnosed using large specimens and possible LCNEC diagnosed using small biopsy specimens. *Int J Clin Oncol.* 2014;19:63–7.
  42. Sun JM, Ahn MJ, Ahn JS, Um SW, Kim H, Kim HK, et al. Chemotherapy for pulmonary large cell neuroendocrine carcinoma: similar to that for small cell lung cancer or non-small cell lung cancer? *Lung Cancer.* 2012;77:365–70.
  43. Shimada Y, Niho S, Ishii G, Hishida T, Yoshida J, Nishimura M, et al. Clinical features of unresectable high-grade lung neuroendocrine carcinoma diagnosed using biopsy specimens. *Lung Cancer.* 2012;75:368–73.
  44. Yamazaki S, Sekine I, Matsuno Y, Takei H, Yamamoto N, Kunitoh H, et al. Clinical responses of large cell neuroendocrine carcinoma of the lung to cisplatin-based chemotherapy. *Lung Cancer.* 2005;49:217–23.
  45. Fasano M, Della Corte CM, Papaccio F, Ciardiello F, Morgillo F. Pulmonary large-cell neuroendocrine carcinoma: from epidemiology to therapy. *J Thorac Oncol.* 2015;10:1133–41.
  46. Masters GA, Temin S, Azzoli CG, Giaccone G, Baker S Jr, Brahmer JR, et al. Systemic therapy for stage IV non-small-cell lung cancer: American Society of Clinical Oncology Clinical Practice Guideline update. *J Clin Oncol.* 2015;33:3488–515.
  47. Le Treut J, Sault MC, Lena H, Souquet PJ, Vergnenegre A, Le Caer H, et al. Multicentre phase II study of cisplatin-etoposide chemotherapy for advanced large-cell neuroendocrine lung carcinoma: the GFPC 0302 study. *Ann Oncol.* 2013;24:1548–52.
  48. Niho S, Kenmotsu H, Sekine I, Ishii G, Ishikawa Y, Noguchi M, et al. Combination chemotherapy with irinotecan and cisplatin for large-cell neuroendocrine carcinoma of the lung: a multicenter phase II study. *J Thorac Oncol.* 2013;8:980–4.
  49. Iyoda A, Hiroshima K, Nakatani Y, Fujisawa T. Pulmonary large cell neuroendocrine carcinoma—its place in the spectrum of pulmonary carcinoma. *Ann Thorac Surg.* 2007;84:702–7.
  50. Asamura H, Kameya T, Matsuno Y, Noguchi M, Tada H, Ishikawa Y, et al. Neuroendocrine neoplasms of the lung: a prognostic spectrum. *J Clin Oncol.* 2006;24:70–6.
  51. Iyoda A, Makino T, Koezuka S, Otsuka H, Hata Y. Treatment options for patients with large cell neuroendocrine carcinoma of the lung. *Gen Thorac Cardiovasc Surg.* 2014;62:351–6.
  52. Iyoda A, Hiroshima K, Moriya Y, Sekine Y, Shibuya K, Iizasa T, et al. Prognostic impact of large cell neuroendocrine histology in patients with pathological stage 1a pulmonary non-small cell carcinoma. *J Thorac Cardiovasc Surg.* 2006;132:312–5.
  53. Takei H, Asamura H, Maeshima A, Suzuki K, Kondo H, Niki T, et al. Large cell neuroendocrine carcinoma of the lung: a clinicopathologic study of eighty-seven cases. *J Thorac Cardiovasc Surg.* 2002;124:285–92.
  54. Iyoda A, Hiroshima K, Toyozaki T, Haga Y, Baba M, Fujisawa T, et al. Adjuvant chemotherapy for large cell carcinoma with neuroendocrine features. *Cancer.* 2001;92:1108–12.
  55. Rossi G, Cavazza A, Marchioni A, Longo L, Migaldi M, Sartori G, et al. Role of chemotherapy and the receptor tyrosine kinases KIT, PDGFRalpha, PDGFRbeta, and Met in large-cell neuroendocrine carcinoma of the lung. *J Clin Oncol.* 2005;23:8774–855.
  56. Iyoda A, Hiroshima K, Moriya Y, Takiguchi Y, Sekine Y, Shibuya K, et al. Prospective study of adjuvant chemotherapy for pulmonary large cell neuroendocrine carcinoma. *Ann Thorac Surg.* 2006;82:1802–7.
  57. Veronesi G, Morandi U, Alloisio M, Terzi A, Cardillo G, Filosso P, et al. Large cell neuroendocrine carcinoma of the lung: a retrospective analysis of 144 surgical cases. *Lung Cancer.* 2006;53:111–5.
  58. Iyoda A, Hiroshima K, Moriya Y, Iwadate Y, Takiguchi Y, Uno T, et al. Postoperative recurrence and the role of adjuvant chemotherapy in patients with pulmonary large-cell neuroendocrine carcinoma. *J Thorac Cardiovasc Surg.* 2009;138:446–53.
  59. Saji H, Tsuboi M, Matsubayashi J, Miyajima K, Shimada Y, Imai K, et al. Clinical response of large cell neuroendocrine carcinoma of the lung to perioperative adjuvant chemotherapy. *Anticancer Drugs.* 2010;21:89–93.
  60. Sarkaria IS, Iyoda A, Roh MS, Sica G, Kuk D, Sima CS, et al. Neoadjuvant and adjuvant chemotherapy in resected pulmonary large cell neuroendocrine carcinomas: a single institution experience. *Ann Thorac Surg.* 2011;92:1180–6.
  61. Filosso PL, Guerrero F, Evangelista A, Galassi C, Welter S, Rendina EA, ESTS Lung Neuroendocrine Working Group Contributors, et al. Adjuvant chemotherapy for large-cell neuroendocrine lung carcinoma: results from the European Society for Thoracic Surgeons Lung Neuroendocrine Tumours retrospective database. *Eur J Cardiothorac Surg.* 2017;52:339–45.
  62. Kim KW, Kim HK, Kim J, Shim YM, Ahn MJ, Choi YL. Outcomes of curative-intent surgery and adjuvant treatment for pulmonary large cell neuroendocrine carcinoma. *World J Surg.* 2017;41:1820–7.
  63. Wakeam E, Adibfar A, Stokes S, Leighl NB, Giuliani ME, Varghese TK Jr, et al. Defining the role of adjuvant therapy for early-stage large cell neuroendocrine carcinoma. *J Thorac Cardiovasc Surg.* 2019. <https://doi.org/10.1016/j.jtcvs.2019.09.077>.
  64. Dresler CM, Ritter JH, Patterson GA, Ross E, Bailey MS, Wick MR. Clinical-pathologic analysis of 40 patients with large

- cell neuroendocrine carcinoma of the lung. *Ann Thorac Surg.* 1997;63:180–5.
65. Iyoda A, Travis WD, Sarkaria IS, Jiang SX, Amano H, Sato Y, et al. Expression profiling and identification of potential molecular targets for therapy in pulmonary large-cell neuroendocrine carcinoma. *Exp Ther Med.* 2011;2:1041–5.
  66. De Pas TM, Giovannini M, Manzotti M, Trifirò G, Toffalorio F, Catania C, et al. Large-cell neuroendocrine carcinoma of the lung harboring EGFR mutation and responding to gefitinib. *J Clin Oncol.* 2011;29:e819–e822822.
  67. Yanagisawa S, Morikawa N, Kimura Y, Nagano Y, Murakami K, Tabata T. Large-cell neuroendocrine carcinoma with epidermal growth factor receptor mutation: possible transformation of lung adenocarcinoma. *Respirology.* 2012;17:1275–7.
  68. Sakai Y, Yamasaki T, Kusakabe Y, Kasai D, Kotani Y, Nishimura Y, et al. Large-cell neuroendocrine carcinoma of lung with epidermal growth factor receptor (EGFR) gene mutation and co-expression of adenocarcinoma markers: a case report and review of the literature. *Multidiscip Respir Med.* 2013;8:47.
  69. Yoshida Y, Ota S, Murakawa T, Takai D, Nakajima J. Combined large cell neuroendocrine carcinoma and adenocarcinoma with epidermal growth factor receptor mutation in a female patient who never smoked. *Ann Thorac Cardiovasc Surg.* 2014;20(Suppl):582–4.
  70. Makino T, Mikami T, Hata Y, Otsuka H, Koezuka S, Isobe K, et al. Comprehensive biomarkers for personalized treatment in pulmonary large cell neuroendocrine carcinoma: a comparative analysis with adenocarcinoma. *Ann Thorac Surg.* 2016;102:1694–701.
  71. Christopoulos P, Engel-Riedel W, Grohé C, Kropf-Sanchen C, von Pawel J, Gütz S, et al. Everolimus with paclitaxel and carboplatin as first-line treatment for metastatic large-cell neuroendocrine lung carcinoma: a multicenter phase II trial. *Ann Oncol.* 2017;28:1898–902.
  72. Miyoshi T, Umemura S, Matsumura Y, Mimaki S, Tada S, Makinoshima H, et al. Genomic profiling of large-cell neuroendocrine carcinoma of the lung. *Clin Cancer Res.* 2017;23:757–65.
  73. Wang VE, Urisman A, Albacker L, Ali S, Miller V, Aggarwal R, et al. Checkpoint inhibitor is active against large cell neuroendocrine carcinoma with high tumor mutation burden. *J Immunother Cancer.* 2017;5:75.
  74. Odate S, Nakamura K, Onishi H, Kojima M, Uchiyama A, Nakano K, et al. TrkB/BDNF signaling pathway is a potential therapeutic target for pulmonary large cell neuroendocrine carcinoma. *Lung Cancer.* 2013;79:205–14.
  75. Araki K, Ishii G, Yokose T, Nagai K, Funai K, Kodama K, et al. Frequent overexpression of the c-kit protein in large cell neuroendocrine carcinoma of the lung. *Lung Cancer.* 2003;40:173–80.
  76. Casali C, Stefani A, Rossi G, Migaldi M, Bettelli S, Parise A, et al. The prognostic role of c-kit protein expression in resected large cell neuroendocrine carcinoma of the lung. *Ann Thorac Surg.* 2004;77:247–53.
  77. Pelosi G, Masullo M, Leon ME, Veronesi G, Spaggiari L, Pasini F, et al. CD117 immunoreactivity in high-grade neuroendocrine tumors of the lung: a comparative study of 39 large-cell neuroendocrine carcinomas and 27 surgically resected small-cell carcinomas. *Virchows Arch.* 2004;445:449–55.
  78. Yokouchi H, Kitahashi M, Oshitari T, Yamamoto S. Intravitreal bevacizumab for iris tumor metastasized from large cell neuroendocrine carcinoma of lung. *Graefes Arch Clin Exp Ophthalmol.* 2013;251:2243–5.
  79. Derks JL, Leblay N, Thunnissen E, van Suylen RJ, den Bakker M, Groen HJM, et al. Molecular subtypes of pulmonary large-cell neuroendocrine carcinoma predict chemotherapy treatment outcome. *Clin Cancer Res.* 2018;24:33–42.
  80. Rekhtman N, Pietanza MC, Hellmann MD, Naidoo J, Arora A, Won H, et al. Next-generation sequencing of pulmonary large cell neuroendocrine carcinoma reveals small cell carcinoma-like and non-small cell carcinoma-like subsets. *Clin Cancer Res.* 2016;22:3618–29.
  81. Rekhtman N, Pietanza CM, Sabari J, Montecalvo J, Wang H, Habeeb O, et al. Pulmonary large cell neuroendocrine carcinoma with adenocarcinoma-like features: napsin A expression and genomic alterations. *Mod Pathol.* 2018;31:111–21.
  82. Tanaka Y, Ogawa H, Uchino K, Ohbayashi C, Maniwa Y, Nishio W, et al. Immunohistochemical studies of pulmonary large cell neuroendocrine carcinoma: a possible association between staining patterns with neuroendocrine markers and tumor response to chemotherapy. *J Thorac Cardiovasc Surg.* 2013;145:839–46.
  83. Minami K, Tanaka Y, Ogawa H, Jimbo N, Nishio W, Yoshimura M, Itoh T, Maniwa Y. Neuroendocrine marker staining pattern categorization of small-sized pulmonary large cell neuroendocrine carcinoma. *Thorac Cancer.* 2019;10:2152–60.
  84. Kusafuka K, Ferlito A, Lewis JS Jr, Woolgar JA, Rinaldo A, Slootweg PJ, et al. Large cell neuroendocrine carcinoma of the head and neck. *Oral Oncol.* 2012;48:211–5.
  85. Ose N, Inoue M, Morii E, Shintani Y, Sawabata N, Okumura M. Multimodality therapy for large cell neuroendocrine carcinoma of the thymus. *Ann Thorac Surg.* 2013;96:e85–e8787.
  86. Embry JR, Kelly MG, Post MD, Spillman MA. Large cell neuroendocrine carcinoma of the cervix: prognostic factors and survival advantage with platinum chemotherapy. *Gynecol Oncol.* 2011;120:444–8.
  87. Yoseph B, Chi M, Truskinovsky AM, Dudek AZ. Large-cell neuroendocrine carcinoma of the cervix. *Rare Tumors.* 2012;4:e18.
  88. Oberstein PE, Kenney B, Krishnamoorthy SK, Woo Y, Saif MW. Metastatic gastric large cell neuroendocrine carcinoma: a case report and review of literature. *Clin Colorectal Cancer.* 2012;11:218–23.
  89. Evans AJ, Humphrey PA, Belani J, van der Kwast TH, Srigley JR. Large cell neuroendocrine carcinoma of prostate: a clinicopathologic summary of 7 cases of a rare manifestation of advanced prostate cancer. *Am J Surg Pathol.* 2006;30:684–93.
  90. Shimono C, Suwa K, Sato M, Shirai S, Yamada K, Nakamura Y, et al. Large cell neuroendocrine carcinoma of the gallbladder: long survival achieved by multimodal treatment. *Int J Clin Oncol.* 2009;14:351–5.
  91. National Comprehensive Cancer Network. Small cell lung cancer. NCCN guidelines, version 2.2018. NCCN Clinical Practice Guidelines in Oncology. [https://www.nccn.org/professionals/physician\\_gls/default.aspx](https://www.nccn.org/professionals/physician_gls/default.aspx).
  92. Noda K, Nishiwaki Y, Kawahara M, Negoro S, Sugiura T, Yokoyama A, et al. Irinotecan plus cisplatin compared with etoposide plus cisplatin for extensive small cell lung cancer. *N Engl J Med.* 2002;346:85–91.
  93. Jiang J, Liang X, Zhou X, Huang L, Huang R, Chu Z, Zhan Q. A meta-analysis of randomized controlled trials comparing irinotecan/platinum with etoposide/platinum in patients with previously untreated extensive-stage small cell lung cancer. *J Thorac Oncol.* 2010;5:867–73.
  94. Lima JP, dos Santos LV, Sasse EC, Lima CS, Sasse AD. Camptothecins compared with etoposide in combination with platinum analog in extensive stage small cell lung cancer: systematic review with meta-analysis. *J Thorac Oncol.* 2010;5:1986–93.
  95. Horn L, Mansfield AS, Szczesna A, Havel L, Krzakowski M, Hochmair MJ, et al. First-line atezolizumab plus chemotherapy in extensive-stage small-cell lung cancer. *N Engl J Med.* 2018;379:2220–9.
  96. Varghese AM, Zakowski MF, Yu HA, Won HH, Riely GJ, Krug LM, et al. Small-cell lung cancers in patients who never smoked cigarettes. *J Thorac Oncol.* 2014;9:892–6.

**Publisher's Note** Springer Nature remains neutral with regard to jurisdictional claims in published maps and institutional affiliations.



# Selected neuroendocrine tumour markers, growth factors and their receptors in typical and atypical bronchopulmonary carcinoids

Stężenia wybranych markerów nowotworów neuroendokrynych, czynników wzrostu i ich receptorów w rakowiakach typowych i atypowych płuc

Aleksandra Telega, Beata Kos-Kudła, Wanda Foltyn, Jolanta Blicharz-Dorniak, Violetta Rosiek

Division of Endocrinology, Department of Pathophysiology and Endocrinology, Silesian Medical University in Katowice, Poland

## Abstract

**Introduction:** Bronchopulmonary neuroendocrine tumours (BP NET) cause many diagnostic and therapeutic problems. There is an ongoing search for biochemical markers of activity of these tumours. The use of polypeptide growth factors seems potentially feasible in establishing the diagnosis, prognosis and treatment of these tumours.

**Material and methods:** We included 41 patients aged 25 to 78 years with histopathologically confirmed typical and atypical bronchopulmonary carcinoid tumours and 20 healthy volunteers. We assessed the levels of specific and non-specific markers of these tumours and of selected growth factors relative to TNM classification.

**Results:** The levels of specific markers (serotonin and its metabolite, 5-hydroxyindoleacetic acid [5HIAA]) and non-specific markers (chromogranin A [CgA]) were significantly higher in patients with atypical carcinoid tumours. The serum levels of hepatocyte growth factor (HGF), vascular endothelial growth factor (VEGF) and VEGF receptor-1 (VEGFR-1) were significantly higher in patients with carcinoid tumours versus the control group. The levels of VEGFR-1 closely correlated with TNM classification. No such correlation could, however, be confirmed for the levels of HGF, VEGF or VEGFR-2.

**Conclusions:** Determination of CgA, serotonin and 5HIAA may be useful in the diagnosis of BP NET, particularly in atypical carcinoid tumours, and their levels depend on the presence of distant metastases. Determination of growth factors (VEGF and its receptor, VEGFR-1, and HGF) may prove useful in the clinical diagnosis of these tumours, while the assessment of VEGFR-1 expression may be helpful in tumour staging. (*Endokrynol Pol* 2012; 63 (6): 477-482)

**Key words:** chromogranin A, serotonin, 5HIAA, growth factors, VEGF, VEGFR, HGF, typical and atypical lung carcinoid tumour

## Streszczenie

**Wstęp:** Nowotwory neuroendokryne płuc sprawiają wiele trudności diagnostycznych i leczniczych. Trwają więc poszukiwania biochemicznych wskaźników aktywności tych nowotworów. Wykorzystanie polipeptydowych czynników wzrostu wydaje się potencjalnie możliwe w diagnostyce, rokowaniu i leczeniu.

**Materiał i metody:** Badaniem objęto 41 chorych w wieku 25-78 lat z potwierdzonymi histopatologicznie rakowiakami typowymi i atypowymi płuc oraz 20 zdrowych wolontariuszy, u których oceniono zależność stężeń specyficznych i niespecyficznych markerów tych nowotworów oraz wybranych czynników wzrostu w zależności od stopnia zaawansowania w skali TNM.

**Wyniki:** Stężenia badanych markerów specyficznych (serotonina oraz jej metabolit — kwas 5-hydroksyindoloctowy [5HIAA]) i niespecyficznych (chromogranina A [CgA]) były istotnie wyższe u chorych z rakowiakiem atypowym. Stężenia czynnika wzrostu hepatocytów (HGF), czynnika wzrostu śródbłonna naczyniowego (VEGF) i jego receptorów R1 (VEGFR-1) było istotnie większe u chorych z rakowiakami w porównaniu z grupą kontrolną. Stężenia VEGFR-1 korelowały ściśle ze stopniem zaawansowania w skali TNM, czego nie udało się potwierdzić badając stężenia HGF oraz VEGF i VEGFR-2.

**Wnioski:** Oznaczanie stężeń CgA, serotoniny i 5HIAA może być przydatne w diagnostyce rakowiaków atypowych płuc a wielkość tych stężeń zależy od istnienia przerzutów odległych. Potencjalną rolę oznaczeń czynników wzrostu (VEGF i jego receptorów VEGFR-1 oraz HGF) upatrujemy w diagnostyce klinicznej tych nowotworów, natomiast ocena ekspresji receptorów VEGFR-1 może być użyteczna w ocenie stopnia zaawansowania procesu nowotworowego. (*Endokrynol Pol* 2012; 63 (6): 477-482)

**Słowa kluczowe:** chromogranina A, serotonina, 5HIAA, czynniki wzrostu, VEGF, VEGFR, HGF, rakowiak typowy i atypowy płuc

## Introduction

Bronchopulmonary neuroendocrine tumours (BP NET) are a group of neoplasms originating from endocrine cells disseminated throughout the human body. Neu-

roendocrine cells of the respiratory tract, also known as enterochromaffin cells (Kulchitsky cells), account for 0.17% of all the cells of the respiratory tract epithelium and are located in the basal layer of the bronchial epithelium and bronchial glands [1]. The aetiology and pathogenesis of



Jolanta Blicharz-Dorniak M.D., Department of Endocrinology, Division of Pathophysiology and Endocrinology, Silesian Medical University in Katowice, e-mail: jblicharz@poczta.fm  
Tłumaczenie: Paweł Baka

BP NET are unclear, which to possesses difficulties in determining their clinical course and prognosis [2–4]. Due to the untypical nature of this rare group of tumours, there is an ongoing search for biochemical markers that might be helpful in establishing the diagnosis and predicting progression of the disease in various stages of the tumour. Laboratory evaluation of these tumours involves the determination of specific markers (serotonin and its metabolite 5-hydroxyindoleacetic acid [5HIAA]) and non-specific markers (chromogranin A [CgA]) [5]. There are scarce and conflicting reports on the use of polypeptide growth factors involved in the processes of neoplastic transformation, proliferation and angiogenesis as potential biochemical markers of activity of these tumours. Angiogenesis is strictly related to tumour growth and metastatic potential of tumours. Neuroendocrine tumours have long been known to be highly vascular. In the past, carcinoid tumours were believed to be characterised by a benign clinical course. However, it has been proved in the past 20 years that these are in fact malignant tumours, and the prognosis and treatment outcomes depend on cell type, differentiation and stage of the disease. Compared to other malignant tumours of the lung, carcinoid tumours tend to occur at a younger age and have a more favourable prognosis than other primary tumours of the lung, although this strictly depends on tumour type and stage. Studies have demonstrated that levels of such angiogenic factors as vascular endothelial growth factor (VEGF) [6], which exerts its actions through specific tyrosine kinase receptors (VEGFR), and hepatocyte growth factor (HGF) correlate with the aggressiveness of tumours in various organs and may be used as prognostic factors. The activity of VEGF is not limited to the vascular endothelium but may extend to certain other cell types (VEGF may, for instance, stimulate migration of monocytes or macrophages). *In vitro* experiments have shown that VEGF stimulates mitosis and migration of endothelial cells and increases the permeability of capillaries. HGF is secreted by mesenchymal cells and acts as a cytokine mainly on cells of epithelial origin, cells of mesothelial origin and on the precursors of haematopoietic cells, regulating their growth, mobility and morphogenesis. Studies have demonstrated that when released from its regulatory mechanisms, HGF causes a fulminant invasion of tumour cells into adjacent tissues and is closely linked to the metastatic potential of various types of tumours [7]. Studies in patients with non-small-lung carcinoma show a significant role in the growth of solid tumours of the lung and suggest a relationship with dissemination of the underlying disease [8, 9].

The aims of our study were to: assess the levels of specific markers (serotonin and its metabolite 5HIAA), non-specific markers (CgA) and selected growth factors (VEGF, HGF, VEGFR1, VEGFR2) in patients with typical and atypical carcinoid tumours of the lung;

— assess the relationship between CgA, serotonin, 5HIAA, VEGF, VEGFR and HGF and the TNM stage in these patients.

## Material and methods

We enrolled 41 patients aged from 25 to 78 years (mean age 59.4 years) with histopathologically confirmed bronchopulmonary carcinoid tumours and 20 sex- and age-matched healthy volunteers serving as controls. Typical carcinoid tumours were present in 54% (22/41) of the patients (Group 1) and atypical ones in 46% (19/41) of the patients (Group 2). Women accounted for 72.7% (16/22) and men for 27.3% (6/22) of the patients in Group 1. The respective percentages in Group 2 were 42.1% (8/19) and 57.9% (11/19). Patients with co-existing tumours in other organs were excluded from the study. Levels of the selected parameters were determined in the serum.

All the study subjects provided informed consent to participate in the study. The study protocol was approved by the relevant ethics committee.

In both patient groups, the patients were classified according to the TNM classification published in 2009 by Travis et al. [10] (Fig. 1, 2).

Fasting blood samples for hormone determinations were collected at 8.00am from an arm vein. The serum obtained by centrifugation was stored at  $-70^{\circ}\text{C}$  until analysis. The levels of the non-specific neuroendocrine tumour marker (CgA), specific neuroendocrine tumour markers (serotonin, 5HIAA), selected growth factors (VEGF, HGF) and binding proteins (VEGFR-1, VEGFR-2) were determined by enzyme-linked immunosorbent assay (ELISA). Serum levels of CgA and serotonin and 24-hour urine levels of 5HIAA were determined using the  $\mu$ Quant (Bio-Tek), the Serotonin ELISA (ALPCO) and the 5-HIAA ELISA (IBL International), respectively. The respective analytical sensitivities of these tests were as follows: 2.0 U/L (normal range: 2–18 U/L); 5 ng/mL (normal ranges: 80–450 ng/mL [women] and 40–400 ng/mL [men]) and 0.06 mg/L (normal range: 6–10 ng/mL). Serum levels of HGF, VEGF VEGFR-1 and VEGFR-2 were determined using the Quantikine (R&D Systems) at the analytical sensitivities of 40 pg/mL, 5 pg/mL, 3.5 pg/mL and 4.6 pg/mL, respectively.

The results were analysed using statistical methods. The analysis involved a comparison of the data in the study patient groups and an assessment of their correlations with the pTNM stage. Linear regression curves were applied to the observed correlations. The differences between the specific variables in the study patient groups were evaluated using univariate analysis of variance. P values of  $< 0.05$  were considered statistically significant. The statistical calculations were performed

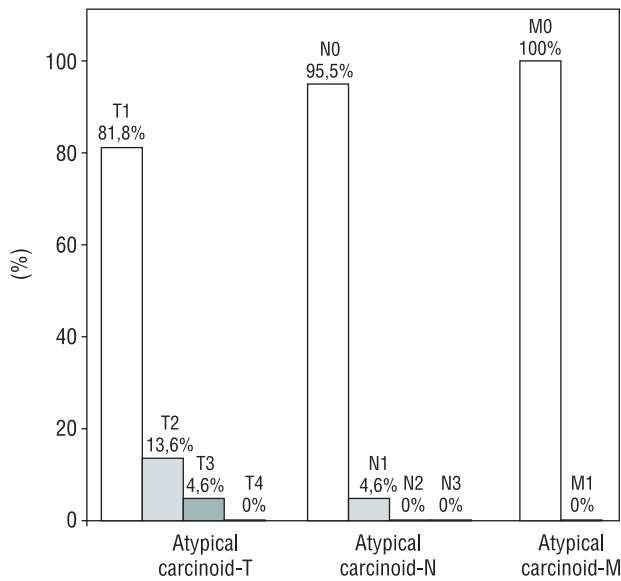


**Figure 1.** Percentage distribution of patients with typical bronchopulmonary carcinoid tumours (Group 1) according to the TNM classification

**Rycina 1.** Rozkład procentowy grupy chorych z rakowiakami typowymi (grupa 1) w zależności od stopnia zaawansowania w skali TNM

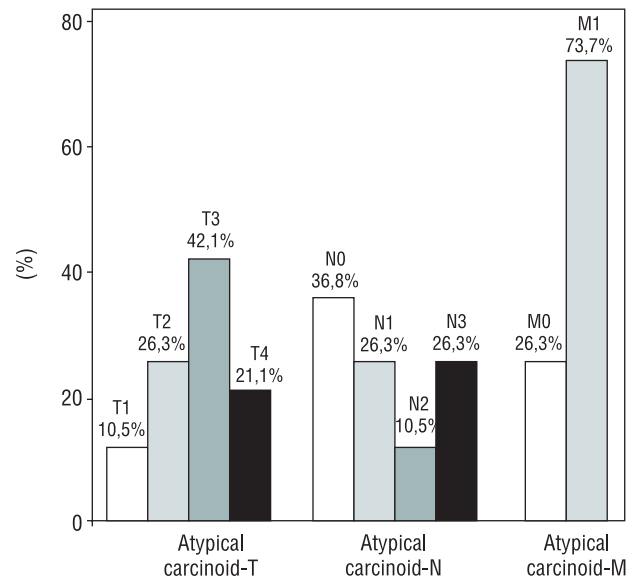


**Figure 2.** Percentage distribution of patients with atypical bronchopulmonary carcinoid tumours (Group 2) according to the TNM classification

**Rycina 2.** Rozkład procentowy grupy chorych z rakowiakami atypowymi (grupa 2) w zależności od stopnia zaawansowania w skali TNM

**Table I.** Mean levels of non-specific markers (CgA) and specific markers (serotonin and 5HIAA) in the study patient groups with BP NET and the control group

**Tabela I.** Średnie stężenia markerów niespecyficznego (CgA) oraz specyficznego (serotoniny i 5HIAA) w grupach badanych

	CgA [U/L] (normal range: 2–18 U/L)	Serotonin [ng/mL] (normal range: 80–450 ng/mL)	5HIAA [mg/24 h] (normal range: 2–6 mg/24 h)
Typical carcinoid tumour group	13.02 (SD 9.10)	164.18 (SD 242.00)	5.75 (SD 3.48)
Atypical carcinoid tumour group	1020.28 (SD 3638.46)	363.94 (SD 333.98)	50.32 (SD 148.90)
Control group	8.09 (SD 6.23)	146.31 (SD 210.30)	4.23 (SD 2.69)
	p = 0.026	p = 0.014	p = 0.048
	p = 0.018	p = 0.021	p = 0.032

using MedCalc. The values calculated for quantitative variables were expressed as arithmetic means.

## Results

In the study patient population, serum levels of CgA and serotonin and 24-hour urine levels of 5HIAA were significantly elevated ( $p < 0.02$ ,  $p < 0.01$  and  $p < 0.04$ , respectively) in patients with atypical bronchopulmonary carcinoid tumours versus patients with typical carcinoid tumours and the control group (Table I).

The mean levels of CgA, serotonin and 5HIAA did not show any significant differences relative to the

tumour size (T) or nodal invasion (N) but were significantly higher in patients with distant metastases (M). Summary results for patients with typical and atypical carcinoid tumours are provided in Figures 3 to 5.

Levels of selected growth factors (VEGF HGF) were determined in the study patient groups and the control group.

Levels of VEGF (mean  $\pm$  SD) in patients with BP NET were significantly higher than in the control group ( $359.26 \pm 281.03$  pg/mL v.  $207.08 \pm 157.84$  pg/mL;  $p = 0.0115$ ) (Fig. 6).

Levels of VEGF did not differ significantly between patients with typical lung carcinoid tumours and patients with atypical carcinoid tumours, and there

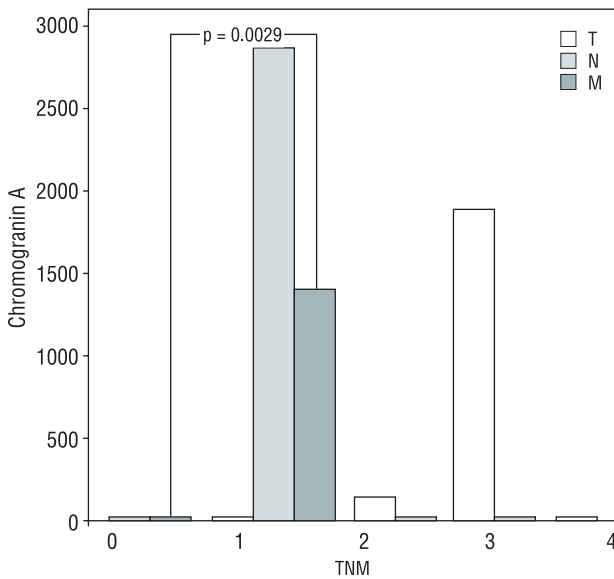


**Figure 3.** CgA levels (U/L) according to the TNM classification in patients with carcinoid tumours of the lung

**Rycina 3.** Stężenia chromograniny A [U/l] w zależności od stopnia zaawansowania według skali TNM u chorych z rakowiakami płuc

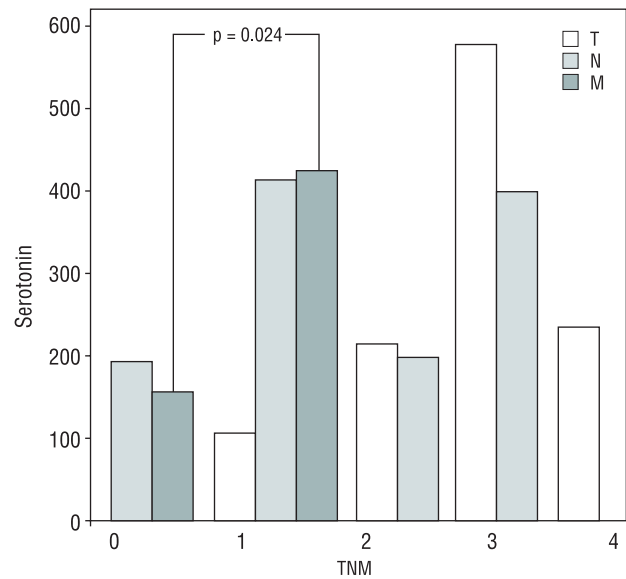


**Figure 4.** Serotonin levels [ng/mL] according to the TNM classification in patients with carcinoid tumours of the lung

**Rycina 4.** Stężenia serotoniny [ng/ml] w zależności od stopnia zaawansowania według skali TNM u chorych z rakowiakami płuc

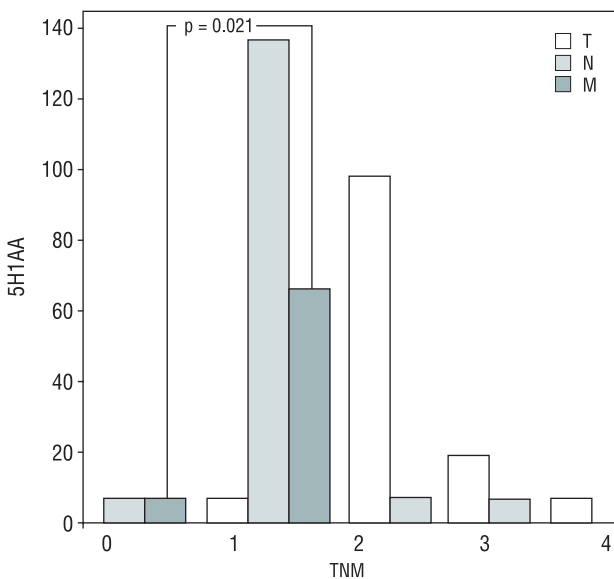


**Figure 5.** 5HIAA levels [mg/24 h] according to the TNM classification in patients with carcinoid tumours of the lung

**Rycina 5.** Stężenia kwasu 5HIO [mg/24 h] w zależności od stopnia zaawansowania według skali TNM u chorych z rakowiakami płuc

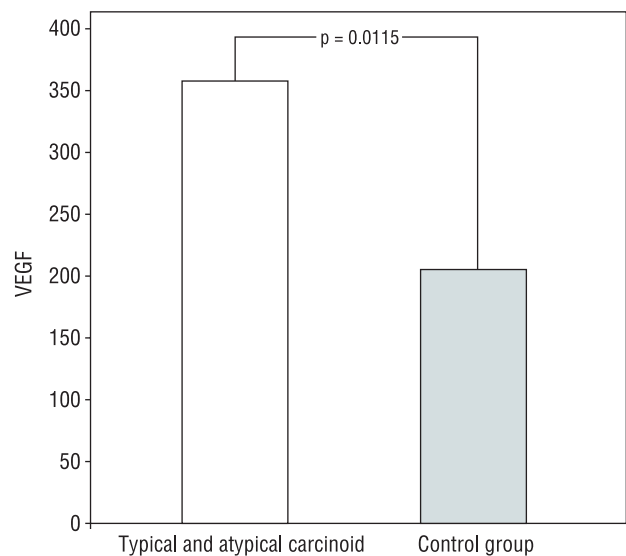


**Figure 6.** Levels of VEGF (pg/mL) in patients with carcinoid tumours of the lung and in the control group

**Rycina 6.** Stężenia VEGF [pg/ml] u chorych z rakowiakami płuc oraz w grupie kontrolnej

were no significant differences according to the TNM classification.

Assessment of VEGFR expression revealed that patients with neuroendocrine tumours of the lung showed higher expression of VEGFR1 than controls ( $p = 0.002$ ). VEGFR1 levels were higher in the group of the most advanced tumours according to the TNM

classification, taking into account the tumour size, nodal invasion and presence of distant metastases (Fig. 7). No such correlations were observed for VEGFR2.

HGF levels (mean  $\pm$  SD) were significantly higher in patients with carcinoid tumours than in the control group ( $1,297.60 \pm 362.19$  pg/mL *v.*  $996.04 \pm 365.85$ ;

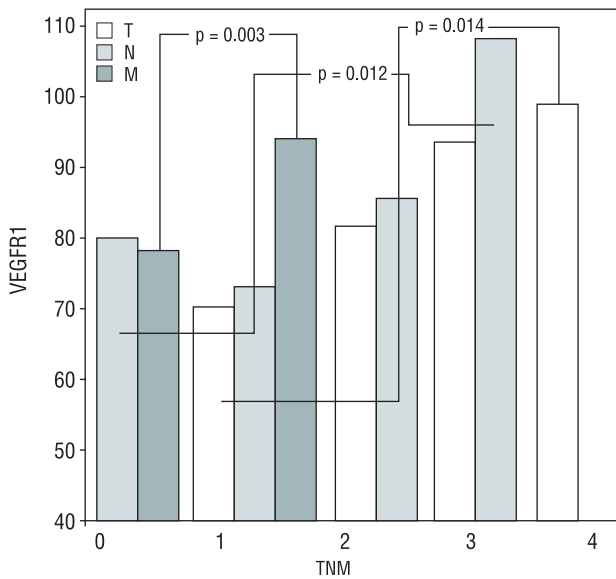


**Figure 7.** Dependence between VEGFR1 expression [pg/mL] and the TNM classification in patients with bronchopulmonary carcinoid tumours

**Rycina 7.** Zależność ekspresji receptorów VEGFR1 [pg/ml] od stopnia zaawansowania w skali TNM w nowotworach neuroendokrynnych płuc

$p = 0.001$ ). HGF levels were also significantly higher in patients with atypical versus typical carcinoid tumours ( $p = 0.046$ ) (Fig. 8). There was no correlation between HGF levels and TNM stage.

## Discussion

Chromogranin A and serotonin are markers used in the laboratory evaluation of neuroendocrine tumours, although, as shown in other studies and confirmed in ours, their levels in bronchopulmonary neuroendocrine tumours may be within reference ranges or be slightly elevated before distant metastases appear (Fig. 3 and 4). CgA and serotonin levels were within reference ranges in Group 1 patients (none of whom had distant metastases), while patients in Group 2 had considerably elevated CgA levels (nearly 74% of these patients had distant metastases).

According to the available literature, 5HIAA levels are within reference ranges in patients with BP NET due to the lack of the enzyme aromatic amino acid decarboxylase, which we managed to confirm in the group of patients with typical bronchopulmonary carcinoid tumours. The high 5HIAA levels in the group of patients with atypical carcinoid tumours might be explained by the presence of metastases in the majority of these patients, with the metastases mostly involving the liver, where the enzyme necessary for serotonin metabolism is present (Table I). The absence of correlation between

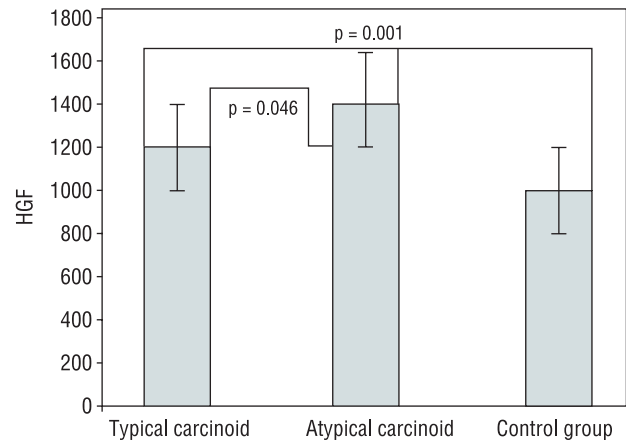


**Figure 8.** Levels of HGF [pg/mL] in the two study patient groups (typical and atypical carcinoid tumours of the lung) and in the control group

**Rycina 8.** Stężenia HGF [pg/ml] w dwóch grupach badanych (rakowiak typowy i atypowy) oraz w grupie kontrolnej

tumour size or nodal involvement and 5HIAA levels and the presence of a correlation between the presence of distant metastases and 5HIAA levels observed in our study confirms this finding (Fig. 5). These observations do suggest a role for these markers in the diagnosis of BP NET despite the many conflicting literature reports on their usefulness in these tumours.

Previous studies have shown that serum levels of VEGF and VEGFR correlate with the aggressiveness of tumours of various organs and targeted therapies that affect angiogenesis and target VEGF, among other factors, raising significant hopes among biologists, oncologists and chemotherapists [11–15].

Our study showed significantly higher serum levels of VEGF in patients with BP NET compared to the control group, which may suggest the potential usefulness of VEGF in the diagnosis, and a potential use of antiangiogenic agents in the treatment of these patients [16–20]. We did not observe any differences in VEGF levels relative to the primary tumour size, presence of distant metastases, or the histologic type (Fig. 6) and therefore could not confirm their usefulness as a prognostic factor. We did, however, obtain promising results when we evaluated VEGFR-1 levels. We observed significantly higher levels in patients versus controls, a close correlation between elevated levels and: primary tumour size, development of nodal involvement and development of distant metastases (Fig. 7), which — in addition to use in the diagnosis and treatment — seems to be an important prognostic factor, which obviously needs to be confirmed in multicentre randomised studies.

The available literature provides data on the significance of HGF in non-neuroendocrine small-cell and non-

small-cell lung carcinomas in the diagnosis, prediction of disease progression and assessment of response to drug treatment [16–18]. Based on the results of our study, where HGF levels were significantly higher in BP NET patients than in controls, it may be concluded that the histological type of the tumour (typical versus atypical carcinoid tumour) plays a significant role, while no correlation has been demonstrated between HGF levels and the TNM classification. It is worth noting that HGF levels were determined in serum rather than tissue samples, which might have affected the determination results in patients in various stages of the underlying illness.

It would be valuable to continue this study in a larger number of patients, as it would allow us to investigate the biology of tumours in greater detail, including the role of growth factors. This would, in turn, enable us to make better use of them in diagnostic evaluation.

In conclusion, our study has shown a potential usefulness of determining the levels of specific markers (serotonin, 5HIAA) and non-specific markers (CgA) in the diagnosis and in the evaluation for distant metastases in bronchopulmonary carcinoid tumours, particularly in atypical tumours. We see a potential role for the selected growth factors, VEGF and HGF, and of the VEGFR1 in the clinical diagnosis of these tumours, while the assessment of VEGFR-1 expression may be useful in tumour staging.

## References

- Corrin B, Nicholson AG. Pathology of the lungs. Churchill Livingstone 2006: 1–35: 527–608.
- Lim E., Goldstraw P, Nicholson A.G. i wsp. Proceedings of the IASLC International Workshop on Advances in Pulmonary Neuroendocrine Tumors 2007. *J. Thorac Oncol* 2008; 3: 1194–1201.
- Warren W.H., Welker M., Gattuso P. Well-differentiated neuroendocrine carcinomas: the spectrum of histologic subtypes and various clinical behaviors. *Semin Thorac Cardiovasc Surg* 2006; 18: 199–205.
- Morandi U, Casali C, Rossi G. Bronchial typical carcinoid tumors. *Semin Thorac Cardiovasc Surg* 2006; 18: 191–198.
- Travis WD, Brambilla E, Muller-Hermelink HG. Pathology and genetics: tumours of the lung, pleura, thymus and heart. IARC Press, Lyon 2004.
- Prager GW, Poettler M. Angiogenesis in cancer. Basic mechanisms and therapeutic advances. *Hamostaseologie* 2012; 32: 105–114.
- Cecchi F, Rabe DC, Bottaro DP. Targeting the HGF/Met signalling pathway in cancer. *Eur J Cancer*. 2010; 46: 1260–1270.
- Gumustekin M, Kargi A, Bulut G et al. HGF/c-Met Overexpressions, but not Met Mutation, Correlates with Progression of Non-small Cell Lung Cancer. *Pathol Oncol Res* 2012; 18: 209–218.
- Korobko IV, Zinov'eva MV, Allakhverdiev AK et al. c-Met and HGF expression in non-small-cell lung carcinomas. *Mol Gen Mikrobiol Virusol* 2007; 2: 18–21.
- William D Travis. Reporting lung cancer pathology specimens. Impact of the anticipated 7th Edition TNM Classification based on recommendations of the IASLC Staging Committee. *Histopathology* 2009; 54: 3–11.
- Bich Trinh X, van Dam PA, Vermeulen PB et al. VEGF-A-independent and angiogenesis-dependent tumour growth in patients with metastatic breast cancer. *Clin Transl Oncol* 2011; 13: 805–808.
- Pircher A, Hilbe W, Heidegger I et al. Biomarkers in tumor angiogenesis and anti-angiogenic therapy. *Int J Mol Sci* 2011; 12: 7077–7099.
- Kajdaniuk D, Marek B, Foltyn W et al. Vascular endothelial growth factor (VEGF) — part 2: in endocrinology and oncology. *Endokrynol Pol* 2011; 62: 456–64.
- Zhao S, Ma D, Dai H i wsp. Biologically inhibitory effects of VEGF siRNA on endometrial carcinoma cells. *Arch Gynecol Obstet* 2011; 284: 1533–1541.
- Blakely C, Jahan T. Emerging antiangiogenic therapies for non-small-cell lung cancer. *Expert Rev Anticancer Ther* 2011; 11: 1607–1618.
- Han JY, Kim JY, Lee SH et al. Association between plasma hepatocyte growth factor and gefitinib resistance in patients with advanced non-small cell lung cancer. *Lung Cancer* 2011; 74: 293–299.
- Ma PC, Tretiakova MS, Nallasura V, Jagadeeswaran R et al. Downstream signalling and specific inhibition of c-MET/HGF pathway in small cell lung cancer: implications for tumour invasion. *Br J Cancer* 2007; 97: 368–377.
- Ma PC, Blaszkowsky L, Bharti A et al. Circulating tumor cells and serum tumor biomarkers in small cell lung cancer. *Anticancer Res* 2003; 23: 49–62.
- Kajdaniuk D, Marek B, Foltyn W et al. Vascular endothelial growth factor (VEGF) — part 1: in physiology and pathophysiology. *Endokrynol Pol* 2011; 62: 444–455.
- Wiedenmann B, Pavel M, Kos-Kudla B. From targets to treatments: a review of molecular targets in pancreatic neuroendocrine tumors. *Neuroendocrinology* 2011; 94: 177–190.

# Axitinib—a selective inhibitor of the vascular endothelial growth factor (VEGF) receptor

Ronan J. Kelly · Olivier Rixe

Received: 25 March 2009 / Accepted: 16 October 2009 / Published online: 30 October 2009  
© Springer-Verlag 2009

**Abstract** An improved understanding of the molecular biology involved in many solid tumors has led to the development of novel targeted agents. Axitinib is a potent and selective inhibitor of vascular endothelial growth factor (VEGF) receptor tyrosine kinases 1, 2, and 3. This review presents preclinical and clinical data available for axitinib, including findings from key phase II clinical trials in a wide variety of tumors including melanomas and renal, pancreatic, thyroid, breast, lung, and colorectal carcinomas. The differences between axitinib and other VEGFR inhibitors are explored and details of the possible use of blood pressure elevation and erythropoietin blood levels as predictive markers of VEGF/VEGFR pathway inhibition are outlined. Ongoing Phase III studies in pancreatic and metastatic renal cell carcinoma should help to determine the optimum utilization of these agents at the appropriate stage of disease.

**Keywords** Axitinib · VEGF receptor inhibitor · Renal cell carcinoma · Pancreatic carcinoma · Tyrosine kinase inhibitor

## Introduction

Angiogenesis is a multistep process that is tightly controlled by balancing endogenous positive and negative regulators that emanate from cancer cells, endothelial cells, stromal cells, blood and the extracellular matrix (ECM) [1]. Vascular endothelial growth factor (VEGF) is a potent endothelial cell mitogen, which is normally seen in certain physiologic situations (fetal development, menstruation, wound healing). Overexpression of VEGF has been associated with tumor progression and poor prognosis in several tumor types including renal cell carcinoma, colorectal carcinoma, gastric carcinoma, pancreatic carcinoma, breast cancer, prostate cancer, lung cancer, and melanoma [2, 3]. The increasingly recognized importance of VEGF signaling in promoting tumor angiogenesis has led to the development and clinical validation of several agents that selectively target this pathway in patients with advanced-stage malignancies. These include neutralizing anti-VEGF monoclonal antibodies, soluble VEGF receptors, and small-molecule inhibitors of VEGF receptor function, administered either as monotherapy or in combination with chemotherapy.

The VEGF gene family consists of four known VEGFs (VEGF-A to -C and placental growth factor [PLGF]) and four platelet-derived growth factors (PDGF-A to -D) [4]. These factors function primarily in a paracrine manner to promote angiogenesis and vasculogenesis [5]. VEGF and PDGF peptides circulate as homo- or heterodimers and regulate cellular processes such as proliferation and migration via binding to tyrosine kinase (TK) receptors. These receptors are expressed on the surface of target cells [6], and are VEGFR-1 (also known as FMS-like tyrosine kinase [FLT]1), VEGFR-2 (also known as kinase insert domain-containing receptor [KDR]/foetal liver kinase (Flk)-1), and

---

R. J. Kelly  
National Cancer Institute, Medical Oncology Branch,  
Center for Cancer Research,  
Bethesda, MD 20892, USA

O. Rixe (✉)  
Division of Hematology/Oncology,  
University of Cincinnati College of Medicine,  
231 Albert Sabin Way ML 0562,  
Cincinnati, OH 45267-0562, USA  
e-mail: olivier.rix@uc.edu

VEGFR-3 (also known as FLT4) [7]. The interaction between the ligand and the receptor triggers autophosphorylation and initiates a series of downstream signaling processes that promotes the proliferation, migration, and survival of endothelial cells. In tumor vascularization, these processes form the framework of immature new neoplastic vessels [3]. VEGFR-2 is the predominant VEGF isoform responsible for the majority of downstream effects.

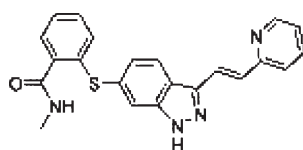
VEGFR-2 is a type III transmembrane kinase receptor, first isolated in 1991 by Terman et al [8]. The *VEGFR-2* gene is located on chromosomes 4q11–q12 and encodes a full-length receptor of 1356 amino acids [9]. It belongs with the 7-Ig/5-Ig protein tyrosine kinase superfamily, and is thus closely related to the platelet-derived growth factor receptors (PDGFRs), fms receptor and c-Kit receptor [10]. Within the cell, the VEGFR-2 protein is translated as a 150 kDa protein without significant glycosylation. It is then processed, by a series of glycosylations, to a mature 230 kDa form that is expressed on the cell surface [11]. VEGF-A binds to the second and third extracellular Ig-like domains of VEGFR-2. Ligand binding induces receptor dimerisation and autophosphorylation. VEGFR-2 is the principal mediator of several physiological and pathological effects of VEGF-A on endothelial cells including enhanced proliferation, migration, survival and permeability. Studies involving anti-VEGF receptor therapies have demonstrated that these agents can potently inhibit angiogenesis and tumor growth in preclinical models [3].

Axitinib is an indazole derivative and is an oral and selective inhibitor of receptor tyrosine kinases with picomolar potency against VEGFR-1, -2 and -3 and nanomolar potency against PDGFR-beta [12]. In recent years axitinib has been investigated both as a single agent and in combination with different chemotherapeutic backbones in many phase II clinical trials and phase III studies are ongoing.

### Molecular structure

The molecular formula for axitinib is  $C_{22}H_{18}N_4OS$  and its structure is shown in Fig. 1. The binding of axitinib to the kinase domain of VEGF receptors stabilizes an inactive conformation of the kinase, thus inhibiting signal transduction by VEGF. In the x-ray crystal structure of the complex with VEGFR-2, axitinib fits tightly into a tunnel in the interior of the kinase and forms many stabilizing interactions.

**Fig. 1** Structure of axitinib



### In vivo/in vitro pre-clinical data

Axitinib blocks VEGF-mediated endothelial cell adhesion and migration on extracellular matrix proteins and induces early endothelial apoptosis. It has also been shown to produce rapid and potent inhibition of endothelial nitric oxide (eNOS), protein kinase B (Akt), and mitogen activated protein kinases (ERK 1/2) phosphorylation at concentrations that correlated with its potency for VEGFRs [13].

#### In vitro pre-clinical data

Preclinical data involving axitinib showed that at subnanomolar concentrations it had a high specificity and potency for recombinant kinases of the VEGF receptor, PDGFR- $\beta$ , and c-Kit. Axitinib has demonstrated additive or synergistic antitumor activity with docetaxel in models of murine lung cancer and human breast cancer, with carboplatin in a model of ovarian cancer, and with gemcitabine in a model of human pancreatic cancer, which resulted in an improvement in antitumor efficacy ranging from efficacy enhancement to an additive effect and synergism [12]. In Vitro metabolism studies show that axitinib metabolism in the liver is predominantly mediated by CYP3A4, and to a lesser extent by CYP1A2 [12]. The pharmacokinetics of axitinib may be affected by CYP3A4 inhibitors and inducers. Systemic exposure of axitinib may be affected by drugs that are substrates or inhibitors of P-glycoprotein.

#### In vivo pre-clinical data

In vivo, dynamic contrast-enhanced magnetic resonance imaging (DCE-MRI) studies showed that axitinib treatment decreases the overall tumor blood flow/permeability at an early stage after initiation of treatment, with a maximum reduction in tumor endothelial transfer constant ( $K^{trans}$ )—an indicator of vascular leakage to the extracellular space—observed on day 7 after dosing. The studies also showed that the changes in vascular  $K^{trans}$  correlated with decreased microvessel density, cellular viability, and tumor growth [14]. The antiangiogenesis activity of axitinib was also assessed by measuring tumor microvessel density (MVD, measured by CD-31 staining) after either acute or prolonged treatment in xenograft tumor models. Based on these observations, a continuous daily dosing of axitinib is considered optimal for antiangiogenesis [13].

#### Phase I trial/pharmacokinetic data

In the phase I, multicenter clinical trial of axitinib in patients ( $n = 36$ ) with refractory tumors, the maximum tolerated dose for further phase II clinical trials was

established as 5 mg bid daily [12]. This trial demonstrated durable response in two patients, one with renal cell carcinoma and the second with adenoid cystic carcinoma. Two non-small cell lung cancer (NSCLC) patients exhibited lung cavitations indicating an antiangiogenic effect. Pharmacokinetic data indicated that axitinib in the fed state is absorbed rapidly, with peak plasma concentrations occurring within 2 to 6 h after dosing [12]. The rate and extent of absorption of the drug was higher in the overnight fasted state with peak concentrations occurring 1 to 2 h after dosing, indicating a significant food effect [12]. However, further studies have confirmed that overnight fasting is not required and ongoing studies recommend subjects take axitinib with food. The plasma elimination half-life ranges between 2 and 5 h [13]. Studies have demonstrated that the effect of pH on absorption of axitinib was not considered to be clinically significant, but in patients taking axitinib, antacids or proton pump inhibitors should be administered at times other than 2 h before and 2 h after drug dosing [12].

## Phase II studies

### Renal cell carcinoma

In the last 10 years many new promising treatments and investigational drugs inhibiting angiogenesis have been evaluated in renal cell carcinoma (RCC). Two pivotal studies investigating patients with cytokine-refractory metastatic RCC, have described a median progression-free survival of 4.8 months in patients treated with high dose bevacizumab [15] and 5.5 months in those treated with sorafenib [16], with objective responses of 10% for both drugs. A third drug sunitinib has shown an objective response rate of 40% in patients who have failed cytokine treatment [17], and a high objective response (31%) and longer progression-free survival compared with interferon alfa in previously untreated patients [18].

Sunitinib and sorafenib have a broad multi-targeted approach and simultaneously inhibit numerous tyrosine kinase receptors, including VEGF receptor, the platelet-derived growth factor receptor, and the tyrosine kinases c-KIT, and FLT3. It was hoped that the high specificity and picomolar potency of axitinib, against the VEGF receptors 1, 2, and 3, which play an important role in renal cell cancer pathogenesis, would account for significant anti-tumor activity.

The efficacy of axitinib (5 mg bid) in patients ( $n = 52$ ) with metastatic RCC whose disease was refractory to cytokine treatment was demonstrated in a phase II, non-randomized clinical trial [19]. Patients were treated in 28-day treatment cycles until disease progression or

unacceptable toxicity. Analysis of results demonstrated two complete (see Fig. 2) and 21 partial responses, for an objective response rate of 44.2% (95% CI 30.5–58.7). Median response duration was 23.0 months. Twenty-two patients showed stable disease lasting for longer than 8 weeks, including 13 patients with stable disease for at least 24 weeks. Stable disease was noted in the only patient with papillary histology, who had a 27.3% decrease in tumor diameter (as defined by the response evaluation criteria in solid tumors [RECIST]) on day 71. Median time to progression was 15.7 months and median overall survival was 29.9 months. In ancillary studies in 13 of the patients (7 responders and 6 non-responders), decreased tumor perfusion was observed in patients who responded to treatment. Decreased perfusion correlated with improved response in 4 out of 6 patients with stable or progressive disease [20]. The results obtained from this phase II study indicate that axitinib is a potent agent for the treatment of metastatic renal cell carcinoma and to date is the only VEGFR tyrosine kinase inhibitor (TKI) to show complete and durable responses in this disease.

A phase II non-randomized, open-label, single-group clinical trial evaluated axitinib (5 mg po, twice daily) in patients ( $n = 62$ ) with advanced and refractory RCC who had also failed sorafenib-based therapy [21]. A partial response was observed in 13 patients (21%), stable disease in 21 patients (34%), and progressive disease in 16 patients (26%). Tumor shrinkage to some extent was experienced by 57% of patients. A preliminary analysis after a median follow-up of 8.1 months indicated an overall median progression-free survival of 7.4 months. These preliminary results suggest the absence of cross-resistance between axitinib and sorafenib for a limited but significant subset of patients.

### Pancreatic cancer

The overall effect of systemic therapy in advanced pancreatic cancer is modest [22]. Gemcitabine has been the standard of care for many years but the addition of targeted agents to this cytotoxic drug has been disappointing [23, 24]. VEGF is recognized as a promising target in this tumor type as it has a role in promoting tumor growth in pancreatic ductal adenocarcinoma [25]. High VEGF expression is associated with increased microvessel density [26], and is a predictor of early tumor recurrence after curative resection and of poor outcome [27]. The addition of bevacizumab to gemcitabine failed to show a survival advantage compared with gemcitabine alone in advanced pancreatic cancer [28].

A phase II, randomized, open-label clinical trial was conducted to determine the relative survival rates of patients ( $n = 103$ ) with metastatic pancreatic cancer receiving either a combination of axitinib and gemcitabine or gemcitabine



## Thyroid cancer

The treatment of thyroid cancer has benefited from a growing understanding of the molecular biology of this disease. A number of targeted agents have been investigated in different types of thyroid cancer. Anaplastic thyroid cancer is relatively rare but it is typically unresectable at presentation and is resistant to radioactive iodine (RAI) and chemotherapy. Medullary thyroid cancer is derived from parafollicular C cells and it has a worse prognosis than the more common papillary thyroid tumors. RAI does not have a role in the management of this cancer [32]. Many advanced thyroid cancers will eventually develop lack of iodine avidity, making chemotherapy the only viable option for systemic treatment. Doxorubicin is an approved therapy in incurable thyroid cancer based on response rates of 10% to 37% [33, 34].

Thyroid cancers are highly vascular and have elevated levels of VEGF compared with normal thyroid tissue [35]. Microvessel density is also higher in papillary thyroid cancer than in normal thyroid tissue [36]. In human thyroid tumor specimens, VEGF levels are correlated with stage, large tumor size, nodal involvement, extra-thyroidal invasion, and distant metastasis [37]. These observations support evaluating axitinib in this disease.

In a phase II multicenter clinical trial in patients ( $n = 60$ ) with measurable metastatic or unresectable locally advanced thyroid cancer that was refractory to or unsuitable for  $^{131}$ iodine treatment, patients received axitinib at an oral dose of 5 mg twice daily [38]. Partial responses were observed in 18 patients, yielding an objective response rate (ORR) of 30% (95% CI, 18.9–43.2). Stable disease lasting  $\geq 16$  weeks was reported in another 23 patients (38%). Objective responses were noted in all histological subtypes. Median PFS was 18.1 months (95% CI, 12.1 to not estimable). Axitinib was generally well tolerated with the most common grade  $\geq 3$  treatment-related adverse event being hypertension ( $n = 7$ ; 12%). Eight patients (13%) discontinued treatment because of adverse events. Axitinib selectively decreased sVEGFR-2 and sVEGFR-3 plasma concentrations versus sKIT, demonstrating its targeting of VEGFR.

## Other solid tumors

Axitinib has been evaluated in other solid tumors including non-small cell lung cancer (NSCLC), melanoma, and advanced colorectal cancer. A phase II, non-randomized, open-label, uncontrolled clinical trial of axitinib was conducted in patients ( $n = 32$ ) with metastatic NSCLC or advanced NSCLC with malignant pleural effusion [39]. Patients were orally administered axitinib (5 mg bid), with doses up to 10 mg permitted, until unacceptable toxicity or disease progression. Three responses were confirmed, with

a median duration of response of 9.4 months. There were ten patients with stable disease and nine with progressive disease. Median survival and progression-free survival were 12.5 and 5.8 months, respectively. Treatment was discontinued for 26 patients mostly due to a lack of efficacy.

A phase II, single-arm, multi-center, open-label, clinical trial in patients ( $n = 32$ ) with metastatic melanoma was presented by Fruehauf et al at the American Society of Clinical Oncology (ASCO) 2008 annual meeting [40]. The primary objective of this study is ORR by RECIST. An investigator report shows an ORR of 19% (95% CI: 7%–36%) including one durable complete response. Median duration of response was 7.9 months, median progression-free survival was 2.3 months (95% CI 1.8–5.7), and median overall survival for all patients was 6.8 months (95% CI 5.2–10.4). These results compare favorably with other agents developed in the same indication, and support further evaluations.

Two phase II, multicenter, non-randomized, open-label clinical trials to study the effect of axitinib in combination with bevacizumab and standard chemotherapy regimens have been initiated in patients with metastatic colorectal cancer. In the first trial, 123 patients receive FOLFOX, and either axitinib (5 mg bid), bevacizumab (5 mg/kg every 2 weeks), or axitinib (5 mg bid) plus bevacizumab (2 mg/kg every 2 weeks) [41]. This trial is currently ongoing. In a second, ongoing study, patients who have previously failed treatment with irinotecan- or oxaliplatin-based therapy were to be administered axitinib in conjunction with either FOLFOX or FOLFIRI or bevacizumab with FOLFIRI or FOLFOX [42]. See Table 1.

## Phase III studies

Axitinib has now entered phase III testing in two tumor types. A phase III, randomized, double blind, active-controlled clinical trial has been initiated to compare treatment with axitinib plus gemcitabine with gemcitabine plus placebo, in patients ( $n = 596$ ) with advanced pancreatic cancer. Patients receive gemcitabine (1,000 mg/m<sup>2</sup> iv) on days 1, 8 and 15 of every 4 weeks, either with or without oral axitinib (5 mg bid), until disease progression or unacceptable toxicity. The primary endpoint in this trial is overall survival [43].

In metastatic renal cell carcinoma a phase III trial investigating axitinib as second-line therapy after failing one prior systemic first-line regimen has commenced recruiting (Axis Trial) [44].

## Toxicity

For single-agent axitinib the most common adverse events reported are hypertension, fatigue, and gastrointestinal

**Table 1** Summary of results from phase II trials

Tumor Type	Number of patients	Phase	Response Rate (%)	PFS (months)	Reference
RCC Cytokine-refractory	52	II	44.2	15.7	[19]
Sorafenib-refractory	62	II	21%	7.4	[21]
Pancreatic	103	II	7	4.2	[29]
Breast	168	II	40	8.2	[30, 31]
Thyroid	60	II	30	18.1	[38]
NSCLC	32	II	9	5.8	[39]
Melanoma	32	II	19	2.3	[40]

toxicity. These side-effects are considered manageable and are an expected class effect.

In phase I studies, the dose-limiting toxicity (DLT) was hypertension, which was responsive to medications and was reversible with drug cessation. None of the patients receiving 5 mg bid had hypertension that could not be managed with standard antihypertensive medications. In ongoing clinical programs, subjects receive a starting dose of 5 mg bid with home monitoring of blood pressure (before each dose) and in-clinic monitoring at the time of scheduled visits. Those subjects who tolerate axitinib with no adverse events above Common Terminology Criteria for Adverse Events (CTCAE) grade 2 for 2 consecutive weeks increase their dose step-wise to 7 mg bid and then to 10 mg bid, unless blood pressure is >150/90 mm Hg or the subject is receiving antihypertensive medication. Bleeding events that have occurred among the phase I studies have included 1 fatal case of hemoptysis in a subject with lung adenocarcinoma, epistaxis, breast hemorrhage, hemochezia, rectal hemorrhage, and vaginal hemorrhage. Asymptomatic proteinuria was seen in early studies and consequently, the phase I protocol was amended to exclude subjects with proteinuria at baseline (>500 mg/24 h) and to require dose modifications of axitinib on the basis of proteinuria. The maximum tolerated dose was defined as a 5 mg bid starting dose.

In the phase II study conducted in metastatic renal cell carcinoma [19], axitinib was given as a single agent and toxicities are reported in Table 2. The most commonly reported treatment related adverse events of severity grade 3 or higher were hypertension (14%), fatigue (10%), diarrhea (4%), palmar plantar erythrodysesthesia syndrome (3%), hypertension aggravated (2%), and stomatitis (2%). Laboratory abnormalities for subjects with solid tumors who received single-agent axitinib were grade 3/4 hyperglycemia in 5.5%, hyponatremia or elevation in creatinine in 4.6%, elevations in AST in 4.0%, and proteinuria in 0.8%. Hematological abnormalities were grade 3 or 4 neutropenia in 0.8% and thrombocytopenia in 1.0%. Grade 3/4 lymphopenia was reported in 19%. Preliminary evidence suggests that axitinib is safe and has a side-effect profile that gives an advantage over other

antiangiogenic drugs. The continuous administration and the constant dose appear to be safe, and compatible with long-term administration. In the phase II RCC study, patients have received axitinib for more than 3 years, with the absence of cumulative toxicity [19].

### Drug interactions

The metabolism of axitinib is primarily mediated by the CYP3A4 drug-metabolizing enzyme, and to a lesser extent by CYP1A2 as determined by in vitro studies with human liver microsomes [12]. There is a mechanistic potential for altered concentrations of axitinib in plasma in the presence of drugs that are CYP3A4 inhibitors (e.g., ketoconazole) or CYP3A4 inducers (e.g., rifampin).

### Comparison of axitinib to other VEGFR inhibitors

Axitinib has been classed as a second-generation VEGFR inhibitor and is a selective inhibitor of VEGFR-1, -2 and -3. Sunitinib and sorafenib are both Food and Drug Administration (FDA)-approved agents in multiple tumor types and their spectrum of targets is wider than that of axitinib. The activity of these agents is related to both the structure of the molecule and the spectrum of kinase inhibition [45]. Sorafenib was initially developed as a Raf kinase inhibitor, but it is now recognized as an active multikinase inhibitor targeting VEGFR-1, -2, and -3; platelet-derived growth factor receptor  $\beta$  (PDGFR $\beta$ ); FMS-like tyrosine kinase 3 (Flt-3); c-Kit protein (c-Kit); and RET receptor tyrosine kinases [16]. Sunitinib is an inhibitor of VEGFR, PDGFR, Flt3, and c-KIT [18].

### Blood pressure elevation as a predictive marker of VEGF pathway inhibition

Hypertension is commonly observed during treatment with axitinib and other VEGFR inhibitors. Increases in blood

**Table 2** Treatment-related adverse events occurring in at least 10% of patients ( $n = 52$ ) [19]

	All grades (number of patients)	Grades 3–4, (number of patients)
Diarrhea	31	5
Hypertension	30	8
Fatigue	27	4
Nausea	23	0
Hoarseness	19	0
Anorexia	18	1
Dry skin	17	0
Weight loss	14	0
Dyspepsia	12	0
Vomiting NOS	11	0
Limb pain	10	2
Stomatitis	9	1
Headache	8	0
Dry mouth	8	0
Nail disorder	7	0
Arthralgia	7	1
Constipation	7	0
Abdominal pain NOS	6	0
Rash	6	0
Dysgeusia	6	0
Myalgia	6	1

pressure have been proposed as an efficacy marker for VEGF pathway inhibitors. Post-hoc, combined analyses of data from 2 phase II studies of axitinib in metastatic RCC (mRCC) were performed to explore the possible association between diastolic blood pressure  $\geq 90$  mm Hg and efficacy endpoints [46]. The 2 studies included 111 patients (59 and 52 with sorafenib and cytokine refractory mRCC, respectively) evaluable for changes in diastolic blood pressure (BP). Seventy patients (63.1%) had  $\geq 1$  diastolic BP measurement  $\geq 90$  mm Hg. The objective response rate (ORR) was 48.4% for patients with diastolic BP measurement  $\geq 90$  mm Hg vs 12.2% for patients without. Median overall survival (30.0 vs 9.8 months;  $p < 0.0001$ ) and progression-free survival (17.6 vs 7.1 months;  $p < 0.0001$ ) were longer in patients with diastolic BP measurement  $\geq 90$  mm Hg than in those without. The frequencies of most commonly reported adverse events were greater in patients with diastolic BP measurement  $\geq 90$  mm Hg than in those without, including fatigue (80.0% vs 41.5%), diarrhea (72.9% vs 41.5%), hypertension reported as an adverse event (67.1% vs 24.4%), nausea (52.9% vs 43.9%), and anorexia (51.4% vs 34.1%). Further studies are required to prospectively validate the occurrence of diastolic BP measurement  $\geq 90$  mm Hg as a biomarker of axitinib activity. A post-hoc exploratory analysis in the phase II pancreatic study [29] also showed an improvement in overall survival in patients with at least one diastolic blood pressure measurement of 90 mm Hg or more during treatment.

Dose-escalation in pancreatic trials, adapted to the blood pressure level is promising but remains to be validated.

#### Erythropoietin blood level as a predictive marker of VEGF/VEGFR modulation

Drug-induced erythrocytosis has been reported with the use of the tyrosine kinase inhibitors sunitinib and sorafenib [47]. Studies showing hepatic erythropoietin (EPO) synthesis related to VEGF blockage could explain this iatrogenic polycythemia [48]. It has been proposed that axitinib can lead to VEGF starvation in organs such as the liver through VEGFR-2 blockade which results in increased hepatic EPO production. An alternative pathway involving axitinib and hypoxia-inducible factor (HIF) has been suggested. The HIF pathway induces nitric oxide release leading to a modification of cutaneous vascular flow and increased systemic EPO expression [49]. The utility of using EPO blood levels as a marker of VEGF/VEGFR inhibition requires further investigation.

#### Conclusion

The utilization of the molecular differences displayed between the vasculature of normal tissue and tumor tissue may herald the beginning of a new frontier. The “vascular

zip code” has been used to describe the unique expression of cell-surface molecules found in each vascular bed. The characterization of tumor blood vessels includes selective over-expression of a heterogeneous group of proteins (proteases, integrins, growth factor receptors and proteoglycans). Even in a situation of absolute specificity, antiangiogenic agents would have limited efficacy. This effect was predicted at an early stage when it was realized that antiangiogenesis would merely arrest tumor growth, but would not generally eliminate all the tumor cells. The limited percentage of complete remissions achieved by antiangiogenics in the clinic when used as single-agent therapies have confirmed this observation.

Axitinib does however present original characteristics and advantages in comparison with the other antiangiogenic compounds: a favorable profile of toxicity with the absence of cumulative dose-limiting toxicity, a large spectrum of activity, a constant and manageable schedule of administration, and the occurrence of complete responses in renal cell carcinoma with the emergence of long-term survivors.

Cross-resistance between antiangiogenic compounds needs to be addressed in the future. Preliminary preclinical studies tried to demonstrate the putative mechanisms involved in acquired resistance to antivascular agents. They underline the heterogeneity of the endothelial cell, angiogenic factors and tumor cells, the role of the microenvironment and the potential for angiogeno-independence. Based on the study in metastatic RCC [19], axitinib has demonstrated a different spectrum of activity from other VEGFR inhibitors, suggesting a potential absence of cross-resistance in a subset of patients.

The definitive role of axitinib for the treatment of solid tumors will be determined in the two ongoing phase III studies conducted in pancreatic and renal carcinoma. The pursuit of reliable predictive factors demonstrating VEGFR inhibitor activity is continuing. Biomarkers in addition to clinical parameters (such as blood pressure or erythropoietin level) are currently being evaluated with promising preliminary results.

**Conflict of interest statement** No funds were received in support of this review and no benefits in any form have been or will be received from a commercial party related to the subject of this article.

## References

- Carmeliet P, Jain RK (2000) Angiogenesis in cancer and other diseases. *Nature* 407:249–257
- Rini BI, Small EJ (2005) Biology and clinical development of vascular endothelial growth factor-targeted therapy in renal cell carcinoma. *J Clin Oncol* 23:1028–1043
- Hicklin DJ, Ellis LM (2005) Role of the vascular endothelial growth factor pathway in tumor growth and angiogenesis. *J Clin Oncol* 23:1011–1027
- Ferrara N, Gerber HP, LeCouter J (2003) The biology of VEGF and its receptors. *Nat Med* 9:669–676
- Leung DW, Cachianes G, Kuang WJ, Goeddel DV, Ferrara N (1989) Vascular endothelial growth factor is a secreted angiogenic mitogen. *Science* 246:1306–1309
- Cross MJ, Dixelius J, Matsumoto T, Claesson-Welsh L (2003) VEGF-receptor signal transduction. *Trends Biochem Sci* 28:488–494
- Nilsson M, Heymach JV (2006) Vascular endothelial growth factor (VEGF) pathway. *J Thorac Oncol* 1:768–770
- Terman BI, Carrion ME, Kovacs E, Rasmussen BA, Eddy RL, Shows TB (1991) Identification of a new endothelial cell growth factor receptor tyrosine kinase. *Oncogene* 6:1677–1683
- Sait SN, Dougher-Vermazen M, Shows TB, Terman BI (1995) The kinase insert domain receptor gene (KDR) has been relocated to chromosome 4q11→q12. *Cytogenet Cell Genet* 70:145–146
- Shibuya M (2002) Vascular endothelial growth factor receptor family genes: when did the three genes phylogenetically segregate? *Biol Chem* 383:1573–1579
- Takahashi T, Shibuya M (1997) The 230 kDa mature form of KDR/Flk-1 (VEGF receptor-2) activates the PLC-gamma pathway and partially induces mitotic signals in NIH3T3 fibroblasts. *Oncogene* 14:2079–2089
- Rugo HS, Herbst RS, Liu G et al (2005) Phase I trial of the oral antiangiogenesis agent AG-013736 in patients with advanced solid tumors: pharmacokinetic and clinical results. *J Clin Oncol* 23:5474–5483
- Hu-Lowe DD, Zou HY, Grazzini ML et al (2008) Nonclinical antiangiogenesis and antitumor activities of axitinib (AG-013736), an oral, potent, and selective inhibitor of vascular endothelial growth factor receptor tyrosine kinases 1, 2, 3. *Clin Cancer Res* 14:7272–7283
- Wilmes LJ, Pallavicini MG, Fleming LM et al (2007) AG-013736, a novel inhibitor of VEGF receptor tyrosine kinases, inhibits breast cancer growth and decreases vascular permeability as detected by dynamic contrast-enhanced magnetic resonance imaging. *Magn Reson Imaging* 25:319–327
- Yang JC, Haworth L, Sherry RM et al (2003) A randomized trial of bevacizumab, an anti-vascular endothelial growth factor antibody, for metastatic renal cancer. *N Engl J Med* 349:427–434
- Escudier B, Eisen T, Stadler WM et al (2007) Sorafenib in advanced clear-cell renal-cell carcinoma. *N Engl J Med* 356:125–134
- Motzer RJ, Michaelson MD, Redman BG et al (2006) Activity of SU11248, a multitargeted inhibitor of vascular endothelial growth factor receptor and platelet-derived growth factor receptor, in patients with metastatic renal cell carcinoma. *J Clin Oncol* 24:16–24
- Motzer RJ, Hutson TE, Tomczak P et al (2007) Sunitinib versus interferon alfa in metastatic renal-cell carcinoma. *N Engl J Med* 356:115–124
- Rixe O, Bukowski RM, Michaelson MD et al (2007) Axitinib treatment in patients with cytokine-refractory metastatic renal-cell cancer: a phase II study. *Lancet Oncol* 8:975–984
- Rixe O, Meric J-B, Bloch J et al (2005) Surrogate markers of activity of AG-013736, a multi-target tyrosine kinase receptor inhibitor, in metastatic renal cell cancer (RCC). *J Clin Oncol* 23:3003 (Meeting Abstracts)
- Rini BI, Wilding GT, Hudes G et al (2007) Axitinib (AG-013736; AG) in patients (pts) with metastatic renal cell cancer (RCC) refractory to sorafenib. *J Clin Oncol* 25:5032 (Meeting Abstracts)
- Burriss HA 3rd, Moore MJ, Andersen J et al (1997) Improvements in survival and clinical benefit with gemcitabine as first-line

- therapy for patients with advanced pancreas cancer: a randomized trial. *J Clin Oncol* 15:2403–2413
23. Moore MJ, Goldstein D, Hamm J et al (2007) Erlotinib plus gemcitabine compared with gemcitabine alone in patients with advanced pancreatic cancer: a phase III trial of the National Cancer Institute of Canada Clinical Trials Group. *J Clin Oncol* 25:1960–1966
  24. Philip PA, Benedetti J, Fenoglio-Preiser C et al (2007) Phase III study of gemcitabine [G] plus cetuximab [C] versus gemcitabine in patients [pts] with locally advanced or metastatic pancreatic adenocarcinoma [PC]: SWOG S0205 study. *J Clin Oncol* 25:LBA4509 (Meeting Abstracts)
  25. Korc M (2003) Pathways for aberrant angiogenesis in pancreatic cancer. *Mol Cancer* 2:8
  26. Seo Y, Baba H, Fukuda T, Takashima M, Sugimachi K (2000) High expression of vascular endothelial growth factor is associated with liver metastasis and a poor prognosis for patients with ductal pancreatic adenocarcinoma. *Cancer* 88:2239–2245
  27. Niedergethmann M, Hildenbrand R, Wostbrock B et al (2002) High expression of vascular endothelial growth factor predicts early recurrence and poor prognosis after curative resection for ductal adenocarcinoma of the pancreas. *Pancreas* 25:122–129
  28. Kindler HL, Niedzwiecki D, Hollis D et al (2007) A double-blind, placebo-controlled, randomized phase III trial of gemcitabine (G) plus bevacizumab (B) versus gemcitabine plus placebo (P) in patients (pts) with advanced pancreatic cancer (PC): A preliminary analysis of Cancer and Leukemia Group B (CALGB). *J Clin Oncol* 25:4508 (Meeting Abstracts)
  29. Spano JP, Chodkiewicz C, Maurel J et al (2008) Efficacy of gemcitabine plus axitinib compared with gemcitabine alone in patients with advanced pancreatic cancer: an open-label randomised phase II study. *Lancet* 371:2101–2108
  30. Phase II study of AG-013736 in combination with docetaxel versus docetaxel alone for patients with metastatic breast cancer. *Clinicaltrials.gov* 2006 July 25. <http://clinicaltrials.gov/ct2/show/NCT00076024>. Accessed on 15 Oct 2009
  31. Rugo HS, Stopeck A, Joy AA et al (2007) A randomized, double-blind phase II study of the oral tyrosine kinase inhibitor (TKI) axitinib (AG-013736) in combination with docetaxel (DOC) compared to DOC plus placebo (PL) in metastatic breast cancer (MBC). *J Clin Oncol* 25:1003 (Meeting Abstracts)
  32. Cupisti K, Wolf A, Raffel A et al (2007) Long-term clinical and biochemical follow-up in medullary thyroid carcinoma: a single institution's experience over 20 years. *Ann Surg* 246:815–821
  33. Gottlieb JA, Hill CS Jr (1974) Chemotherapy of thyroid cancer with adriamycin. Experience with 30 patients. *N Engl J Med* 290:193–197
  34. Shimaoka K, Schoenfeld DA, DeWys WD, Creech RH, DeConti R (1985) A randomized trial of doxorubicin versus doxorubicin plus cisplatin in patients with advanced thyroid carcinoma. *Cancer* 56:2155–2160
  35. Viglietto G, Maglione D, Rambaldi M et al (1995) Upregulation of vascular endothelial growth factor (VEGF) and downregulation of placenta growth factor (PlGF) associated with malignancy in human thyroid tumors and cell lines. *Oncogene* 11:1569–1579
  36. Kilicarslan AB, Ogus M, Arici C, Pestereli HE, Cakir M, Karpuzoglu G (2003) Clinical importance of vascular endothelial growth factor (VEGF) for papillary thyroid carcinomas. *APMIS* 111:439–443
  37. Klein M, Picard E, Vignaud JM et al (1999) Vascular endothelial growth factor gene and protein: strong expression in thyroiditis and thyroid carcinoma. *J Endocrinol* 161:41–49
  38. Cohen EE, Rosen LS, Vokes EE et al (2008) Axitinib is an active treatment for all histologic subtypes of advanced thyroid cancer: results from a phase II study. *J Clin Oncol* 26:4708–4713
  39. Schiller JH, Larson T, Ou SI et al (2007) Efficacy and safety of axitinib (AG-013736; AG) in patients (pts) with advanced non-small cell lung cancer (NSCLC): A phase II trial. *J Clin Oncol* 25:7507 (Meeting Abstracts)
  40. Fruehauf JP, Lutzky J, McDermott DF et al (2008) Axitinib (AG-013736) in patients with metastatic melanoma: a phase II study. *J Clin Oncol* 26:9006 (Meeting Abstracts)
  41. Phase II study with AG-013736 combined with chemotherapy and bevacizumab in patients with metastatic colorectal cancer. *Clinicaltrials.gov* 2008 April 17. <http://clinicaltrials.gov/ct2/show/NCT00460603>. Accessed 15 Oct 2009
  42. A study combining FOLFOX or FOLFIRI with AG-013736 or avastin in patients with metastatic colorectal cancer after failure of one first line regimen. *Clinicaltrials.gov* 2008 April 07. <http://clinicaltrials.gov/ct2/show/NCT00615056>. Accessed 15 Oct 2009
  43. Randomized study of gemcitabine plus AG-013736 versus gemcitabine for advanced pancreatic cancer. *Clinicaltrials.gov* 2007 May 07. <http://clinicaltrials.gov/ct2/show/NCT00471146>. Accessed 15 Oct 2009
  44. Axitinib as second line therapy for metastatic renal cell cancer: Axis trial. *Clinicaltrials.gov* 2009. <http://clinicaltrials.gov/ct2/show/NCT00678392>. Accessed 15 Oct 2009
  45. Karaman MW, Herrgard S, Treiber DK et al (2008) A quantitative analysis of kinase inhibitor selectivity. *Nat Biotechnol* 26:127–132
  46. Rixe O, Dutcher JP, Motzer RJ (2008) Association between diastolic blood pressure  $\geq 90$  mmHg and efficacy in patients with metastatic renal cell carcinoma receiving axitinib (AG-013736). *ESMO 2008 Meeting abstract*
  47. Alexandrescu DT, McClure R, Farzanmehr H, Dasanu CA (2008) Secondary erythrocytosis produced by the tyrosine kinase inhibitors sunitinib and sorafenib. *J Clin Oncol* 26:4047–4048
  48. Tam BY, Wei K, Rudge JS et al (2006) VEGF modulates erythropoiesis through regulation of adult hepatic erythropoietin synthesis. *Nat Med* 12:793–800
  49. Boutin AT, Weidemann A, Fu Z et al (2008) Epidermal sensing of oxygen is essential for systemic hypoxic response. *Cell* 133:223–234

## DRUG EVALUATION

For reprint orders, please contact: [reprints@futuremedicine.com](mailto:reprints@futuremedicine.com)

# Axitinib for the treatment of metastatic renal cell carcinoma

Hiral Parekh<sup>\*1</sup>, Julianne Griswold<sup>1</sup> & Brian Rini<sup>1</sup>

Renal cell carcinoma is a cancer that results from a genetic inactivation of the *VHL* tumor suppressor gene leading to an upregulation of VEGF. Targeted therapies against VEGF receptors have piqued substantial interest among clinicians and researchers, and these drugs are now the standard of care in the treatment of advanced renal cell carcinoma. One of these VEGF receptor inhibitors, axitinib, has been shown to be a superior second-line therapy when compared with sorafenib. Although axitinib has clinical activity and a manageable safety profile in patients with treatment-naïve metastatic renal cell carcinoma, utility in the front-line setting is area of ongoing investigation. Another area of ongoing research is dose titration of axitinib to achieve the maximum clinical benefit. Interestingly, the axitinib-related side effect of hypertension has shown to be associated with more favorable clinical outcomes. This article describes the development of axitinib and discusses the current indications for clinical use in the management of metastatic renal cell carcinoma.

First draft submitted: 2 October 2015; Accepted for publication: 18 November 2015; Published online: 15 January 2016

## Renal cell carcinoma

Renal cell carcinoma (RCC) accounts for 90–95% of neoplasms arising from the kidney, and accounts for 3% of all malignancies in the adult population with an estimated incidence of 62,000 new cases and almost 14,000 deaths from RCC each year in USA [1]. Pathophysiologically, RCC originates from the epithelium of the proximal renal tubule and occurs either sporadically (non-hereditary) or hereditarily with both forms stemming from structural mutations in the short arm of chromosome 3 [2]. These mutations typically arise from the *VHL* gene (a tumor suppressant gene), which leads to both a decrease in degradation of hypoxia-inducing factor and upregulation of VEGF expression [3]. The role of VEGF in RCC pathogenesis is multifaceted, but it primarily acts as a potent inducer of tumor-associated angiogenesis [4]. VEGF works by binding to receptors on the surface of endothelial cells leading to an intracellular cascade, which ultimately causes angiogenesis and subsequent vascularization of the neoplastic cells. Activation of VEGF receptors has also been shown to produce downstream effects including the inhibition of apoptosis within the tumor cells [5].

### • VEGF inhibitor therapy in mRCC

The expression of VEGF is implicated in a number of cancers but the level of expression in RCC is virtually unparalleled, resulting in their highly vascular nature. As such, treatment of RCC over the course of the past decade has been revolutionized by the advent of targeted therapies, which work as inhibitors of VEGF.

## KEYWORDS

• axitinib • renal cell carcinoma • VEGF receptor inhibitor

<sup>1</sup>Cleveland Clinic Taussig Cancer Institute, 9500 Euclid Avenue, Mail Code R35, Cleveland, OH 44195, USA

\*Author for correspondence: [parekhh@ccf.org](mailto:parekhh@ccf.org)

In 2005, the US FDA approved sorafenib, a multi-target inhibitor of VEGFR-1–3, based on a study in 903 patients previously treated with cytokines. The study showed a significant improvement in progression-free survival (PFS; hazard ratio [HR]: 0.88; 95% CI: 0.63–0.95;  $p = 0.015$ ) with sorafenib as compared with placebo [12]. Following this advancement in therapy, in 2006 and 2009, the FDA approved two other VEGFR inhibitors, sunitinib and pazopanib, respectively, for the treatment of advanced RCC [13,14]. Bevacizumab, a monoclonal antibody against the extracellular domain of VEGF-A, is approved for the treatment of metastatic RCC (mRCC) along with IFN- $\alpha$  [15].

January 2012 brought the FDA approval of axitinib, which is indicated for advanced RCC after failure of one prior systemic therapeutic agent. Axitinib is a somewhat unique VEGF inhibitor given its receptor specificity and potency [16]. The development of the drug, preclinical and clinical studies and current role of axitinib in the management of mRCC with future directions to improve efficacy and minimize the toxicity, are reviewed in this article.

### Axitinib

#### • Preclinical development

Axitinib, formerly AG-013736, manufactured by Pfizer and marketed as Inlyta<sup>®</sup>, is an indazole-derived inhibitor of tyrosine kinases particularly VEGFRs: VEGFR-1, VEGFR-2 and VEGFR-3 [17] (chemical information illustrated in **Box 1**; pharmacokinetic information can be seen in **Box 2**; chemical structure illustrated in **Figure 1**).

Initially in the preclinical setting, axitinib was thought to display similar potency inhibiting VEGFR and PDGFR. This effect, however, was not supported at clinically achieved plasma concentrations, and anti-PDGFR activity was found to be approximately eight-times weaker than anti-VEGFR activity when observed *in vivo* [5].

Box 1. Chemical information for axitinib.	
<b>Chemical name</b>	<ul style="list-style-type: none"> <li>• N-methyl-2-[3-((E)-2-pyridin-2-yl-vinyl)-1H-indazol-6-ylsulfanyl]-benzamide</li> </ul>
<b>Molecular weight</b>	<ul style="list-style-type: none"> <li>• 386.47</li> <li>• Formula</li> <li>• C<sub>22</sub>H<sub>18</sub>N<sub>4</sub>OS</li> </ul>
Data taken from [18].	

This selectivity to VEGFR likely accounts for the on-target efficacy and toxicity profile of axitinib. The half maximal inhibitory concentration (IC<sub>50</sub>) of axitinib is 0.1 nM for VEGFR-1, 0.2 nM for VEGFR-2 and 0.1–0.3 nM for VEGFR-3 [19].

#### • Phase I clinical trials

Phase I study of axitinib to determine maximum tolerated dose included 36 patients with advanced solid tumors [20]. Axitinib was administered in the fixed dose schedule of 5–30 mg twice daily dosing. Based on this study, it was determined that axitinib was absorbed rapidly and achieved peak plasma concentration after 2–6 h of administration and 5 mg twice daily in fasted state was recommended as dose for Phase II studies. Important dose-limiting toxicities included hypertension (HTN), hemoptysis and stomatitis at higher dose levels. HTN was managed with medication, and stomatitis was managed with dose reductions and interruptions. The incidence and severity of HTN were proportional to drug dosage. In this study, two of the six patients with RCC achieved an objective partial response, supporting the drug's activity in this disease. Subsequently, Phase I studies of axitinib in advanced solid tumors in Japanese patient population verified the tolerability and toxicity profile of 5 mg twice daily dosing in non-Caucasian population [21].

#### • Phase II clinical trials

Based on initial Phase I studies, axitinib was evaluated in three Phase II studies (**Table 1**). The initial Phase II trial (n = 52) examined a population of patients who had failed prior treatment with cytokine therapy to determine the safety and activity of axitinib dosed 5 mg twice daily [6]. Patients with uncontrolled HTN and prior exposure to antiangiogenic agents were excluded from the study. The primary end point was objective response rate (ORR), which was 44% (95% CI: 31–59%). The median time to progression was 15.7 months (95% CI: 8.4–23.4) and median overall survival (OS) was 29.9 months (95% CI: 20.3–not estimable; range: 2.4–35.8). The most commonly reported treatment-related side effects were diarrhea, HTN, fatigue, nausea and hoarseness. Updated long-term follow-up data showed 5 year OS of 20.6% and no new toxicity signals [22].

A second Phase II trial recruited 62 patients and aimed to examine the effectiveness of axitinib

in patients who had received prior therapy with sorafenib. The starting dose was 5 mg twice daily and dose escalation was permitted up to 10 mg twice daily (53% of patients having dose titration >5 mg twice daily and 35.5% of patients requiring dose decrease to <5 mg twice daily) with a primary end point of ORR defined by Response Evaluation Criteria In Solid Tumors (RECIST). In these patients, the ORR was 22.6% (95% CI: 12.9–35) with a median duration of response of 17.5 months. Median PFS (mPFS) was 7.4 months (95% CI: 6.7–11) and median OS (mOS) was 13.6 months (95% CI: 8.4–18.8). The most common grade 3 and 4 adverse effects (AEs) were hand–foot syndrome, fatigue, HTN, dyspnea and diarrhea [7]. A third Phase II study reported response rate of 51.6% , mPFS of 11.0 months (95% CI: 9.2–12.0) and mOS of 37.3 months (95% CI: 28.6–49.9) in 64 Japanese patients supporting the role of axitinib after cytokine therapy in a non-Caucasian patient population [8].

Axitinib has also been studied in neoadjuvant setting in a Phase II trial, where 24 patients were treated with axitinib and showed median reduction of 28.3% in primary renal tumor diameter. Eleven patients had a partial response and 13 patients had stable disease [23]. Axitinib was well-tolerated with similar safety profile. Use of axitinib in neoadjuvant setting warrants further investigation at this time.

#### • Phase III clinical trials

At the time the second Phase II trial was published in 2009, the AXIS trial, a Phase III trial examining axitinib with sorafenib in patients who have advanced renal cell carcinoma refractory to one first-line therapy, was underway. The AXIS trial was the first trial to compare the effectiveness of one VEGFR inhibitor against another in the treatment of advanced RCC [9]. This trial included 723 patients with mRCC who had initially received sunitinib (54%), bevacizumab plus IFN- $\alpha$  (8%), temsirolimus (3%) or cytokine therapy (35%). Patients were randomized in 1:1 ratio to axitinib at a starting dose of 5 mg twice daily or sorafenib 400 mg twice daily. Dose adjustments in those receiving axitinib to 7 or 10 mg twice daily were allowed in patients who did not exhibit HTN (defined by >150/90 mmHg) or other adverse reaction >grade 2 as defined by the Common Terminology Criteria for Adverse Events (CTCAE). The primary end point of this study was PFS, and OS was a secondary end point.

#### Box 2. Pharmacokinetics of axitinib.

##### Absorption

- 58% bioavailability

##### Distribution

- Highly bound (>99%) to plasma proteins
- Metabolism
- Hepatic; primarily by CYP3A4/5 and to a lesser extent by CYP1A2, CyP2C19, UGT1A1

##### Excretion

- Metabolites excreted primarily in the feces

Data taken from [18].

Results were significant with a median PFS in the axitinib group of 6.7 months compared with a median PFS of 4.7 months in those patients who received sorafenib (HR: 0.665; 95% CI: 0.544–0.812; one-sided  $p < 0.0001$ ). Benefit with regards to improvement in mPFS was seen across the clinical trial regardless of prior therapy, with prior cytokine therapy mPFS was 12.1 months with axitinib as compared with 6.5 months with sorafenib (HR: 0.464; 95% CI: 0.318–0.676) and with prior sunitinib mPFS 4.8 months compared with 3.4 months (HR: 0.741; 95% CI: 0.573–0.958). Objective response rate was assessed in this study by masked blinded radiology review committee using RECIST criteria. ORR in the axitinib group was 19% (95% CI: 15.4–23.9), and 9% (95% CI: 6.6–12.9) in the sorafenib group ( $p = 0.0001$ ). No difference was observed between treatment arms in terms of OS (20.1 months with axitinib as compared with 19.2 months with sorafenib; HR: 0.969; 95% CI: 0.800–1.174; one-sided  $p = 0.3744$ ). The lack of survival benefit could be secondary to the fact that both the arms included active therapy and 54% of the axitinib group and 57% of the sorafenib group received additional therapy upon progression, and that 23 and 25% of each drug group, respectively, went on to receive two or more subsequent treatments.



**Figure 1. Axitinib.**

Data taken from [18].

**Table 1. Summary of pertinent clinical trials of axitinib in metastatic renal cell carcinoma.**

Study (year)	Phase	n	Prior therapy	Intervention	ORR (%)	Median PFS (months)	Median OS (months)	Ref.
Rixi <i>et al.</i> (2007)	II	52	Cytokine	Axitinib 5 mg p.o. b.i.d.	44.2	15.7 (TTP)	29.9	[6]
Rini <i>et al.</i> (2009)	II	62	Sorafenib	Axitinib 5 mg p.o. b.i.d. with dose titration	22.6	7.4	13.6	[7]
Eto <i>et al.</i> (2014)	II	64	Cytokine	Axitinib 5 mg p.o. b.i.d.	51.6	11	37.3	[8]
Rini <i>et al.</i> (2011)	III	723	Cytokine, sunitinib, bevacizumab or temsirolimus (one prior regimen)	Axitinib 5 mg p.o. b.i.d. with dose titration (n = 361) Sorafenib 400 mg p.o. b.i.d. (n = 362)	19 9 (p < 0.0001)	6.7 4.7 (HR: 0.665; p < 0.0001)	20.1 19.2	[9]
Rini <i>et al.</i> (2013)	II	213	None	Axitinib dose titration up to 10 mg p.o. b.i.d. (n = 56) Placebo titration (n = 56) No titration (n = 101)	54 34 59	14.5 15.7 16.6	NR NR NR	[10]
Hutson <i>et al.</i> (2013)	III	288	None	Axitinib 5 mg p.o. b.i.d. with dose titration	32	10.1	NR	[11]

b.i.d.: Twice daily; HR: Hazard ratio; NR: Not reported; ORR: Objective response rate; OS: Overall survival; PFS: Progression-free survival; p.o.: Oral; TTP: Time to progression.

The adverse events (all grades) most common in patients treated with axitinib were diarrhea (55%), HTN (40%) and fatigue (39%) and decreased appetite (34%). The adverse events most common in patients receiving sorafenib included diarrhea (53%), hand-foot syndrome (51%), as well as alopecia, fatigue and rash (all occurring in 32% of patients). Hypothyroidism requiring initiation or change in the levothyroxine dose occurred more commonly with axitinib as compared with sorafenib (27 vs 14%). As compared with sorafenib, axitinib was associated with higher rate of grade 3 or higher HTN (16% axitinib; 11% sorafenib), fatigue (11% axitinib; 5% sorafenib) and diarrhea (11% axitinib; 7% sorafenib) and less frequent cutaneous toxicity (5% axitinib, 16% sorafenib) and anemia (1% axitinib, 4% sorafenib). Three patients in the AXIS trial discontinued axitinib therapy due to a transient ischemic attack, while no transient ischemic attack was reported for sorafenib. There was a decreased rate of treatment discontinuation (4% axitinib, 8% sorafenib) and dose reduction (31% axitinib, 52% sorafenib) as compared with sorafenib.

The AXIS trial assessed patient reported quality of life outcomes with use of the Functional Assessment of Cancer Therapy Kidney Symptoms Index (FKS) and FKSI-Disease Related Symptoms (FKSI-DRS). Analysis of the composite end point of occurrence of death, progression of disease and deterioration of symptoms found 17% reduction in FKSI (p = 0.014)

and 16% reduction in FKSIDRS (p = 0.0203) with axitinib compared with sorafenib.

Another Phase III trial randomized 288 previously untreated mRCC patients to either axitinib (192) or sorafenib (96) [11]. Sorafenib was given at the standard dose of 400 mg twice daily and axitinib was given at the dose of 5 mg twice daily with possible titration up to 10 mg twice daily as per criteria described in AXIS trial. Unfortunately, this study did not meet statistical significance with a median PFS of 10.1 months with axitinib as compared with 6.5 months in sorafenib arm (HR: 0.77; 95% CI: 0.56–1.05; p = 0.038). In the preplanned subgroup of patients with good performance status (PS = 0), the median PFS reported was significantly superior in the axitinib group as compared with the sorafenib group (13.7 vs 6.6 months; HR: 0.64; 95% CI: 0.42–0.99; p = 0.022). AE profile was similar to AXIS study with higher rate HTN, diarrhea and hypothyroidism with axitinib and more skin toxicity with sorafenib arm. Based on the results of this study, axitinib currently remains indicated only for second-line therapy of mRCC.

### Axitinib in clinical practice

Axitinib is currently FDA approved for use in the treatment of advanced renal cell carcinoma in patients who have previously failed treatment with a first-line agent and also approved by EMA for advanced RCC after failure of prior sunitinib or cytokine.

### • Dosing & administration

The current initial dosing regimen is 5 mg twice daily with dose adjustment based on the individual safety and tolerability. It can be taken with or without food and achieves steady state within 2–3 days with a plasma half-life of 2.5–6.1 h [18].

In the AXIS trial, dose titration of axitinib was permitted from the starting dose of 5–7 mg twice daily and up to 10 mg twice daily if patients had blood pressure <150/90 mmHg and not higher than grade 2 toxicity of drug. This was based on the concept that patients who tolerate 5 mg twice daily dose may have sub-therapeutic drug levels and dose titration would achieve therapeutics drug levels [9].

Subsequently, dose titration was formally evaluated in a randomized, double-blind, Phase II trial [10,24]. The trial enrolled 213 patients; they all received starting dose of axitinib 5 mg twice daily during a 4 week lead in period. After the 4 weeks, patients with blood pressure <150/90 mmHg (on no more than two antihypertensive agents) and no grade 3 or 4 toxic effects were stratified by Eastern Cooperative Oncology Group (ECOG) performance status and were then randomly (1:1) assigned to either titration with axitinib (56 patients) or placebo titration (stayed on 5 mg twice daily; 56 patients). Dose titration in the axitinib group was to 7 mg twice daily which, if tolerated, was increased to 10 mg twice daily. The patients who did not meet the criteria for dose escalation continued on the initial dose of axitinib (a total of 91 patients).

At the end of the study, 30 patients (54%; 95% CI: 40–67) in the axitinib dose titration group had an objective response compared with 19 patients (34%; 95% CI: 22–48) in the group receiving placebo titration (risk ratio: 1.58; 95% CI: 1.02–2.45; one-sided  $p = 0.019$ ). In the patients who did not meet criteria for dose titration, 54 of them had an objective response (59%, 95% CI: 49–70). Median PFS for all patients in the study was 14.6 months (95% CI: 11.5–17.5). The hazard ratio for PFS with axitinib titration versus placebo titration was 0.85 (95% CI: 0.54–1.35; one sided stratified  $p = 0.24$ ), favoring the titrated group. In the axitinib titration group, median PFS was 14.5 months (95% CI: 9.2–24.5); in the placebo titration group, it was 15.7 months (95% CI: 8.3–19.4) and 16.6 months (95% CI: 11.2–22.5) in patients who were nonrandomized. Median OS was 42.7 months (95% CI: 24.7–not estimable) in the axitinib titration arm versus 30.4 months (95% CI: 23.7–45.0) in the placebo

titration arm (HR: 0.785;  $p = 0.1616$ ) [25]. Pharmacokinetic data was collected from subset of patients ( $n = 73$ ), which showed that dose titration eligible patients had both lower area under the plasma concentration–time curve and lower maximum observed plasma concentration at baseline when compared with the group not eligible for dose titration, and that exposure increased with an increasing dose [24].

The most common grade 3 or worse adverse effect was HTN (18% of axitinib titration group, 9% of the placebo group and 49% of the nontitration group). Common grade 3 or worse adverse events in axitinib titration group as compared with placebo titration were HTN, diarrhea, anorexia and nausea. All the patients meeting clinical dose titration criteria did not tolerate dose titration. This was evidenced by the ten patients (18%) who required dose reductions after meeting the criteria for dose increase. In these patients, axitinib was increased to 7 mg twice daily, which resulted in an overtitration (as it is a 40% increase in dose, which could be substantial) and subsequently lead to adverse events, which required dose reduction to 5 mg (or less) twice daily.

This trial demonstrated that axitinib exposure can be increased with upward titration in patients who tolerate the initial dose, and that this can lead to a greater objective response rate. However, PFS was not significantly increased. This latter point may be due to the fact that toxicity from titration limited the duration of titration or moreover the total duration of axitinib therapy. It can be hypothesized that smaller titration increments may be a strategy to optimize axitinib titration. This hypothesis requires prospective testing. It is also true in clinical practice that brief (2–3 days) interruptions of axitinib can reduce toxicity and overall lead to more days on an adequate dose of drug. This practice, however, also requires prospective testing.

### • Axitinib in the context of alternate therapies

Everolimus, an mTOR inhibitor, is approved as second-line therapy for mRCC based on PFS benefit as compared with placebo [26]. In RECORD-1 trial, patients with mRCC, which had progressed on sunitinib, sorafenib or both, were randomly assigned to receive everolimus 10 mg once daily ( $n = 272$ ) or placebo ( $n = 138$ ), in conjunction with best supportive care. Everolimus was associated with mPFS of 4.9

months as compared with 1.9 months with placebo (HR: 0.33;  $p < 0.001$ ) with no difference in OS [27]. However, it should be noted that most of the included patients who received everolimus were not truly second line, only 21% ( $n = 89$ ) of patients received everolimus in the second-line setting. In contrast, AXIS trial included pure second-line patients, but neither AXIS nor RECORD-1 trial has demonstrated prolonged OS compared with placebo. The rationale for sequential use of two tyrosine kinase inhibitors (TKIs) originates from numerous case series and INTORSECT study, a randomized Phase III trial comparing temsirolimus versus sorafenib as a second-line treatment option in patients with mRCC who had progressed on sunitinib in the first-line setting [28]. In this study, there was a significant OS difference in favor of sorafenib compared with temsirolimus (HR: 1.31; 95% CI: 1.05–1.63;  $p = 0.01$ ). The results of this study might suggest sequencing with VEGFR (a TKI) may be more optimal than sequencing with mTOR inhibitor.

There are several other ongoing trials assessing role of newer agents in the refractory setting. Recently, results of the Phase III trial of a check point inhibitor, nivolumab, compared with everolimus in 821 patients with advanced clear-cell RCC previously treated with one or two VEGF-TKI agents were published. In this trial, nivolumab was associated with improvement in OS with mOS of 25.0 months as compared with 19.6 months with everolimus (HR: 0.73; 98.5% CI: 0.57–0.93;  $p = 0.002$ ) [29]. Another agent, cabozantinib (XL-184), a multikinase inhibitor of VEGFR-2, MET, KIT and RET, was compared with everolimus in 658 patients with mRCC met its primary end point of a statistically significant increase in mPFS. In this study, cabozantinib was associated with mPFS of 7.4 months as compared with 3.8 months with everolimus (HR: 0.58; 95% CI: 0.45–0.75;  $p < 0.001$ ). OS was longer with cabozantinib but did not cross the significant boundary for the interim analysis [30]. These agents are likely to significantly alter the therapeutic landscape in refractory RCC.

• **Safety & tolerability**

As defined by the AXIS trial, the most common of all adverse events associated with the use of axitinib are diarrhea, HTN, fatigue, anorexia, nausea and dysphonia [9]. Grade 3 or higher laboratory abnormalities include lipase

elevation, lymphopenia, hypophosphatemia and neutropenia, although none of these tend to be clinically-relevant. In both the Phase III trials, sorafenib was more commonly associated with cutaneous toxicity, hand–foot syndrome (palmar–plantar erythrodysesthesia [PPE]) and myelosuppression [9,11].

The most important components of side effect management are patient-focused education, close monitoring, pharmacological and nonpharmacological management of toxicity and treatment modification including interruption and dose modification if required to minimize the toxicity. Patients with a history of HTN should be on an optimal regimen prior to starting therapy, and patients with comorbidities of heart disease, diabetes or renal dysfunction should be closely monitored while on therapy [31]. Management of axitinib-associated gastrointestinal side effects includes dietary and medication interventions, and PPE requires ongoing assessment and management to control the extent and severity of this adverse event. The ‘3C’ approach has been recommended for the management of PPE, which includes controlling calluses, comforting with cushions and covering with creams and covers like cotton gloves or socks [31,32].

• **HTN as a biomarker**

Similar to other therapies that inhibit VEGF–VEGFR signaling, axitinib induces HTN, which appears to be a biomarker for drug activity [33].

In a retrospective analysis of five Phase II trials of axitinib used for the treatment of four different tumor types, 230 patients were evaluated for a relationship between diastolic blood pressure  $\geq 90$  mmHg and efficacy of axitinib as determined by OS, PFS and ORR. This study concluded that patients with a diastolic BP  $\geq 90$  mmHg had a significantly lower relative risk of death than those with a diastolic blood pressure (dBp)  $< 90$  mmHg (adjusted HR: 0.55; 95% CI: 0.39–0.77;  $p < 0.001$ ). This analysis also found the objective response rate was 43.9 versus 12% in patients with an elevated diastolic blood pressure. The median OS and median PFS were also higher in patients with diastolic BP  $\geq 90$  mmHg (25.8 vs 14.9 months and 10.2 vs 7.1 months, respectively) [34].

The OS benefit of axitinib-induced diastolic blood pressure elevation was echoed in a post-hoc analysis of the AXIS trial. In this analysis, OS in the axitinib group was longer in patients with a diastolic blood pressure  $> 90$  mmHg

(20.7 months [95% CI: 18.4–24.6]) compared with patients with a diastolic blood pressure <90 mmHg (12.9 months [10.1–20.4]) [9]. Axitinib dose titration study also showed longer PFS in patients with dBP change from baseline  $\geq 10$  (n = 176) versus <10 mmHg (n = 27; median: 16.6 vs 5.7 months; HR: 0.40; 95% CI: 0.25–0.65; one-sided p < 0.001) [24]. However, there was a weak correlation ( $R^2 = 0.225$ ) between axitinib plasma steady-state exposure and mean change from baseline in dBP on cycle 1/day 15.

Elevations in diastolic blood pressure can be used as one potential marker of efficacy of the VEGFR inhibitor. Importantly, however, as noted above in the dose titration study, the data to-date do not yet support a ‘dose to HTN’ strategy as a method of optimizing patient dose and clinical outcome. Moreover, treatment of HTN at baseline or during axitinib therapy would not compromise the efficacy of the treatment [33]. Hence, aggressive management of HTN is necessary to prevent HTN-related sequelae. Further investigation of how to exploit the association of HTN and axitinib efficacy in clinical practice is needed.

#### • Drug interactions

When studied *in vitro*, axitinib is thought to be metabolized primarily by CYP3A4/5 and to a lesser extent by CYP1A2, CYP2C19 and UGT1A1. Coadministration of axitinib with strong CYP3A4/5 inhibitors (e.g., grapefruit, ketoconazole, itraconazole, clarithromycin, atazanavir) may increase axitinib plasma concentrations. On the other hand, coadministration with strong CYP3A4/5 inducers (e.g., rifampin, dexamethasone, phenytoin, carbamazepine, rifabutin, and St John’s Wort) may decrease plasma concentrations. Coadministration of axitinib with CYP3A4/5 inhibitors/inducers should be avoided when possible and coadministration is required, dose adjustment of axitinib is recommended [18].

#### • Specific patient groups

##### Hepatic & renal impairment

Axitinib is eliminated by hepatobiliary excretion and Phase I studies have suggested <1% excretion of the drug in urine [20]. Dose modifications are not recommended for patients with mild hepatic impairment (Child-Pugh A). The recommended starting dose is 50% for patients with moderate hepatic failure (Child-Pugh B) and it has not been studied in severe hepatic failure (Child-Pugh C). No starting dose adjustments

have been recommended in pre-existing mild-to-severe renal impairment, but caution is advised in end-stage renal disease (creatinine clearance <15 ml/min) [18,35].

#### Special population

Axitinib is pregnancy category D (positive evidence of human fetal risk). There are no studies of axitinib in pregnant women. Based on the known mechanism of action of the drug, it should be avoided in pregnant women and was shown in mouse models to be teratogenic, embryotoxic and fetotoxic at levels lower than the equivalent recommended starting dose in humans. Use of axitinib in lactating female has not been studied. It is also not studied in pediatric population. AXIS trial included 34% of patients above the age of 65 years and greater sensitivity in some older individuals cannot be ruled out, no overall differences were observed and no dose adjustments are recommended based on the age [18].

#### Conclusion

Axitinib is a potent VEGFR inhibitor, currently approved for second-line therapy in patients with metastatic RCC. It has shown superiority in PFS when compared against another drug in its class (sorafenib). Although demonstrated activity and tolerable safety profile in treatment naïve mRCC patients, its use in first-line setting needs further investigation. The starting dose of axitinib is 5 mg twice daily, and dose titration of axitinib has been shown to have a superior objective response rate when compared with patients who met criteria of dose titration but did not receive increased doses of the medication. The optimal method for selecting appropriate patients and the optimal schema for titration for the best clinical outcome requires further study. Refinement of axitinib-specific dose titration criteria and the use of intermediate dosing regimens must also be investigated so that the benefits of the drug can be maximized while minimizing toxic therapeutic effects.

#### Financial & competing interests disclosure

*In the past 36 months, B Rini has served as a consultant or advisor to and/or has received research funding from Pfizer. The authors have no other relevant affiliations or financial involvement with any organization or entity with a financial interest in or financial conflict with the subject matter or materials discussed in the manuscript apart from those disclosed.*

*No writing assistance was utilized in the production of this manuscript.*

## EXECUTIVE SUMMARY

- Clear cell renal cell carcinoma involves inactivation of the *VHL* gene on chromosome 3, which causes an upregulation of VEGF.
- Axitinib is a potent inhibitor of the VEGF receptor.
- Axitinib has been shown to be superior to sorafenib as a second-line therapy in treating advanced renal cell carcinoma in regard to objective response rate and progression-free survival.
- The recommended dose of axitinib is 5 mg twice daily for metastatic renal cell carcinoma with upward dose titration encouraged in patients who tolerate initial therapy.
- Important axitinib-related side effects include hypertension, diarrhea, fatigue and loss of appetite.
- Axitinib-induced increases in blood pressure are associated with more favorable clinical outcome.

## References

Papers of special note have been highlighted as:  
• of interest

- Siegel RL, Miller KD, Jemal A. Cancer statistics, 2015. *CA Cancer J. Clin.* 65(1), 5–29 (2015).
- Cohen HT, Mcgovern FJ. Renal-cell carcinoma. *N. Engl. J. Med.* 353(23), 2477–2490 (2005).
- Albiges L, Salem M, Rini B, Escudier B. Vascular endothelial growth factor-targeted therapies in advanced renal cell carcinoma. *Hematol. Oncol. Clin. North Am.* 25(4), 813–833 (2011).
- Rini BI, Small EJ. Biology and clinical development of vascular endothelial growth factor-targeted therapy in renal cell carcinoma. *J. Clin. Oncol.* 23(5), 1028–1043 (2005).
- Hu-Lowe DD, Zou HY, Grazzini ML *et al.* Nonclinical antiangiogenesis and antitumor activities of axitinib (AG-013736), an oral, potent, and selective inhibitor of vascular endothelial growth factor receptor tyrosine kinases 1, 2, 3. *Clin. Cancer. Res.* 14(22), 7272–7283 (2008).
- Rixe O, Bukowski RM, Michaelson MD *et al.* Axitinib treatment in patients with cytokine-refractory metastatic renal-cell cancer: a Phase II study. *Lancet Oncol.* 8(11), 975–984 (2007).
- Rini BI, Wilding G, Hudes G *et al.* Phase II study of axitinib in sorafenib-refractory metastatic renal cell carcinoma. *J. Clin. Oncol.* 27(27), 4462–4468 (2009).
- Eto M, Uemura H, Tomita Y *et al.* Overall survival and final efficacy and safety results from a Japanese Phase II study of axitinib in cytokine-refractory metastatic renal cell carcinoma. *Cancer Sci.* 105(12), 1576–1583 (2014).
- Rini BI, Escudier B, Tomczak P *et al.* Comparative effectiveness of axitinib versus sorafenib in advanced renal cell carcinoma (AXIS): a randomised Phase 3 trial. *Lancet* 378(9807), 1931–1939 (2011).
- Phase III trial of axitinib that lead to axitinib approval.**
- Rini BI, Melichar B, Ueda T *et al.* Axitinib with or without dose titration for first-line metastatic renal-cell carcinoma: a randomised double-blind Phase 2 trial. *Lancet Oncol.* 14(12), 1233–1242 (2013).
- Phase II study that studies dose titration formerly.**
- Hutson TE, Lesovoy V, Al-Shukri S *et al.* Axitinib versus sorafenib as first-line therapy in patients with metastatic renal-cell carcinoma: a randomised open-label Phase 3 trial. *Lancet Oncol.* 14(13), 1287–1294 (2013).
- Axitinib in frontline setting.**
- Escudier B, Eisen T, Stadler WM *et al.* Sorafenib for treatment of renal cell carcinoma: final efficacy and safety results of the Phase III treatment approaches in renal cancer global evaluation trial. *J. Clin. Oncol.* 27(20), 3312–3318 (2009).
- Motzer RJ, Hutson TE, Tomczak P *et al.* Overall survival and updated results for sunitinib compared with interferon  $\alpha$  in patients with metastatic renal cell carcinoma. *J. Clin. Oncol.* 27(22), 3584–3590 (2009).
- Sternberg CN, Hawkins RE, Wagstaff J *et al.* A randomised, double-blind Phase III study of pazopanib in patients with advanced and/or metastatic renal cell carcinoma: final overall survival results and safety update. *Eur. J. Cancer* 49(6), 1287–1296 (2013).
- Escudier B, Pluzanska A, Koralewski P *et al.* Bevacizumab plus interferon  $\alpha$ -2a for treatment of metastatic renal cell carcinoma: a randomised, double-blind Phase III trial. *Lancet* 370(9605), 2103–2111 (2007).
- Mittal K, Wood LS, Rini BI. Axitinib in metastatic renal cell carcinoma. *Biol. Ther.* 2, 5 (2012).
- Patson B, R BC, Olszanski AJ. Pharmacokinetic evaluation of axitinib. *Expert Opin. Drug Metab. Toxicol.* 8(2), 259–270 (2012).
- Inlyta® (Axitinib), package insert. NPL, NY, USA.
- Escudier B, Gore M. Axitinib for the management of metastatic renal cell carcinoma. *Drugs R. D.* 11(2), 113–126 (2011).
- Rugo HS, Herbst RS, Liu G *et al.* Phase I trial of the oral antiangiogenesis agent AG-013736 in patients with advanced solid tumors: pharmacokinetic and clinical results. *J. Clin. Oncol.* 23(24), 5474–5483 (2005).
- Mukohara T, Nakajima H, Mukai H *et al.* Effect of axitinib (AG-013736) on fatigue, thyroid-stimulating hormone, and biomarkers: a Phase I study in Japanese patients. *Cancer Sci.* 101(4), 963–968 (2010).
- Motzer RJ, Harzstark AI, Rini BI *et al.* Axitinib second-line therapy for metastatic renal cell carcinoma (mRCC): five-year (yr) overall survival (OS) data from a Phase II trial. *J. Clin. Oncol.* 29(Suppl.), Abstract 4547 (2011).
- Karam JA, Devine CE, Urbauer DL *et al.* Phase 2 trial of neoadjuvant axitinib in patients with locally advanced nonmetastatic clear cell renal cell carcinoma. *Eur. Urol.* 66(5), 874–880 (2014).
- Rini BI, Melichar B, Fishman MN *et al.* Axitinib dose titration: analyses of exposure, blood pressure and clinical response from a randomized Phase II study in metastatic renal cell carcinoma. *Ann. Oncol.* 26(7), 1372–1377 (2015).

- **Role of biomarkers with axitinib use.**
- 25 Rini BI TY, Melichar B. Overall survival analysis from a randomized Phase II study of axitinib with or without dose titration for first-line metastatic renal cell carcinoma. *J. Clin. Oncol.* 33(Suppl.), Abstract 4545 (2015).
- 26 Motzer RJ, Escudier B, Oudard S *et al.* Efficacy of everolimus in advanced renal cell carcinoma: a double-blind, randomised, placebo-controlled Phase III trial. *Lancet* 372(9637), 449–456 (2008).
- 27 Motzer RJ, Escudier B, Oudard S *et al.* Phase 3 trial of everolimus for metastatic renal cell carcinoma: final results and analysis of prognostic factors. *Cancer* 116(18), 4256–4265 (2010).
- 28 Hutson TE, Escudier B, Esteban E *et al.* Randomized Phase III trial of temsirolimus versus sorafenib as second-line therapy after sunitinib in patients with metastatic renal cell carcinoma. *J. Clin. Oncol.* 32(8), 760–767 (2014).
- 29 Motzer RJ, Escudier B, McDermott DF *et al.* Nivolumab versus everolimus in advanced renal-cell carcinoma. *N. Engl. J. Med.* 373(19), 1803–1813 (2015).
- **Emerging therapy – PD-1 inhibitor, role of nivolumab in metastatic renal cell carcinoma.**
- 30 Phase TK, Escudier B, Powles T *et al.* Cabozantinib versus everolimus in advanced renal-cell carcinoma. *N. Engl. J. Med.* 373(19), 1814–1823 (2015).
- **Newer agent – role of cabozantinib in metastatic renal cell carcinoma**
- 31 Maitland ML, Bakris GL, Black HR *et al.* Initial assessment, surveillance, and management of blood pressure in patients receiving vascular endothelial growth factor signaling pathway inhibitors. *J. Natl Cancer Inst.* 102(9), 596–604 (2010).
- 32 Wood LS LH, Jatoi A *et al.* Practical considerations in the management of hand–foot skin reaction caused by multikinase inhibitors. *Comm. Oncol.* 7, 23–29 (2010).
- 33 Rini BI, Schiller JH, Fruehauf JP *et al.* Diastolic blood pressure as a biomarker of axitinib efficacy in solid tumors. *Clin. Cancer Res.* 17(11), 3841–3849 (2011).
- 34 Rini BI, Garrett M, Poland B *et al.* Axitinib in metastatic renal cell carcinoma: results of a pharmacokinetic and pharmacodynamic analysis. *J. Clin. Pharmacol.* 53(5), 491–504 (2013).
- 35 Nishida H, Fukuhara H, Yamagishi A *et al.* Sequential molecularly targeted drug therapy including axitinib for a patient with end-stage renal failure and metastatic renal cell carcinoma. *Hemodial. Int.* doi:10.1111/hdi.12329 (2015) (Epub ahead of print).

See discussions, stats, and author profiles for this publication at: <https://www.researchgate.net/publication/282911607>

# Axitinib induces DNA damage response leading to senescence, mitotic catastrophe, and increased NK cell recognition in human renal carcinoma cells

Article in *Oncotarget* · October 2015

DOI: 10.18632/oncotarget.5768

CITATIONS

25

READS

272

8 authors, including:



**Maria Beatrice Morelli**

Sapienza University of Rome

83 PUBLICATIONS 3,828 CITATIONS

SEE PROFILE



**Consuelo Amantini**

University of Camerino

120 PUBLICATIONS 4,654 CITATIONS

SEE PROFILE



**Matteo Santoni**

University of Macerata

400 PUBLICATIONS 6,800 CITATIONS

SEE PROFILE



**Alessandra Soriani**

Sapienza University of Rome

88 PUBLICATIONS 2,229 CITATIONS

SEE PROFILE

Some of the authors of this publication are also working on these related projects:



Urothelial carcinoma [View project](#)



Role of ion channels in cancer and inflammation [View project](#)

# Axitinib induces DNA damage response leading to senescence, mitotic catastrophe, and increased NK cell recognition in human renal carcinoma cells

Morelli Maria Beatrice<sup>1,2</sup>, Amantini Consuelo<sup>3</sup>, Santoni Matteo<sup>4</sup>, Soriani Alessandra<sup>2</sup>, Nabissi Massimo<sup>1</sup>, Cardinali Claudio<sup>1,2</sup>, Santoni Angela<sup>2</sup> and Santoni Giorgio<sup>1</sup>

<sup>1</sup> School of Pharmacy, Experimental Medicine Section, University of Camerino, Camerino, Italy

<sup>2</sup> Department of Molecular Medicine, Sapienza University, Rome, Italy

<sup>3</sup> School of Biosciences and Veterinary Medicine, University of Camerino, Camerino, Italy

<sup>4</sup> Department of Medical Oncology, AOU Ospedali Riuniti, Polytechnic University of the Marche Region, Ancona, Italy

**Correspondence to:** Matteo Santoni, **email:** mattymo@alice.it

**Keywords:** renal cell carcinoma, tyrosine kinase inhibitors, cell senescence, mitotic catastrophe, NKG2D ligands

**Received:** August 07, 2015

**Accepted:** September 12, 2015

**Published:** October 14, 2015

This is an open-access article distributed under the terms of the Creative Commons Attribution License, which permits unrestricted use, distribution, and reproduction in any medium, provided the original author and source are credited.

## ABSTRACT

**Tyrosine kinase inhibitors (TKIs) including axitinib have been introduced in the treatment of renal cell carcinoma (RCC) because of their anti-angiogenic properties. However, no evidence are presently available on a direct cytotoxic anti-tumor activity of axitinib in RCC.**

**Herein we reported by western blot analysis that axitinib treatment induces a DNA damage response (DDR) initially characterized by  $\gamma$ -H2AX phosphorylation and Chk1 kinase activation and at later time points by p21 overexpression in A-498 and Caki-2 RCC cells although with a different potency. Analysis by immunocytochemistry for the presence of 8-oxo-7,8-dihydro-2'-deoxyguanosine in cellular DNA and flow cytometry using the redox-sensitive fluorescent dye DCFDA, demonstrated that DDR response is accompanied by the presence of oxidative DNA damage and reactive oxygen species (ROS) generation. This response leads to G2/M cell cycle arrest and induces a senescent-like phenotype accompanied by enlargement of cells and increased senescence-associated  $\beta$ -galactosidase activity, which are abrogated by N-acetyl cysteine (NAC) pre-treatment. In addition, axitinib-treated cells undergo to cell death through mitotic catastrophe characterized by micronucleation and abnormal microtubule assembly as assessed by fluorescence microscopy.**

**On the other hand, axitinib, through the DDR induction, is also able to increase the surface NKG2D ligand expression. Accordingly, drug treatment promotes NK cell recognition and degranulation in A-498 RCC cells in a ROS-dependent manner.**

**Collectively, our results indicate that both cytotoxic and immunomodulatory effects on RCC cells can contribute to axitinib anti-tumor activity.**

## INTRODUCTION

Renal cell carcinoma (RCC) accounts for 2-3% of all malignancies, with approximately 84,400 new cases and 34,700 cancer-related deaths in Europe in 2013 [1]. Almost one third of the patients present metastatic disease at diagnosis and another 20% develop metastases after nephrectomy [2, 3].

Angiogenesis is critical for sustaining RCC growth

and haematogenous dissemination [4]. Tyrosine kinase inhibitors (TKIs) targeting vascular endothelial growth factor receptor (VEGFR), such as sunitinib, sorafenib, pazopanib and axitinib, the anti-VEGF antibody bevacizumab and the mammalian target of rapamycin (mTOR) inhibitors everolimus and temsirolimus, have been sequentially approved by the US Food and Drug Administration (FDA) [5-12].

Axitinib is a potent and selective inhibitor of

VEGFR 1, 2, and 3 approved by FDA in 2012 for the treatment of patients with metastatic RCC (mRCC) after failure of one prior systemic therapy. The European Medicines Agency has approved the use of axitinib in 2015 for the treatment of advanced renal carcinoma after failure of prior treatment with sunitinib or interleukin 2 (IL-2) [13]. Its use as first-line therapy for advanced or mRCC was also reported [14, 15].

In experimental models, axitinib produces a dose-dependent blockade of VEGFR-2 phosphorylation, reduction of vascular permeability and angiogenesis, and induction of apoptosis, providing evidence for therapeutic potential [16]. Moreover, in murine RCC xenografts, axitinib augments CD8<sup>+</sup> T cell-mediated antitumor activity against renal carcinoma via a STAT3-dependent reversal of myeloid suppressor cells (MDSC) accumulation in the spleens and tumor beds [17].

Agents that cause genotoxic stress or DNA-replication inhibitors have been recently shown to activate the DNA damage response (DDR) as well as to increase the expression of stress-induced NKG2D and DNAX accessory molecule-1 (DNAM-1) ligands recognized by the innate immune system [18]. DDR to genotoxic insults involves a class of protein kinases, including ATM, ATR, and DNA-dependent protein kinases, followed by activation of Chk1 and Chk2 kinases that causes temporal cell cycle arrest, and promotes assembly of DNA repair complexes at the damaged sites on chromosomes [19-21]. *In vivo* activation of Chk1 requires phosphorylation on both Ser-345 and Ser-317 [22]. Cell cycle arrest can then lead to different cellular programs including senescence, apoptosis and mitotic catastrophe [23, 24].

Beyond its effects on angiogenesis, axitinib has been recently shown to modulate the function of immune effector cells that play an important role in the control of RCC development, progression and drug response [25,26]. RCC exhibits a prominent immune cell infiltrate consisting of T cells, dendritic cells (DCs), macrophages and natural killer (NK) cells.

NK cells represent one of the main effectors of the immunosurveillance against tumors [27, 28]. NK cell activity depends on the interplay between inhibitory receptors for major histocompatibility complex (MHC) class I molecules and activating receptors, such as NKG2D and DNAM-1 that operate in concert to induce the elimination of tumor cells [29, 30]. Human NKG2D belongs to C-type lectin-like receptor family and recognizes MHC I-related molecules MICA/B and ULBPs (UL16-binding proteins) [31-33]. NKG2D is expressed not only on NK cells, but also on  $\gamma\delta$  T cells, CD8<sup>+</sup> T cells, and a subset of CD4<sup>+</sup> T cells. The expression of NKG2D ligands is largely confined to virus-infected, tumor, and stressed cells [31]. DNAM-1 is a transmembrane glycoprotein constitutively expressed on the majority of T cells, NK cells, and macrophages. DNAM-1 ligands, namely nectin-2 (Nec-2, CD112) and the poliovirus

receptor (PVR, CD155), have been initially described as adhesion molecules and only recently they have been found on a variety of tumors and virus-infected cells [33-35].

In this study, we demonstrated the ability of axitinib treatment to trigger DNA damage response, cell cycle arrest and senescence, and mitotic catastrophe in RCC cells. In addition, we further evaluated axitinib ability to increase NKG2D and DNAM-1 ligand surface expression and to enhance NK cell recognition and activity against RCC cells.

## RESULTS

### Axitinib inhibits RCC cell viability in a dose and time-dependent manner

We first evaluated the effects of axitinib on cell viability in A-498 and Caki-2 RCC lines by performing dose-response and time-course analyses (Figure 1). Axitinib inhibited the growth of RCC lines, with IC50 values of 13.6  $\mu$ M for A-498 and 36  $\mu$ M for Caki-2 cells after 96 h of treatment, indicating that Caki-2 cells are more resistant to axitinib-mediated cytotoxic effects. The lowest effective dose of axitinib inducing growth inhibition (12.5  $\mu$ M for A-498 and 25  $\mu$ M for Caki-2 cells after 96 h treatment) was used for the subsequent experiments.

### Axitinib triggers DDR associated with oxidative DNA damage in RCC cells

To evaluate whether axitinib treatment could trigger DDR in RCC cells, we initially investigated the presence of  $\gamma$ -H2AX (H2AX), a phosphorylated variant of histone 2A that is associated with DNA double-strand breaks [36]. Interestingly, western blot analysis revealed strong induction of the DNA damage marker in both RCC cell lines, being more rapid and sustained in A-498 cells (Figure 2A).  $\gamma$ -H2AX induction was accompanied by Ser317- and Ser345-Chk1 phosphorylation already after 1 h exposure to axitinib and persisting at later points only in A-498 cells (Figure 2B, 2C). Later at 12 h after treatment, a progressive overexpression of p21 that paralleled the decline of Ser345- and Ser317-Chk1 activation and Chk1 protein levels, was mainly observed in A-498 cells (Figure 2B, 2C).

In addition, immunofluorescence analysis with 8-oxo-7,8-dihydro-2-deoxyguanosine (8-oxo-dG), a marker of oxidative DNA damage [37], in cells treated for different times with axitinib alone or in combination with the antioxidant NAC, indicated that axitinib induces oxidative DNA damage in a time-dependent manner, being more rapid and prominent in A-498 cells (Figure 3A); this

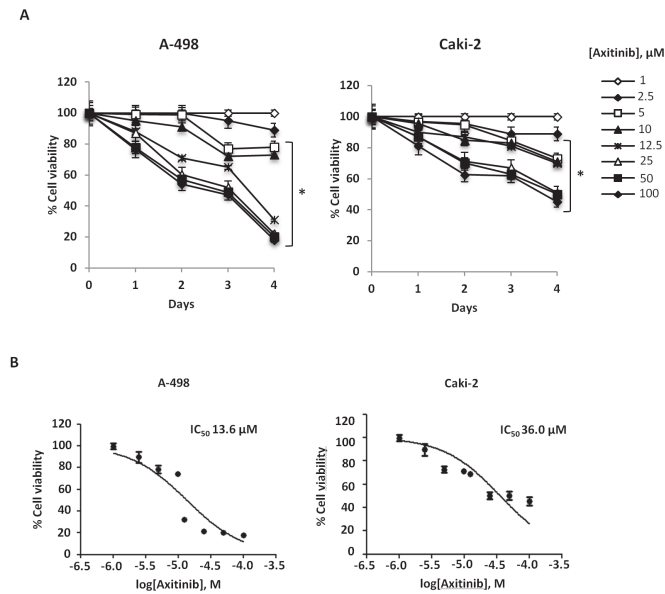


**Figure 1: Axitinib inhibits RCC cell viability in a dose and time-dependent manner.** **A.** A-498 and Caki-2 RCC cell lines were cultured up to 96 h with different doses of axitinib. Cell viability was determined by MTT assay. Data shown are expressed as mean  $\pm$  SD of three separate experiments; \* $p < 0.01$  vs vehicle-treated cells. **B.** RCC cell lines were cultured for 96 h with different doses of axitinib. Cell viability was determined by MTT assay. Data shown are expressed as mean  $\pm$  SE of three separate experiments.

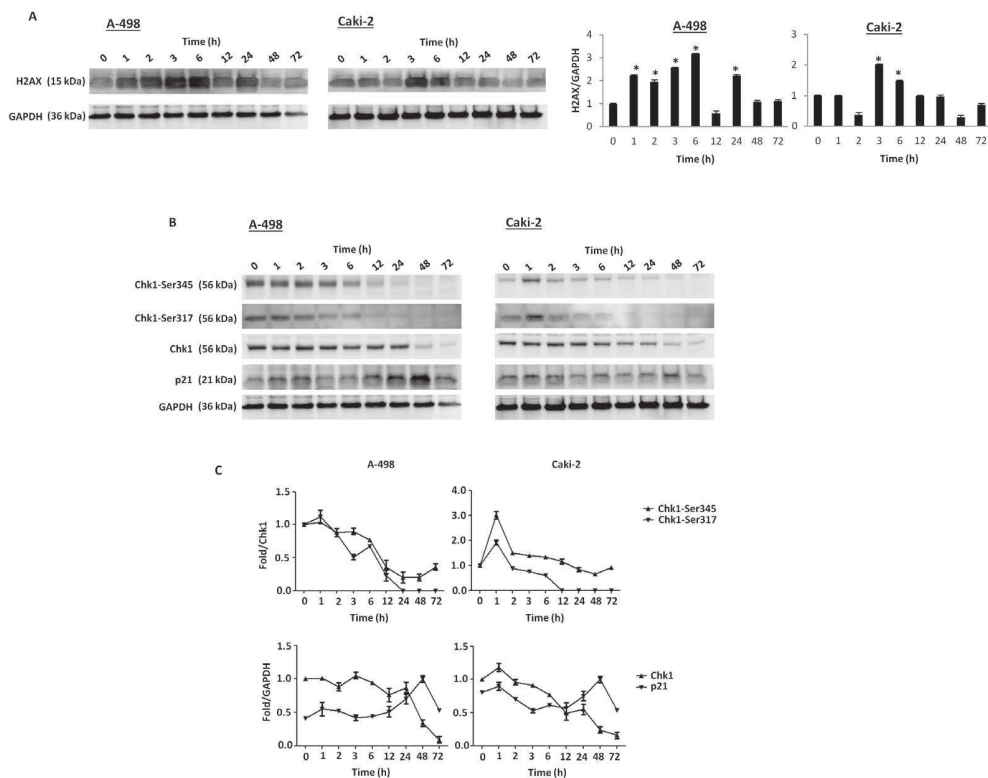


**Figure 2: Axitinib triggers DDR in RCC cells.** **A.** Western blot analysis and densitometry quantification of H2AX protein levels in RCC cells cultured for up to 72 h in the presence of axitinib (12.5  $\mu$ M in A-498 and 25  $\mu$ M in Caki-2). H2AX densitometry values were normalized to GAPDH used as loading control. Blots are representative of one of three separate experiments, \* $p < 0.01$  treated vs untreated cells. **B.** Western blot analysis of Chk1-Ser345, Chk1-Ser317, Chk1 and p21 protein levels in RCC cells cultured for up to 72 h as above described. Blots are representative of one of three separate experiments. **C.** Quantitative representation of the experiment reported in panel B. Chk1 and p21 densitometry values were normalized to GAPDH used as loading control. The Chk1-Ser345 and Chk1-Ser317 protein levels were determined with respect to Chk1 levels. For Chk1-Ser345, Chk1-Ser317 and Chk1, the initial protein levels were taken as 1. For p21, the maximal p21 protein levels were also taken as 1.

response was reverted by pre-treatment of RCC cells with the antioxidant NAC (Figure 3B).

### Axitinib induces G2/M arrest and cell senescence in RCC cells

We then evaluated whether axitinib treatment could result in changes in cell cycle. Thus, we performed cell cycle experiments in the presence of axitinib for 96 h. We observed that treatment of RCC cells induced a significant decrease of G0/G1 phase cell population already at 6 h and this decrease was accompanied by a parallel and progressive increase of G2/M-phase cell population

until 72 h (Figure 4A). Again, the axitinib effects were more potent in A-498 cells as compared to Caki-2 cells. In addition, pre-treatment of RCC cells with NAC reverted the axitinib-induced effects on cell cycle at any experimental time point tested (Figure 4B, and data not shown).

An accumulation of RCC cells with enlarged and flattened morphology was observed at 48 h after axitinib treatment by microscopy and biparametric (forward scatter, FSS vs side scatter, SSC) cytofluorimetric analysis (Supplementary Figure 1). Since these morphological changes are reminiscent of a senescent phenotype, we analyzed the presence of senescence-associated

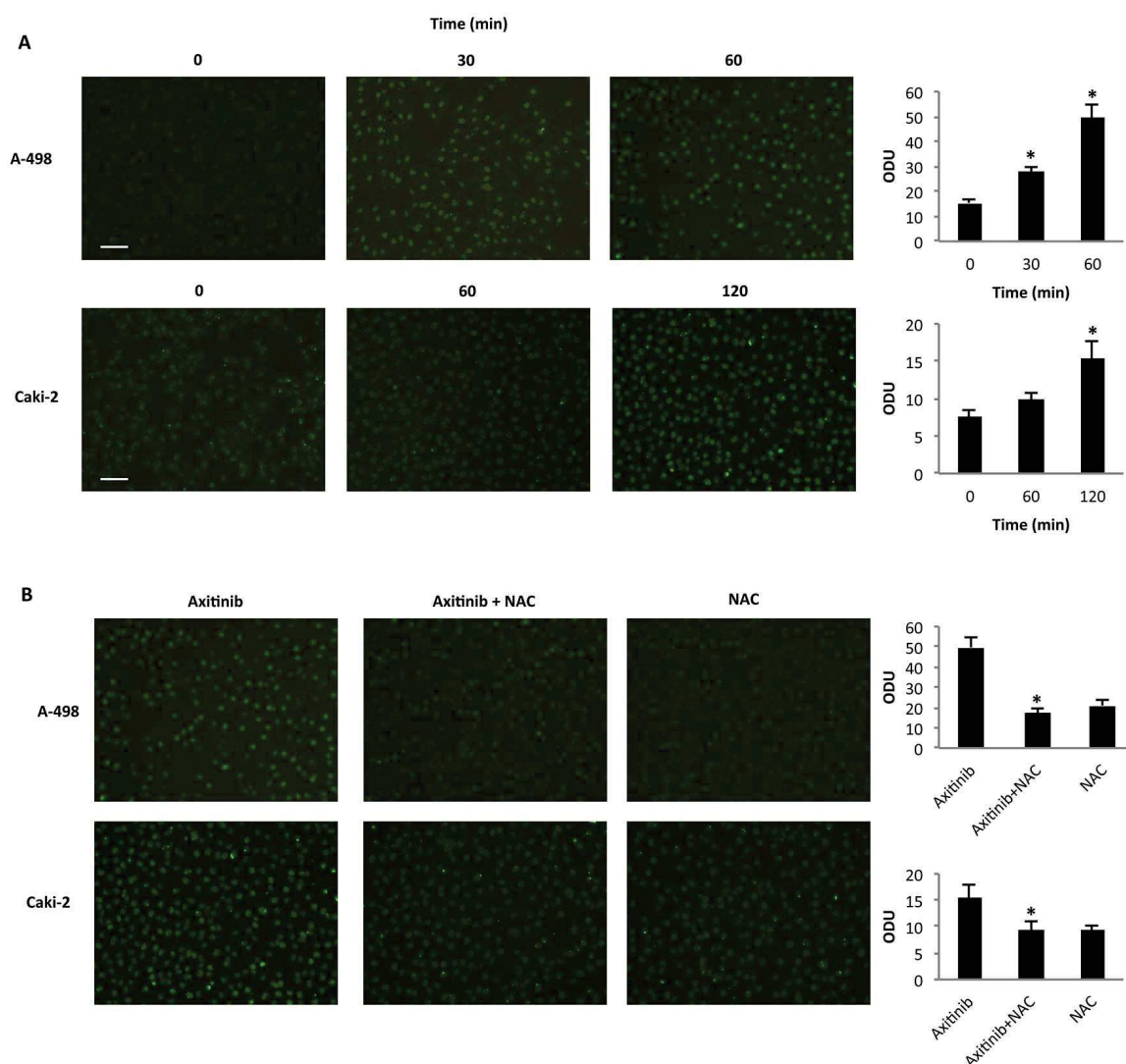


**Figure 3: Axitinib triggers oxidative DNA damage in RCC cells.** **A.** Immunofluorescence analysis of 8-oxo-dG in A-498 and Caki-2 RCC cells treated with axitinib (12.5  $\mu$ M and 25  $\mu$ M, respectively) for different times. Optical Density Units (ODU) were calculated on ten random fields. Data shown are representative of one of three separate experiments, \* $p < 0.01$  vs. untreated cells. Bar: 100  $\mu$ M. **B.** Immunofluorescence analysis of 8-oxo-dG in A-498 cells treated with axitinib 12.5  $\mu$ M for 60 min and in Caki-2 cells treated with axitinib 25  $\mu$ M for 120 min alone or pretreated with NAC (10 mM for 1 h). ODU were calculated on ten random fields. Data shown are representative of one of three separate experiments, \* $p < 0.01$  vs. axitinib treated cells. Bar: 100  $\mu$ M.

$\beta$ -galactosidase (SA- $\beta$ -gal) activity, in axitinib-treated cells [38,39]. Seventy-two hours after axitinib treatment, increased levels of SA- $\beta$ -gal activity were detected in RCC cells stained with the fluorescent  $\beta$ -galactosidase substrate, C<sub>12</sub>FDG as determined by flow cytometry. (Figure 5A).

Recent studies have suggested that reactive oxygen species (ROS) generation by anticancer drug treatment can stimulate cellular senescence [40]. Thus, we evaluated the generation of ROS in RCC cells by flow cytometry using the general redox-sensitive fluorescent dye, DCFDA. As shown in Figure 5B, axitinib stimulated intracellular generation of ROS that was evident at 24 h after exposure, being more rapid and sustained in A-498 cells. These results were also supported by cytochemical assessment of SA- $\beta$ -gal activity that revealed a significant reduction in the percentage of blu-stained axitinib-treated senescent cells after pretreatment with NAC (Figure 5C).

### Axitinib induces mitotic catastrophe in RCC cells

Mitotic catastrophe is a non-apoptotic cell death resulting from cell cycle arrest and abnormal mitosis,

usually ending in the formation of large cells with multiple micronuclei [41]. Thus we decided to study whether axitinib treatment could also result in mitotic catastrophe in RCC cells, by assessing the changes in nuclear morphology using Hoechst 33258 staining. Increased number of micronuclei was observed at 96 h in both RCC cell lines (Figure 6A). In addition, by examining the expression of  $\alpha$ -tubulin, abnormal microtubule assembly was found in axitinib-treated RCC cells at 96 h after treatment (Figure 6B). To further support mitotic catastrophe as the mode of death, FITC-conjugated Annexin V/PI and cytofluorimetric analysis, agarose gel electrophoresis for DNA fragmentation and western blot analysis for caspase-3 activity were performed in untreated or axitinib-treated cells. Axitinib treatment resulted in an increased percentage of cells undergoing necrotic-like death (Annexin V/PI<sup>+</sup>) and secondary necrosis (Annexin V<sup>+</sup>/PI<sup>+</sup>) upon drug exposure in both RCC cell lines, being the frequency of dead cells higher and the cell death program more advanced in A-498 cells as compared to Caki-2 cells (Figure 6C); moreover, neither DNA fragmentation (Figure 6D) or caspase-3 activation (Figure 6E) was evidenced in axitinib-treated RCC cells.

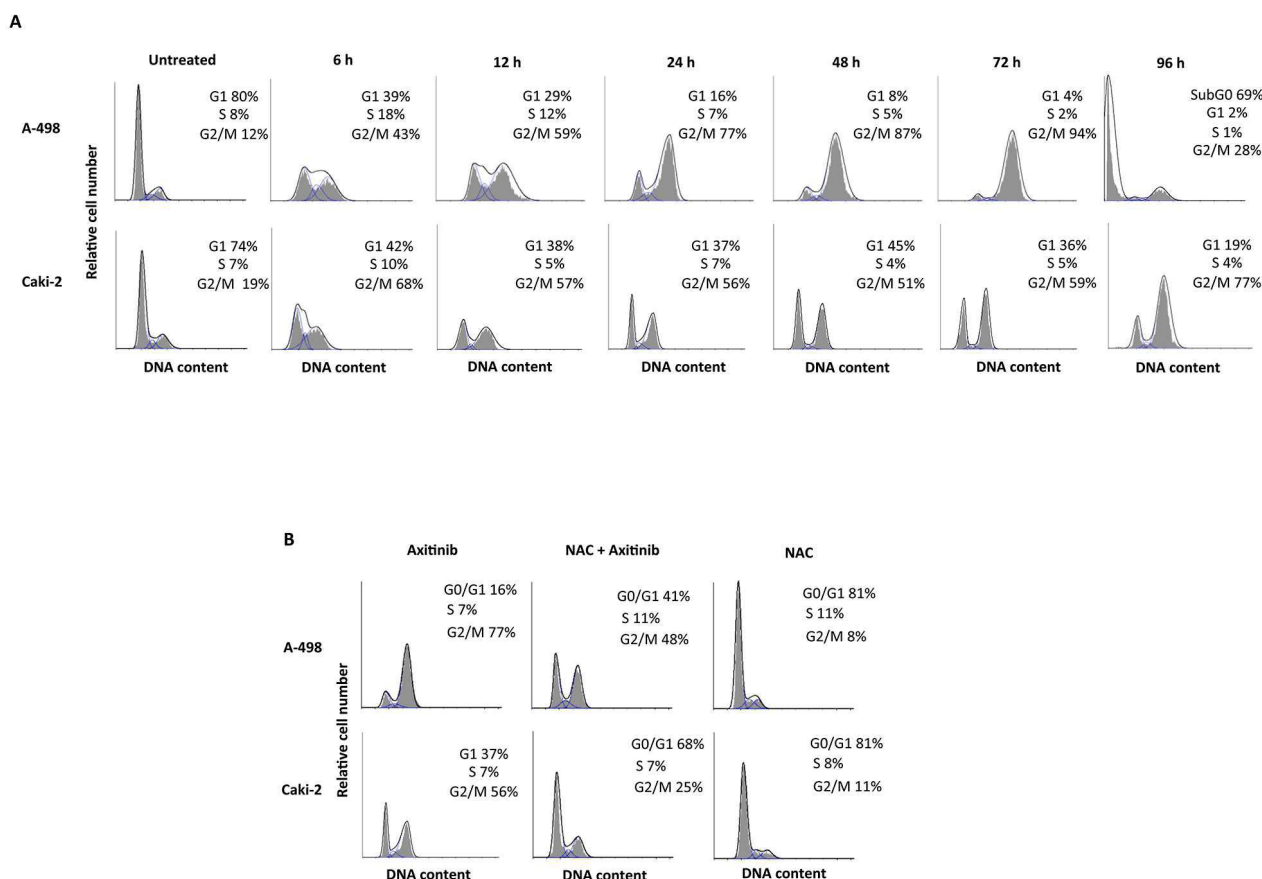


**Figure 4: Axitinib induces cell cycle arrest in ROS-dependent manner. A.** Cell cycle analysis in A-498 cells treated with axitinib 12.5  $\mu$ M and in Caki-2 cells treated with axitinib 25  $\mu$ M for the indicated times. **B.** Representative cell cycle distribution in A-498 and Caki-2 cells pretreated or not with NAC (10 mM for 1 h) before axitinib treatment for 24 h.

Taken together, these results indicate that axitinib induces cell death in RCC cells through mitotic catastrophe.

### Axitinib preferentially increases NKG2D ligand expression in senescent RCC cells

Since chemotherapeutic agents through the activation of the DDR have been shown to enhance the expression of NKG2D and DNAM-1 ligands on human multiple myeloma cells in a ROS-dependent manner [18], we investigated whether axitinib treatment could modulate the expression of the ligands for NKG2D and DNAM-1 activating NK receptors on A-498 and Caki-2 RCC lines, and the involvement of ROS signaling in this event. To this aim we firstly evaluated the basal expression of NKG2D (MICA, MICB, ULBP1, 2, 3, 5, 6) and DNAM-1 (PVR and nectin-2) ligands on A-498 and Caki-2 RCC cells by immunofluorescence and cytofluorimetric analysis. Both cell lines constitutively express MICA and ULBP family NKG2D ligands, and PVR and nectin-2 DNAM-1 ligands, but with a different profile (Figure 7A). Seventy-two hour treatment of RCC cells with axitinib induced MICB expression in A-498 cells, and increased the expression of

ULBP1 and MICA in Caki-2 cells, respectively (Figure 7A). In addition, down-regulation of nectin-2 and PVR DNAM-1 ligands was observed in Caki-2 cells upon drug exposure (Figure 7A). Moreover, we found that MICB was preferentially expressed on FDG-positive A-498 cells undergoing senescence as demonstrated by double immunofluorescence and flow cytometry (Figure 7B).

We next investigated the expression of MICB, MICA and ULBP1 on PI A-498 and Caki-2 RCC cells, respectively, in the presence of anti-oxidant NAC. Exposure of RCC cells to NAC resulted in complete inhibition of MICB and ULBP1 expression in A-498 and Caki-2 cells, respectively (Figure 8A and 8B), whereas NAC pretreatment did not significantly reduce axitinib-induced increase of MICA expression on Caki-2 cells that exhibited a weaker oxidative stress response.

### Enhanced NK cell degranulation upon interaction with axitinib-treated A-498 RCC cells

Based on these findings, we evaluated whether axitinib would increase NK cell degranulation upon interaction with drug-treated RCC cells. The expression of the lysosomal marker CD107a, which correlates

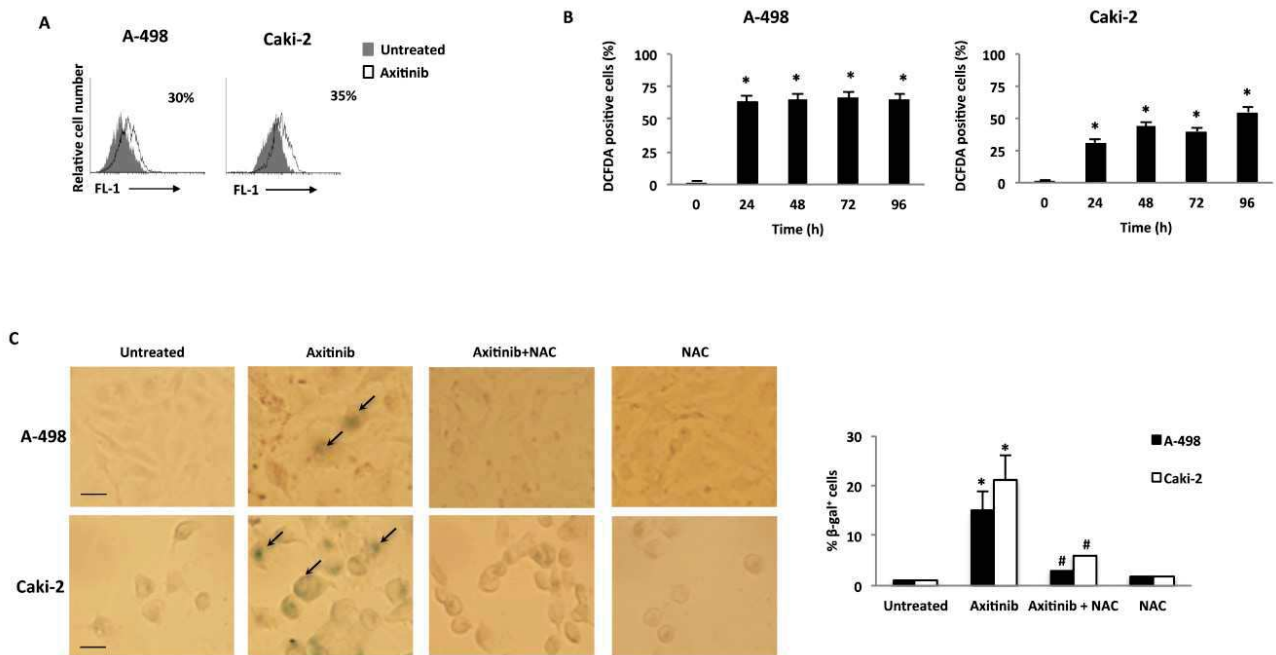


**Figure 5: Axitinib induces cellular senescence in RCC cells in a ROS-dependent manner.** **A.** Representative flow cytometric profiles of RCC cells untreated or treated with axitinib for 72 h, then stained with  $C_{12}$ FDG, a fluorogenic substrate for SA- $\beta$ -galactosidase before analysis. Data represent the percentage of positive cells. **B.** ROS generation in RCC cell lines treated with axitinib for the indicated times. Cells were stained with DCFDA before flow cytometric analysis. Data are expressed as percentage of DCFDA positive cells with respect to untreated cells; \* $p < 0.01$  treated vs. untreated cells. **C.** Cellular senescence was assessed in A-498 cells treated with axitinib 12.5  $\mu$ M and in Caki-2 cells treated with axitinib 25  $\mu$ M for 72 h, with or without pretreatment with NAC 10 mM for 1 h, by detection of SA- $\beta$ -galactosidase activity using cytochemistry. Arrows indicate blue-stained positive cells. Graph represents the percentage of  $\beta$ -galactosidase<sup>+</sup> cells calculated on ten random fields. Data shown are representative of one of three separate experiments, \* $p < 0.01$  vs. untreated cells. # $p < 0.01$  vs. axitinib-treated cells. Bar: 25  $\mu$ M.

with NK cell cytotoxicity [42] was evaluated by immunofluorescence and flow cytometry analysis by gating on CD56<sup>+</sup> human peripheral blood NK cells contacting treated or untreated RCC cells used as target. The expression of CD107a on NK cells from two different healthy donors contacting axitinib treated-RCC target cells, revealed that drug-treated A-498 RCC cells more efficiently triggered NK cell degranulation as compared to untreated cells, and this enhancement is completely blocked by NAC pretreatment, in parallel with inhibition of MICB induction (Figure 9). Conversely, no significant changes in CD107a expression were observed on NK cells contacting axitinib-treated Caki-2 cells (Supplementary

Figure 2), likely attributable to the lower responsiveness of these cells to the axitinib-exerted activity.

## DISCUSSION

TKIs and in particular axitinib have been recently approved for the treatment of advanced mRCC, mainly for their anti-angiogenic properties. Herein, we provide evidence indicating that axitinib anti-tumor activity can be also the result of its ability to induce DDR, cellular senescence and mitotic catastrophe, and to enhance the recognition of RCC cells by innate immune effector cells through the modulation of activating ligands.

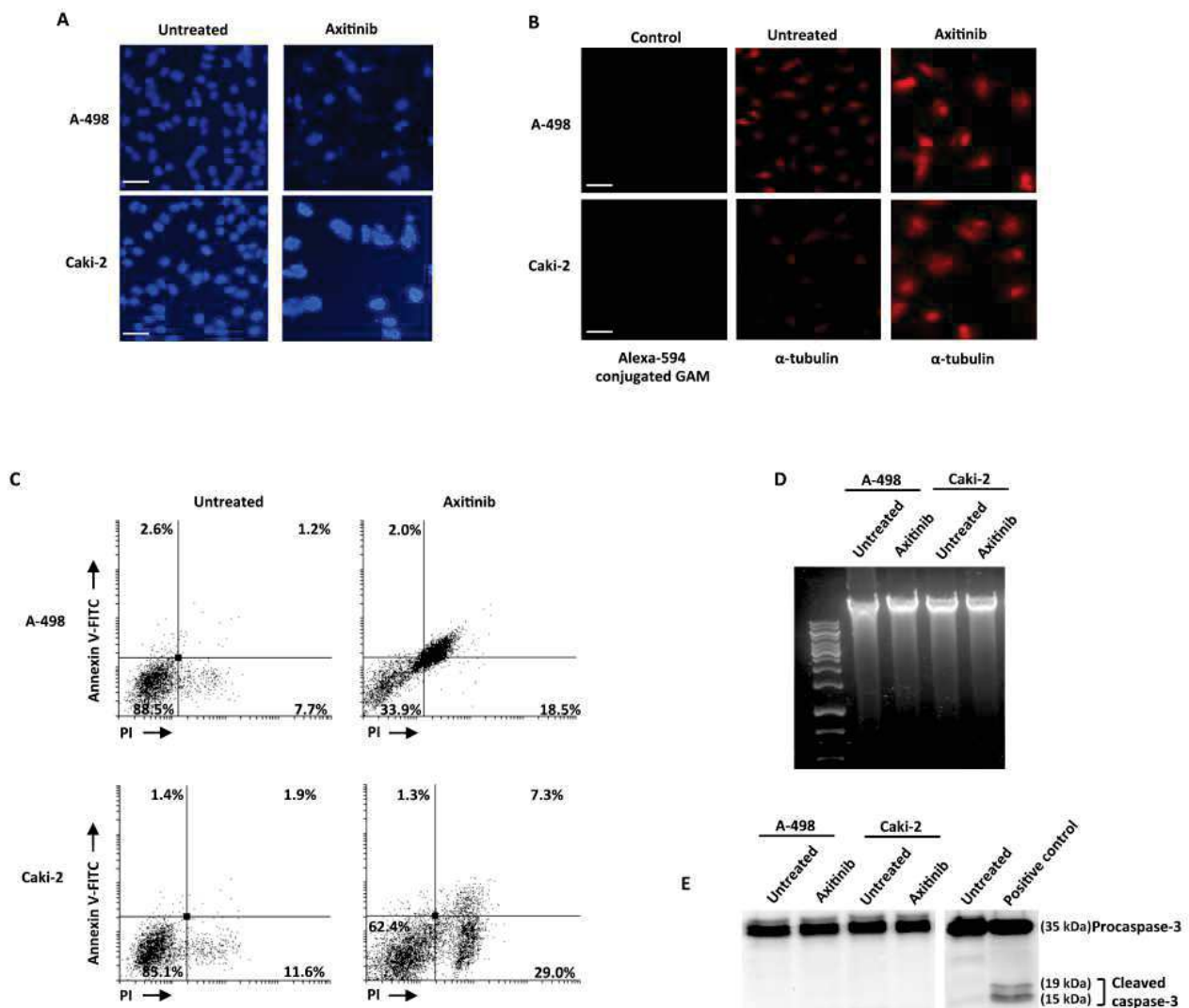


**Figure 6: Axitinib induces mitotic catastrophe in RCC cells.** **A.** Nuclei of RCC cells untreated or treated with axitinib for 96 h were stained with Hoechst 33258 and then analyzed on ten random fields. Cells were observed under a fluorescence microscope. Bar: 50  $\mu$ M. **B.** Representative images of RCC cells treated as above described, and then immunostained with anti- $\alpha$ -tubulin antibody. Bar: 50  $\mu$ M. **C.** RCC cells were cultured for 96 h with axitinib. Flow cytometric analysis was performed on treated cells by Annexin V-FITC and PI double-staining. Data represent the percentage of PI and/or Annexin V positive cells. **D.** Representative agarose gel electrophoresis of DNA extracts obtained from untreated or axitinib treated cells at 96 h for assessment of DNA fragmentation. **E.** Representative immunoblot of caspase-3 in RCC cells treated as above described.

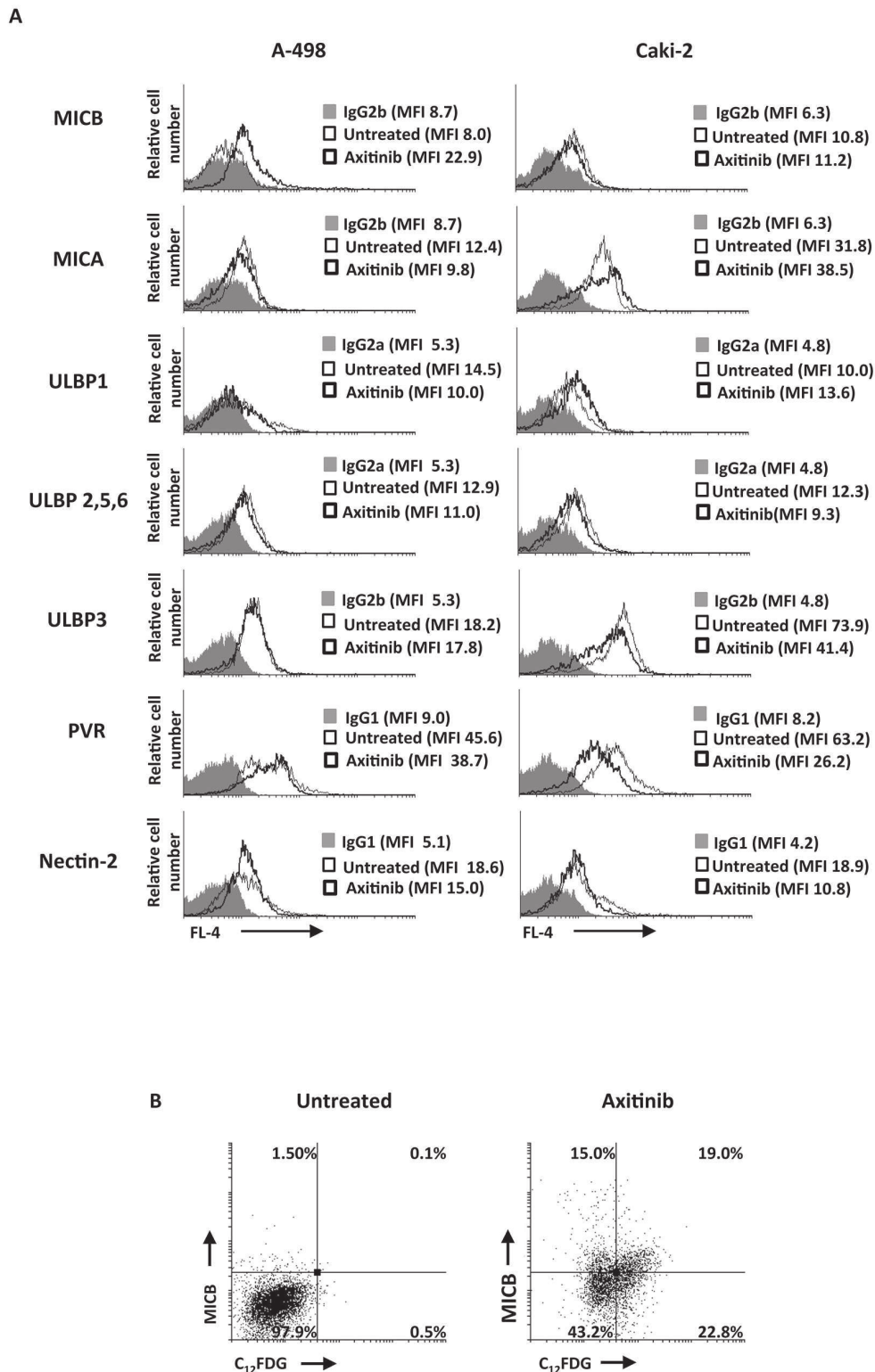


**Figure 7: Modulation of NKG2D and DNAM-1 ligand expression on the RCC cell lines by axitinib treatment.** A. MICB, MICA, ULBP1, ULBP2, 5, 6 and ULBP3, PVR and nectin-2 surface expression was analyzed by flow cytometry on RCC cells treated for 72 h with axitinib or untreated. Light lines represent ligand expression in untreated cells, dark lines represent ligand expression in axitinib-treated RCC cells, whereas gray histogram isotype controls. MFI, mean fluorescence intensity. B. Representative dot plots illustrating the double fluorescence MICB-APC/C<sub>12</sub>FDG in A-498 RCC cells treated as above described. Numbers represent the percentage of cells in each quadrant. Results are representative of 1 of 3 independent experiments.

In particular, we found that treatment of RCC with suboptimal doses of axitinib triggers a DDR evidenced by increased levels of H2AX, Ser317- and Ser345-Chk1 phosphorylation and DNA oxidation, leading to cell cycle arrest at G2/M phase and cellular senescence. At later time points, overexpression of the cell cycle inhibitor p21 was observed and paralleled decreased levels of Chk1 activation and depletion. In this regard, reactivation of a senescence program in PC-3 prostate cancer cells upon a retrovirus-mediated transduction of p21, was described to suppress Chk1 activation [43].

We also investigated the involvement of redox signaling on the ability of axitinib treatment to induce cellular senescence in A-498 and Caki-2 RCC cells. We found that drug exposure increases ROS generation and induces the DNA oxidation, whereas pretreatment with the

antioxidant agent NAC results in impaired cell cycle arrest and decreased percentage of SA- $\beta$ -gal positive cells.

Similarly to our study, treatment of gastric cancer cells with axitinib was reported to induce a senescent phenotype characterized by increased cell size, expression of SA- $\beta$ -galactosidase and arrest in G2 cell cycle phase [44].

Cell cycle arrest and senescence are often associated with mitotic catastrophe. Chk1, the kinase that regulates the G2/M checkpoint, is also particularly important for preventing mitotic catastrophe in cells treated with DNA-damaging agents [45-47]. Mitotic catastrophe has been described as the main form of cell death induced by anticancer drugs [48, 49]. Similarly to necrosis, mitotic catastrophe shows early loss of plasma membrane integrity, with large cells containing uncondensed

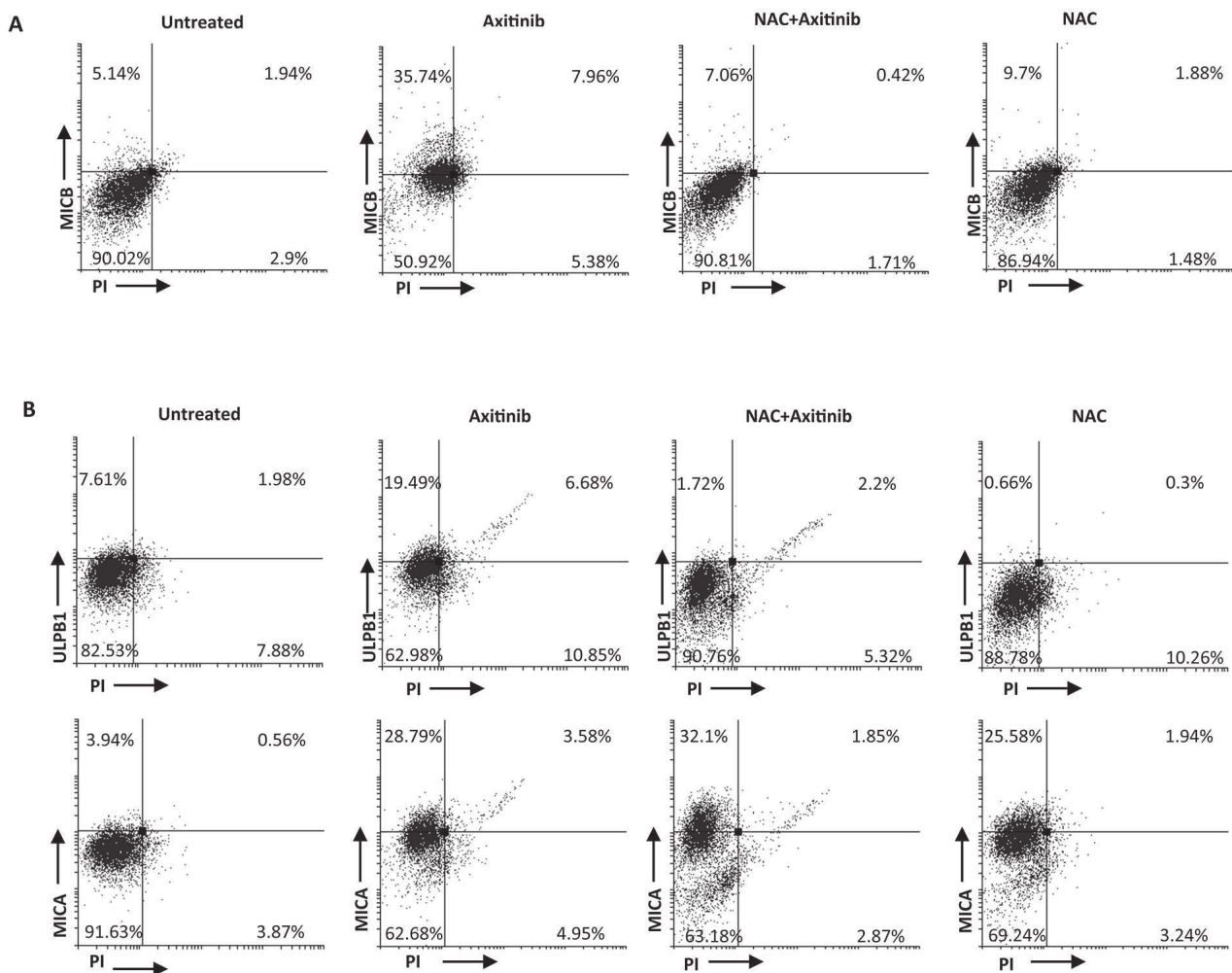


**Figure 8: ROS-dependent axitinib-induced increase of NKG2D ligand expression in the RCC cell lines. A.** Increase of MICB surface expression was analyzed by flow cytometry on A-498 RCC cell line treated with axitinib for 72 h with or without pretreatment with NAC 10 mM for 1 h. Representative dot plots illustrate the double fluorescence ligands-APC/PI. Numbers represent the percentage of cells in each quadrant. Data are representative of 1 of 4 independent experiments. **B.** Increase of MICA and ULBP1 surface expression was analyzed by flow cytometry on Caki-2 RCC cells treated with axitinib for 72 h with or without pretreatment with NAC 10 mM for 1 h. Representative dot plots illustrate the double fluorescence ligands-APC/PI. Numbers represent the percentage of cells in each quadrant. Data are representative of 1 of 4 independent experiments.

chromosomes [50]. Treatment with axitinib caused an increased frequency of cells undergoing necrotic-like death and secondary necrosis as well as mitotic catastrophe characterized by multinucleation, abnormal microtubule assembly, early membrane permeabilization and absence of apoptotic features such as caspase 3 activation and DNA fragmentation.

Our study provides also evidence that axitinib treatment increases the surface expression of stress-induced ligands recognised by innate immune effector cells.

Up-regulation of stress-inducible NK-cell activating ligands is preferentially associated with the onset of a senescent phenotype and arrest in the G2 phase of the cell cycle [51]. Our findings demonstrate that A-498 and Caki-2 RCC cells constitutively express, although at different levels, several NKG2D and DNAM-1 ligands. Axitinib treatment induced MICB expression in A-498 RCC cells and increased ULBP1 and MICA expression in Caki-2 cells. In addition in these latter cells, significative down-regulation of the DNAM-1 ligand PVR was observed.

We also demonstrated that induction of MICB on A-498 RCC cells and ULBP-1 on Caki-2 cells requires ROS signaling as ligand up-regulation was susceptible to NAC pretreatment. By contrast, in Caki-2 cells pretreated with NAC, no reversal of axitinib-induced increase of MICA expression was evident. Moreover, in accordance with previous evidence indicating that NKG2D and DNAM-1 ligand are expressed on tumor cells with senescent phenotype upon treatment with genotoxic agents [52], we found a preferential expression of MICB on axitinib-treated senescent A-498 RCC cells. Like axitinib, other TKIs such as sorafenib and sunitinib have

been described to induce the expression of MICA/B in nasopharyngeal carcinoma cells [53], but their association with a senescent phenotype was not reported.

As far as the mechanisms underlying axitinib-induced MICB expression, a role for Signal transducer and activator of transcription 3 (STAT3) inhibition can be envisaged based on the recent evidences demonstrating that axitinib can stimulate anti-tumor immunity by down-regulating the STAT3 expression in Renca RCC cells [54], and MICA/B expression on cancer cells induced by genotoxic stress is enhanced by inhibition of STAT3 activity [55].

Our results also show increased degranulation activity in NK cells contacting axitinib-treated A-498 but not Caki-2 RCC cells. The failure of axitinib-treated Caki-2 cells to promote NK cell degranulation as compared to A-498 RCC cells may depend on the less potent and sustained DDR induced by axitinib in this tumor cell line. In addition, this result may be related to the drug-induced down-regulation of DNAM-1 ligand expression observed in these cells leading to lack of cooperative signals required for the triggering of NK cell cytotoxic program [56].

Collectively, our findings are consistent with previous evidence describing RCC susceptibility to NK cell-mediated cytotoxicity, and the presence of a high frequency of NK cells in the lymphocytic infiltrate of RCC predicting a better prognosis [57]. Moreover, interleukin-2 (IL-2) in combination with infusion of IL-2-activated NK and LAK cells has been widely employed as immunotherapeutic approach for RCC patients [58].

Based on these findings, the use of axitinib in sequential or combined strategies with other

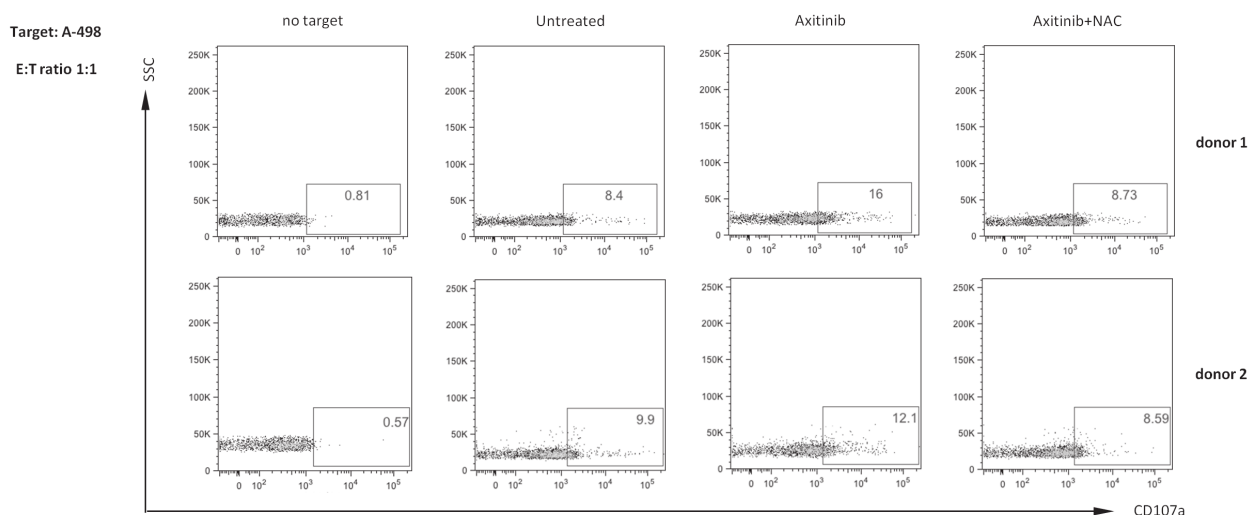


**Figure 9: Enhanced NK cell degranulation upon interaction with axitinib-treated A-498 RCC cells is ROS-dependent.** A-498 RCC cells were treated with axitinib 12.5  $\mu$ M for 72 h with or without pretreatment with NAC 10 mM for 1 h, and then incubated with freshly isolated human peripheral blood NK cells from two different healthy donors at 1:1 ratio for 2 h. Results are expressed as percentage of CD107a<sup>+</sup> NK cells.

immunotherapeutic approaches, such as anti-programmed death-1 (PD-1) or PD-ligand 1 (PD-L1) agents, should be tested in prospective clinical trials. At this regard, a phase I study is in course to assess the safety of axitinib in combination with avelumab (MSB0010718C), an anti-PD-L1 antibody, in patients with advanced RCC (NCT02493751).

Taken together, our study first demonstrate that axitinib not only inhibits angiogenesis, but it can exert direct genotoxic effects on RCC cells by inducing cell cycle arrest and mitotic catastrophe, and activating a cellular senescence program. This direct cytotoxic effect of axitinib in RCC cells may partially explain the relevant gastrointestinal and hematologic toxicity of this agent [12].

In addition, axitinib can also display an immune-mediated antitumor activity by promoting NK cell-mediated recognition and elimination of RCC through the regulation NK activating ligand expression. A better dissection of the functions of immune cells in RCC microenvironment and of the immune-modulatory effects of TKIs will be crucial to optimize immunotherapeutic approaches in RCC advanced patients.

## MATERIALS AND METHODS

### Cell line culture and treatment

Human kidney cancer (Caki-2 and A-498) cell lines were purchased from Cell bank Interlab Cell Line Collection (ICLC, Italy) and cultured at 37°C in a humidified atmosphere of 5% CO<sub>2</sub>. Caki-2 cells were cultured in McCoy's 5a medium (Lonza Bioresearch, Basel, Switzerland) supplemented with 10% (v/v) heat-inactivated fetal bovine serum (FBS), 2mM L-glutamine and 100 IU/ml of penicillin, 100 µg of streptomycin (Lonza). A-498 cells were cultured in EMEM medium (Lonza) supplemented with 10% (v/v) heat-inactivated FBS 2mM L-glutamine and 100 IU/ml of penicillin, 100 µg of streptomycin and 1 mM sodium pyruvate (Lonza).

A-498 and Caki-2 cells were treated with different doses of axitinib (1, 2.5, 5.0, 10.0, 12.5, 25.0, 50.0 and 100 µM) for different times. In some experiments Caki-2 and A-498 cells were pretreated for 1 h with 10 mM of NAC, before axitinib treatment.

### Reagents

Axitinib ((Inlyta®) was kindly provided by Pfizer (New York, NY, USA). The following mouse monoclonal allophycocyanin (APC)-conjugated antibodies (Abs) were used: anti-MICB, anti-MICA, anti-PVR, anti-ULBP1, anti-ULBP 2,5,6, anti-ULBP3 and anti-nectin-2 (R&D Systems, Abingdon, United Kingdom). APC-

conjugated goat affinity purified F(ab')<sub>2</sub> fragment to mouse IgG1, IgG2a, IgG2b were purchased from Jackson ImmunoResearch Laboratories (West Grove, PA). Mouse anti- $\alpha$ -tubulin and anti-p21 antibodies were purchased from Santa Cruz Biotechnology (Santa Cruz, CA). Rabbit anti-H2AX, anti-Chk1-Ser345, anti-Chk1-Ser317, anti-Chk1 and anti-caspase-3 were purchased from Cell Signaling Technology (Danvers, MA). The following secondary antibodies were used: horseradish peroxidase (HRP)-conjugated sheep anti-mouse IgG and HRP-conjugated donkey anti-rabbit IgG (GE Healthcare, Munich, Germany). Annexin V-FITC was purchased from eBioscience (Hatfield, UK). 8-oxo-7,8-dihydro-2'-deoxyguanosine (8-oxo-dG) MAb was purchased from Trevigen (Gaithersburg, MD, USA). Goat anti-mouse (GAM) Alexa Fluor 594 and 5-dodecanoylaminofluorescein di- $\beta$ -D- galactopyranoside (C<sub>12</sub>FDG) were from Invitrogen (San Diego, CA, USA). Bafilomycin A1, dimethyl sulfoxide (DMSO, used as vehicle), Hoechst 33258, propidium iodide (PI, 1 µg/ml), ribonuclease A, 5-bromo-4-chloro-3-indolyl  $\beta$ -D-galactopyranoside (X-Gal), N-acetyl-L-cysteine (NAC), 3-(4,5-dimethylthiazol-2-yl)-2,5-diphenyltetrazolium bromide (MTT) and anti-glyceraldehyde-3-phosphate dehydrogenase (GAPDH)-peroxidase were from Sigma Aldrich (St. Louis, USA).

### MTT assay

The colorimetric MTT assay was used to evaluate the cell viability. Three  $\times 10^5$  RCC cells/ml were seeded into 96-well plates and cultured with different doses of axitinib for up to 96 h. At the end of treatment, 0.8 mg/ml of MTT was added to the samples and incubated for 3 h. Then the supernatants were discarded and coloured formazan crystals dissolved with 100 µl/well of DMSO, were read by an enzyme-linked immunosorbent assay reader (BioTek Instruments, Winooski, USA). Four replicates were used for each treatment.

### Cell cycle analysis

Three  $\times 10^5$  RCC cells/ml were treated with vehicle or axitinib, alone or in combination with NAC, for up to 72 h. Cells were collected and fixed in 70% ethanol and then washed with staining buffer (PBS, 2% FBS and 0.01% NaN<sub>3</sub>). Next, the cells were treated with 100 µg/ml ribonuclease A solution, incubated for 30 min at 37°C, stained for 30 min at room temperature with PI 20 µg/ml and finally analysed by flow cytometry using linear amplification.

## Western blot analysis

Cells were lysed in lysis buffer (1M Tris pH 7.4, 1 M NaCl, 10 mM EGTA, 100 mM NaF, 100 mM NaVO<sub>3</sub>, 100 mM phenylmethylsulfonyl fluoride, 2% deoxycholate, 100 mM EDTA, 10% Triton X-100, 10% glycerol, 10% SDS, 0.1 M Na<sub>4</sub> P<sub>2</sub> O<sub>7</sub>) containing protease inhibitor cocktail (Sigma-Aldrich) by using a Mixer Mill MM300 (Qiagen, Hilden, Germany). Lysates were separated on SDS polyacrylamide gel and transferred onto Hybond-C extra membranes (GE Healthcare). Membrane were incubated overnight at 4°C in primary Abs (anti-caspase 3 1:100; anti-H2AX 1:1000, anti-Chk1-Ser345 1:1000, anti-Chk1-Ser317 1:1000, anti-Chk1 1:1000, anti-p21 1:300), followed by the incubation (room temperature, 1 h) with HRP-conjugated anti-rabbit or anti-mouse secondary Abs. Peroxidase activity was visualized with the LiteAblot®PLUS (EuroClone, Milan, Italy) kit and densitometric analysis was carried out by a Chemidoc using the Quantity One software (Bio-Rad).

## Senescence analysis

We performed the senescence analysis by both microscope and flow cytometry. RCC cells were treated with axitinib or vehicle before performing the senescence-associated  $\beta$ -galactosidase (SA- $\beta$ -Gal) assay. Cells were then fixed for 5 min at room temperature in 3% formaldehyde and incubated overnight at 37°C without CO<sub>2</sub> with fresh SA- $\beta$ -Gal stain solution: 1 mg/mL 5-bromo-4-chloro-3-indolyl  $\beta$ -D-galactoside (X-Gal), 150 mM NaCl, 2 mM MgCl<sub>2</sub>, 40 mM citric acid, 5 mM sodium phosphate (pH 6.0), 5 mM potassium ferrocyanide, and 5 mM potassium ferricyanide. Senescent cells were identified as blue-stained cells by standard light microscopy. Photographs were acquired and analyzed by an Olympus BX51 microscope (Hamburg, Germany) using magnification 40x.

Relatively to flow cytometry, we performed the assay using the fluorogenic substrate C<sub>12</sub>FDG. Drug-treated cells were incubated 1 h at 37°C and 5% CO<sub>2</sub> with 100 nM bafilomycin A1 in culture medium to induce lysosomal alkalization at pH 6 and, then, for 1 h with 33  $\mu$ M C<sub>12</sub>FDG. Samples were immediately analyzed using FACScan cytofluorimeter using the CellQuest software. The C<sub>12</sub>-fluorescein signal was measured on the FL-1 detector, and  $\beta$ -galactosidase activity was estimated using the median fluorescence intensity (MFI) of the population.

## Annexin V and PI staining

Cell death was evaluated using Annexin V-FITC and PI staining followed by biparametric FACS analysis. Three  $\times 10^5$  A-498 and Caki-2 RCC cells were treated with

axitinib or with vehicle for up to 96 h. The percentage of positive cells determined over 10,000 events was analyzed on a FACScan cytofluorimeter using the CellQuest software.

## DNA fragmentation assay

RCC cells were treated as above described for up to 96 h, and genomic DNA was extracted using a DNA extraction kit (Qiagen). The purified samples were then subjected to electrophoresis on a 1.25% agarose gel, and DNA was stained with ethidium bromide. Ultraviolet spectroscopy at 302 nm was used to obtain the results.

## Reactive Oxygen Species (ROS) production

Cells were cultured for up to 96 h with axitinib or vehicle. Cells were washed with PBS, pulsed with DCFDA for 10 min at 37°C, 5% CO<sub>2</sub>, and analyzed by FACScan cytofluorimeter using the CellQuest software.

## $\alpha$ -Tubulin and nuclei staining

Cells cultured as above described were fixed in 2% formaldehyde and 0.5% triton X-100 for 10 min at room temperature and then in 4% formaldehyde and 0.5% triton X-100 for 10 min. To examine the expression of  $\alpha$ -tubulin, fixed cells were permeabilized in 0.1% Tween-20/3% BSA, and stained with mouse anti- $\alpha$ -tubulin antibody (1:50). Cells were further incubated with Alexa-594-conjugated GAM (1:100). For nuclei analysis, cells were fixed in Carnoy's fixative (1:3 glacial acetic acid: absolute methanol) and stained with 0,05  $\mu$ g/ml Hoechst 33258. Stained cells were examined by using the Olympus BX51 microscope.

## Immunofluorescence and microscopic analysis

For immunofluorescence analysis, RCC cells were fixed with 1:1 MeOH, acetone for 20 min at -20°C and labeled with anti-8-hydroxyguanine (8-oxo-dG) antibody (1:250) diluted in 1X PBS containing 1% BSA, 0.01% Tween 20 at 4°C o/n in a humidified chamber according to manufacturer's instructions. Cells were further incubated with Alexa-594-conjugated GAM (1:100). Photographs were acquired and analyzed by an Olympus BX51 microscope.

## Cytofluorimetric analysis

NKG2D and DNAM-1 ligand surface expression on Caki-2 and A-498 cells was analyzed by immunofluorescence staining using anti-MICA, anti-

MICB, anti-ULBP1/2,5,6/3, anti-PVR or anti-nectin-2 APC-conjugated mAbs or relative APC-conjugated IgG isotypes according to manufacturer's instructions. In some experiments, RCC cells were double stained with anti-MICB APC-conjugated mAb and C<sub>12</sub>FDG or with anti-MICB, anti-MICA, anti-ULBP1 APC-conjugated mAbs and PI. Fluorescence was analyzed by FACScan cytofluorimeter using the CellQuest software.

## Degranulation assay

NK cell-mediated cytotoxicity was evaluated using the degranulation lysosomal marker CD107a as described [42]. As source of effector cells freshly purified NK cells were used. Peripheral blood mononuclear cells (PBMC) were separated from buffy coats of healthy donors by Lymphoprep (Nycomed, Oslo, Norway) gradient centrifugation. Freshly isolated NK cells were then isolated from PBMC by negative selection using a magnetically activated cell sorter NK isolation kit (Miltenyi Biotec, Bologna, Italy). This purification protocol resulted in a purity of more than 95% of negatively selected NK cells. After 72 h treatment with axitinib, RCC cells were incubated with NK cells at effector:target (E:T) ratios of 1:1 in a flat-bottom 96-well tissue culture plate in complete medium. In some experiments axitinib-treated where exposed to NAC (10 mM, for 1 h). The plates were then incubated at 37 °C in a 5% CO<sub>2</sub> atmosphere for 2 h. Thereafter, cells were incubated with anti-CD107a/APC (or cIgG/APC) for 45 min at 4 °C. Cells were also stained with anti-CD56/PE to gate NK cell population.

## Statistical analysis

The data presented represent the mean and standard deviation (SD) of at least 3 independent experiments. The statistical significance was determined by Student's t-test and by one way ANOVA; \*,#  $p < 0.01$ . The statistical analysis of IC<sub>50</sub> levels was performed using Prism 5.0a (Graph Pad).

## ACKNOWLEDGMENTS

This study was supported by AIRC IG 2014, cod. 15821. We thank Pfizer Inc for kindly providing the TKI, axitinib.

## CONFLICTS OF INTEREST

There is no conflict of interest.

## REFERENCES

1. Ferlay J, Steliarova-Foucher E, Lortet-Tieulent J, Rosso S, Coebergh JW, Comber H, Forman D, Bray F. Cancer incidence and mortality patterns in Europe: estimates for 40 countries in 2012. *Eur J Cancer*. 2013; 49: 1374-1403.
2. Athar U, Gentile TC. Treatment options for metastatic renal cell carcinoma: a review. *Can J Urol*. 2008; 15: 3954-3966.
3. Motzer RJ, Bander NH, Nanus DM. Renal-cell carcinoma. *N Engl J Med*. 1996; 335: 865-875.
4. Négrier S, Raymond E. Antiangiogenic treatments and mechanisms of action in renal cell carcinoma. *Invest New Drugs*. 2012; 30: 1791-1801.
5. Escudier B, Eisen T, Stadler WM, Szczylik C, Oudard S, Siebels M, Negrier S, Chevreau C, Solska E, Desai AA, Rolland F, Demkow T, Hutson TE, et al. Sorafenib in advanced clear-cell renal-cell carcinoma. *N Engl J Med*. 2007; 356: 125-134.
6. Motzer RJ, Hutson TE, Tomczak P, Michaelson MD, Bukowski RM, Rixe O, Oudard S, Negrier S, Szczylik C, Kim ST, Chen I, Bycott PW, Baum CM, et al. Sunitinib versus interferon alfa in metastatic renal-cell carcinoma. *N Engl J Med*. 2007; 356: 115-124.
7. Hudes G, Carducci M, Tomczak P, Dutcher J, Figlin R, Kapoor A, Staroslawska E, Sosman J, McDermott D, Bodrogi I, Kovacevic Z, Lesovoy V, Schmidt-Wolf IG, et al. Temsirolimus, interferon alfa, or both for advanced renal cell carcinoma. *N Engl J Med*. 2007; 356: 2271-2281.
8. Escudier B, Bellmunt J, Négrier S, Bajetta E, Melichar B, Bracarda S, Ravaud A, Golding S, Jethwa S, Sneller V. Bevacizumab plus interferon alfa-2a for treatment of metastatic renal cell carcinoma: a randomized, double-blind phase III trial. *J Clin Oncol*. 2010; 28: 2144-2150.
9. Motzer RJ, Escudier B, Oudard S, Hutson TE, Porta C, Bracarda S, Grünwald V, Thompson JA, Figlin RA, Hollaender N, Urbanowitz G, Berg WJ, Kay A, et al. Efficacy of everolimus in advanced renal cell carcinoma: a double-blind randomised placebo-controlled phase III trial. *Lancet*. 2008; 372: 449-456.
10. Rini BI, Halabi S, Rosenberg JE, Stadler WM, Vaena DA, Ou SS, Archer L, Atkins JN, Picus J, Czaykowski P, Dutcher J, Small EJ. Bevacizumab plus interferon alfa compared with interferon alfa monotherapy in patients with metastatic renal cell carcinoma: CALGB 90206. *J Clin Oncol*. 2008;26: 5422-5428.
11. Sternberg CN, Davis ID, Mardiak J, Szczylik C, Lee E, Wagstaff J, Barrios CH, Salman P, Gladkov OA, Kavina A, Zarbá JJ, Chen M, McCann L, et al. Pazopanib in locally advanced or metastatic renal cell carcinoma: results of a randomized phase III trial. *J Clin Oncol*. 2010; 28: 1061-1068.
12. Rini BI, Escudier B, Tomczak P, Kaprin A, Szczylik C, Hutson TE, Michaelson MD, Gorbunova VA, Gore ME, Rusakov IG, Negrier S, Ou YC, Castellano D, et al. Comparative effectiveness of axitinib versus sorafenib in advanced renal cell carcinoma (AXIS): a randomised phase 3 trial. *Lancet*. 2011;378: 1931-1939.

13. Tzogani K, Skibeli V, Westgaard I, Dalhus M, Thoresen H, Slot KB, Damkier P, Hofland K, Borregaard J, Ersbøll J, Salmonson T, Pieters R, Sylvester R, et al. The European Medicines Agency approval of axitinib (Inlyta) for the treatment of advanced renal cell carcinoma after failure of prior treatment with sunitinib or a cytokine: summary of the scientific assessment of the committee for medicinal products for human use. *Oncologist*. 2015; 20: 196-201.
14. Hutson TE, Lesovoy V, Al-Shukri S, Stus VP, Lipatov ON, Bair AH, Rosbrook B, Chen C, Kim S, Vogelzang NJ. Axitinib versus sorafenib as first-line therapy in patients with metastatic renal-cell carcinoma: a randomised open-label phase 3 trial. *Lancet Oncol*. 2013; 14: 1287-1294.
15. Koie T, Ohyama C, Yoneyama T, Yamamoto H, Imai A, Hatakeyama S, Hashimoto Y, Yoneyama T, Tobisawa Y, Mori K. Feasibility of axitinib as first-line therapy for advanced or metastatic renal cell carcinoma: a single-institution experience in Japan. *BMC Urol*. 2015; 15: 32.
16. Hu-Lowe DD, Zou HY, Grazzini ML, Hallin ME, Wickman GR, Amundson K, Chen JH, Rewolinski DA, Yamazaki S, Wu EY, McTigue MA, Murray BW, Kania RS, et al. Nonclinical antiangiogenesis and antitumor activities of axitinib (AG-013736), an oral, potent, and selective inhibitor of vascular endothelial growth factor receptor tyrosine kinases 1, 2, 3. *Clin Cancer Res*. 2008; 14: 7272-7283.
17. Yuan H, Cai P, Li Q, Wang W, Sun Y, Xu Q, Gu Y. Axitinib augments antitumor activity in renal cell carcinoma via STAT3-dependent reversal of myeloid-derived suppressor cell accumulation. *Biomed Pharmacother*. 2014; 68 :751-756.
18. Soriani A, Iannitto ML, Ricci B, Fionda C, Malgarini G, Morrone S, Peruzzi G, Ricciardi MR, Petrucci MT, Cippitelli M, Santoni A. Reactive oxygen species- and DNA damage response-dependent NK cell activating ligand upregulation occurs at transcriptional levels and requires the transcriptional factor E2F1. *J Immunol*. 2014;193: 950-960.
19. Bakkenist CJ, Kastan MB. Initiating cellular stress responses. *Cell*. 2004; 118: 9-17.
20. Kastan MB, Bartek J. Cell-cycle checkpoints and cancer. *Nature*. 2004;432: 316-323.
21. Niida H, Nakanishi M. DNA damage checkpoints in mammals. *Mutagenesis*. 2006; 21: 3-9.
22. Zhao H, Piwnicka-Worms H. ATR-mediated checkpoint pathways regulate phosphorylation and activation of human Chk1. *Mol Cell Biol*. 2001;21: 4129-4139.
23. Chen Y, Sanchez Y. Chk1 in the DNA damage response: conserved roles from yeasts to mammals. *DNA Repair (Amst)*. 2004; 3: 1025-1032.
24. Chen Z, Xiao Z, Gu WZ, Xue J, Bui MH, Kovar P, Li G, Wang G, Tao ZF, Tong Y, Lin NH, Sham HL, Wang JY, et al. Selective Chk1 inhibitors differentially sensitize p53-deficient cancer cells to cancer therapeutics. *Int J Cancer*. 2006; 119: 2784-2794.
25. Heine A, Holderried TA, Brossart P. Immunotherapy in renal cell carcinoma. *Immunotherapy*. 2009; 1: 97-107.
26. Heine A, Held SA, Daecke SN, Riethausen K, Kotthoff P, Flores C, Kurts C, Brossart P. The VEGF-Receptor Inhibitor Axitinib Impairs Dendritic Cell Phenotype and Function. *PLoS One*. 2015; 10: e0128897.
27. Cerwenka A, Lanier LL. Ligands for natural killer cell receptors: redundancy or specificity. *Immunol Rev*. 2001; 181: 158-169.
28. Ljunggren HG, Malmberg KJ. Prospects for the use of NK cells in immunotherapy of human cancer. *Nat Rev Immunol*. 2007; 7: 329-339.
29. Lanier LL. NKG2D in innate and adaptive immunity. *Adv Exp Med Biol*. 2005; 560: 51-56.
30. Moretta L, Bottino C, Pende D, Castriconi R, Mingari MC, Moretta A. Surface NK receptors and their ligands on tumor cells. *Semin Immunol*. 2006; 18: 151-158.
31. Raulet DH. Roles of the NKG2D immunoreceptor and its ligands. *Nat Rev Immunol*. 2003; 3: 781-790.
32. Shibuya A, Campbell D, Hannum C, Yssel H, Franz-Bacon K, McClanahan T, Kitamura T, Nicholl J, Sutherland GR, Lanier LL, Phillips JH. DNAM-1, a novel adhesion molecule involved in the cytolytic function of T lymphocytes. *Immunity*. 1996; 4: 573-581.
33. Bottino C, Castriconi R, Pende D, Rivera P, Nanni M, Carnemolla B, Cantoni C, Grassi J, Marcenaro S, Reymond N, Vitale M, Moretta L, Lopez M, et al. Identification of PVR (CD155) and Nectin-2 (CD112) as cell surface ligands for the human DNAM-1 (CD226) activating molecule. *J Exp Med*. 2003; 198: 557-567.
34. Reymond N, Imbert AM, Devillard E, Fabre S, Chabannon C, Xerri L, Farnarier C, Cantoni C, Bottino C, Moretta A, Dubreuil P, Lopez M. DNAM-1 and PVR regulate monocyte migration through endothelial junctions. *J Exp Med*. 2004;199: 1331-1341.
35. Pende D, Spaggiari GM, Marcenaro S, Martini S, Rivera P, Capobianco A, Falco M, Lanino E, Pierri I, Zambello R, Bacigalupo A, Mingari MC, Moretta A, et al. Analysis of the receptor-ligand interactions in the natural killer-mediated lysis of freshly isolated myeloid or lymphoblastic leukemias: evidence for the involvement of the Poliovirus receptor (CD155) and Nectin-2 (CD112). *Blood*. 2005; 105: 2066-2073.
36. Rogakou EP, Pilch DR, Orr AH, Ivanova VS, Bonner WM. DNA double-stranded breaks induce histone H2AX phosphorylation on serine 139. *J Biol Chem*. 1998; 273: 5858-5868.
37. Tsutsui H, Ide T, Shiomi T, Kang D, Hayashidani S, Suematsu N, Wen J, Utsumi H, Hamasaki N, Takeshita A. 8-oxo-dGTPase, which prevents oxidative stress-induced DNA damage, increases in the mitochondria from failing hearts. *Circulation*. 2001; 104: 2883-2885.
38. Collado M, Blasco MA, Serrano M. Cellular senescence in cancer and aging. *Cell*. 2007; 130: 223-233.

39. Roninson IB. Tumor cell senescence in cancer treatment. *Cancer Res.* 2003; 63: 2705-2715.
40. Ewald JA, Desotelle JA, Wilding G, Jarrard DF. Therapy-induced senescence in cancer. *J Natl. Cancer Inst.* 2010; 102: 1536-1546.
41. Eom YW, Kim MA, Park SS, Goo MJ, Kwon HJ, Sohn S, Kim WH, Yoon G, Choi KS. Two distinct modes of cell death induced by doxorubicin: apoptosis and cell death through mitotic catastrophe accompanied by senescence-like phenotype. *Oncogene.* 2005; 24: 4765-4777.
42. Bryceson YT, March ME, Barber DF, Ljunggren HG, Long EO. Cytolytic granule polarization and degranulation controlled by different receptors in resting NK cells. *J Exp Med.* 2005; 202: 1001-1012.
43. Fulda S, Gorman AM, Hori O, Samali A. Cellular stress responses: cell survival and cell death. *Int J Cell Biol.* 2010; 2010: 214074.
44. Gabai VL, O'Callaghan-Sunol C, Meng L, Sherman MY, Yaglom J. Triggering senescence programs suppresses Chk1 kinase and sensitizes cells to genotoxic stresses. *Cancer Res.* 2008; 68: 1834-1842.
45. He Q, Gao J, Ge S, Wang T, Li Y, Peng Z, Li Y, Shen L. Axitinib alone or in combination with chemotherapeutic drugs exerts potent antitumor activity against human gastric cancer cells in vitro and in vivo. *J Cancer Res Clin Oncol.* 2014; 140: 1575-1583.
46. Maugeri-Saccà M, Bartucci M, De Maria R. Checkpoint kinase 1 inhibitors for potentiating systemic anticancer therapy. *Cancer Treat Rev.* 2013; 39: 525-533.
47. Zhou BB, Elledge SJ. The DNA damage response: putting checkpoints in perspective. *Nature.* 2000; 408: 433-439.
48. Bucher N, Britten CD. G2 checkpoint abrogation and checkpoint kinase-1 targeting in the treatment of cancer. *Br J Cancer.* 2008; 98: 523-528.
49. Torres K, Horwitz SB. Mechanisms of Taxol-induced cell death are concentration dependent. *Cancer Res.* 1998; 58: 3620-3626.
50. Cohen-Jonathan E, Toulas C, Ader I, Monteil S, Allal C, Bonnet J, Hamilton AD, Sebti SM, Daly-Schveitzer N, Favre G. The farnesyltransferase inhibitor FTI-277 suppresses the 24-kDa FGF2-induced radioresistance in HeLa cells expressing wild-type RAS. *Radiat Res.* 1999; 152: 404-411.
51. Roninson IB, Broude EV, Chang BD. If not apoptosis, then what? Treatment-induced senescence and mitotic catastrophe in tumor cells. *Drug Resist Updat.* 2001; 4: 303-313.
52. Morisaki T, Onishi H, Katano M. Cancer immunotherapy using NKG2D and DNAM-1 systems. *Anticancer Res.* 2012; 32: 2241-2247.
53. Amin PJ, Shankar BS. Sulforaphane induces ROS mediated induction of NKG2D ligands in human cancer cell lines and enhances susceptibility to NK cell mediated lysis. *Life Sci.* 2015; 126: 19-27.
54. Bedel R, Thierry-Vuillemin A, Grandclement C, Balland J, Remy-Martin JP, Kantelip B, Pallandre JR, Pivot X, Ferrand C, Tiberghien P, Borg C. Novel role for STAT3 in transcriptional regulation of NK immune cell targeting receptor MICA on cancer cells. *Cancer Res.* 2011; 71: 1615-1626.
55. Huang Y, Wang Y, Li Y, Guo K, He Y. Role of sorafenib and sunitinib in the induction of expressions of NKG2D ligands in nasopharyngeal carcinoma with high expression of ABCG2. *J Cancer Res Clin Oncol.* 2011; 137: 829-837.
56. Ardolino M, Zingoni A, Cerboni C, Cecere F, Soriani A, Iannito ML, Santoni A. DNAM-1 ligand expression on Ag-stimulated T lymphocytes is mediated by ROS-dependent activation of DNA-damage response: relevance for NK-T cell interaction. *Blood* 2011; 117: 4778-4786.
57. Eckl J, Buchner A, Prinz PU, Riesenberger R, Siegert SI, Kammerer R, Nelson PJ, Noessner E. Transcript signature predicts tissue NK cell content and defines renal cell carcinoma subgroups independent of TNM staging. *J Mol Med.* 2012; 90: 55-66.
58. Margolin KA. Interleukin-2 in the treatment of renal cancer. *Semin Oncol.* 2000; 27: 194-203.

## Axitinib induces senescence-associated cell death and necrosis in glioma cell lines: The proteasome inhibitor, bortezomib, potentiates axitinib-induced cytotoxicity in a p21(Waf/Cip1) dependent manner

Maria Beatrice Morelli<sup>1,2</sup>, Consuelo Amantini<sup>3</sup>, Massimo Nabissi<sup>1</sup>, Claudio Cardinali<sup>1,2</sup>, Matteo Santoni<sup>4</sup>, Giovanni Bernardini<sup>2,5</sup>, Angela Santoni<sup>2,5</sup>, Giorgio Santoni<sup>1</sup>

<sup>1</sup>School of Pharmacy, University of Camerino, Camerino, Italy

<sup>2</sup>Department of Molecular Medicine, Sapienza University, Rome, Italy

<sup>3</sup>School of Biosciences and Veterinary Medicine, University of Camerino, Camerino, Italy

<sup>4</sup>Department of Medical Oncology, Polytechnic University of Marche, Ancona, Italy

<sup>5</sup>I.N.M. Neuromed, Pozzilli, Isernia, Italy

**Correspondence to:** Giorgio Santoni, **email:** giorgio.santoni@unicam.it

**Keywords:** axitinib, glioblastoma, bortezomib, p21, senescence

**Received:** August 02, 2016

**Accepted:** November 18, 2016

**Published:** December 01, 2016

### ABSTRACT

**Glioblastoma is associated with a poor overall survival despite new treatment advances. Antiangiogenic strategies targeting VEGF based on tyrosine kinase inhibitors (TKIs) are currently undergoing extensive research for the treatment of glioma.**

**Herein we demonstrated that the TKI axitinib induces DNA damage response (DDR) characterized by  $\gamma$ -H2AX phosphorylation and Chk1 kinase activation leading to G2/M cell cycle arrest and mitotic catastrophe in U87, T98 and U251 glioma cell lines. Moreover, we found that p21(Waf1/Cip1) increased levels correlates with induction of ROS and senescence-associated cell death in U87 and T98 cell lines, which are reverted by N-acetyl cysteine pretreatment. Conversely, U251 cell line showed a resistant phenotype in response to axitinib treatment, as evidenced by cell cycle arrest but no sign of cell death.**

**The combinatorial use of axitinib with other therapies, with the aim of inhibiting multiple signaling pathways involved in tumor growth, can increase the efficiency of this TKI. Thus, we addressed the combined effects of axitinib with no toxic doses of the proteasome inhibitor bortezomib on the growth of U87 and T98 axitinib-sensitive and axitinib-resistant U251 cell lines. Compared to single treatments, combined exposure was more effective in inhibiting cell viability of all glioma cell lines, although with different cell death modalities. The regulation of key DDR and cell cycle proteins, including Chk1,  $\gamma$ -H2AX and p21(Waf1/Cip1) was also studied in glioma cell lines.**

**Collectively, these findings provide new perspectives for the use of axitinib in combination with Bortezomib to overcome the therapy resistance in gliomas.**

### INTRODUCTION

Glioblastoma (GBM) is a high angiogenic malignancy. GBM secretes high levels of vascular endothelial growth factor (VEGF) that promotes endothelial cell proliferation, blood brain barrier permeability and angiogenesis [1, 2]. They are aggressive tumors that generally respond poorly to therapy consisting

of surgery, radiation, and conventional chemotherapy. Although advancements in the past decades, no significant increase in the overall survival (OS) of patients is observed, with a median survival of 14.6 months and five-year survival < 10% [3]. Molecularly targeted agents hold significant promise as novel therapeutic adjuncts; however, these new therapies are still in clinical trial phase. Among targeted therapies, a new current focuses on

the angiogenic tyrosine kinase receptors (TRKs) and their signaling pathway inactivation. The anti-VEGF antibody bevacizumab was the first TKI approved in 2009 by the Food and Drug Administration (FDA) as a second-line treatment of recurrent GBM [4].

A novel orally available TKI is axitinib (Inlyta®), a selective and potent inhibitor of VEGFR 1, 2, and 3 that has been approved by FDA in 2012 for the treatment of patients with metastatic renal cell carcinoma (mRCC) after failure of one prior systemic therapy [5, 6]. We have recently reported that axitinib induces activation of DNA damage response (DDR), senescence and mitotic catastrophe in RCC cell lines [7]; however at present, very few data using this TKI have been provided in GBM. Preclinical study showed that systemic treatment with axitinib exerts antiangiogenic effect and survival prolongation in preclinical orthotopic GBM models, including clinically relevant glioma stem cell models [8]. More recently, a randomized multicenter phase II clinical trial demonstrated an increased 6-month progression-free survival (PFS) rate of 34% after axitinib treatment in patients with recurrent GBM with respect to 28 % PFS in the control patients treated with bevacizumab or lomustine, suggesting that in recurrent GBM, axitinib shows clinical activity as single-agent [9]. Finally, a window study on front-line axitinib followed by axitinib and radiation in elderly patients with glioblastoma from University of Cincinnati (NCT01508117) is currently under evaluation.

Other new-targeted therapies interfere with proteasome, the enzymatic complex responsible for the bulk of protein degradation. Proteasome inhibition leads to toxic accumulation of misfolded and abnormal proteins and can also stabilize specific tumor inhibitory factors such as cell cycle regulatory proteins and induce apoptosis [10–14]. The proteasome inhibitor bortezomib (PS-341/Velcade) is FDA-approved for multiple myeloma and mantle cell lymphoma [15]. Bortezomib functions as a selective inhibitor of the 26S proteasome, producing predictable, dose-related, and reversible proteasome inhibition [16]. It exerts antitumor activity in a variety of malignancies [17]. *In vitro* studies have demonstrated that bortezomib alone or in combination with histone

deacetylase (HDAC) [18], the cyclooxygenase-2 inhibitor celecoxib (Celebrex) [19], phosphatidylinositol 3-kinase (ZSTK474) inhibitors [20] or temozolomide [21, 22] stimulates a potent cytotoxic response and causes cell death in GBM cell lines.

Therefore, the aim of the present work was to evaluate the effects of axitinib treatment as monotherapy and in combination with bortezomib on multiple signaling pathways involved in glioma growth. Of particular interest was the cytotoxic synergy of axitinib-bortezomib combination found in different human glioma cell lines that involves the modulation of p21 (Waf1/Cip1) protein levels and leads to enhanced cell death.

## RESULTS

### Axitinib inhibits glioma cell viability in a dose and time-dependent manner

We first evaluated the effects of axitinib on cell viability in U87, T98 and U251 glioma cell lines by performing dose-response and time-course analyses (Supplementary Figure S1A). Axitinib inhibited the growth of U87 and T98 cells, after 72 h of treatment, with  $IC_{50}$  values of 12.7  $\mu$ M and 8.5  $\mu$ M, respectively (Figure 1). Conversely, U251 cells were found to be more resistant to axitinib-mediated cytotoxic effects. Therefore, the lowest effective dose of axitinib in inducing growth inhibition for each cell line (5  $\mu$ M for U87 and T98; 15  $\mu$ M for U251) was used for the subsequent experiments.

### Axitinib triggers the DNA damage response (DDR) and p21 overexpression in glioma cell lines

Axitinib has been found to trigger DDR in RCC lines [7], however at present no data on the effect of axitinib in glioma are available. Thus, to evaluate whether axitinib treatment could trigger the DDR in glioma cells, we initially investigated the presence of  $\gamma$ -H2AX (H2AX), Ser139 phosphorylated variant of histone 2A associated with DNA double-strand breaks [23]. Western blot analysis revealed strong induction of

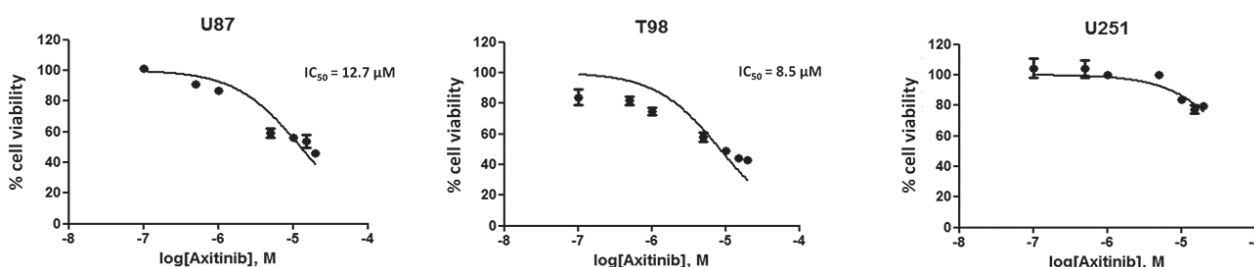


**Figure 1: Axitinib inhibits viability in glioma cell lines.** U87, T98 and U251 glioma cell lines were cultured for 72 h with different doses of axitinib. Cell viability was determined by MTT assay. Data shown are expressed as mean  $\pm$  SE of three separate experiments.

the DNA damage marker expression in all axitinib-treated glioma cell lines, although with different kinetics (Figure 2A and 2B). Interestingly, phospho-H2AX induction was accompanied by Ser345-Chk1 phosphorylation already at 3 h after exposure to axitinib that declined at later time points in all glioma cell lines. The Chk1 protein was expressed in all glioma cell lines until 48 h, and declined at later time points after axitinib treatment (Figure 2A and 2B). At 12 h after treatment, p21 overexpression, that paralleled the decline of Ser345-Chk1 activation, was observed in U87 and T98 cells, but not in U251 cells (Figure 2A and 2B).

### Axitinib induces G2/M arrest and mitotic catastrophe in glioma cell lines

Then we evaluated whether axitinib treatment could result in cell cycle alteration. Thus, we performed cell cycle experiments in the presence of axitinib for different times. We observed that treatment of glioma cells induced a significant early (just at 6 h) and transient decrease of G1-phase which was accompanied by a progressive increase of G2/M-phase cell population until 24 h in U87, T98 glioma cells and 72 h in U251 (Figure 2C and Supplementary Figure S1B). In addition, a decreased percentage of U87 and

T98, but not U251 cells in G2/M-phase cells paralleled by an increase of subG1 phase was observed at 48-72 h after axitinib treatment (Figure 2C and Supplementary Figure S1B). Moreover, treatment with axitinib led to a significant increase in the percentage of cells with polyploidy in all glioma cell lines analyzed (cells with DNA content >4N) (Figure 2C and Supplementary Figure S1B).

Tetraploid tumor cells intrinsically susceptible to mitotic aberrations are particularly sensitive to the induction of mitotic catastrophe [24, 25]. Thus, we decided to investigate whether axitinib treatment could result in mitotic catastrophe in glioma cells, by assessing the changes in nuclear morphology [26]. By Hoechst 33258 staining we observed that the nuclei became significantly larger and some cells contained several nuclei of unequal sizes already after 24 h of drug treatment in U87, T98 and U251 glioma cell lines (Figure 3A). Further, in order to assess mitochondrial changes in mitotic catastrophe, JC-1 staining was used to analyze mitochondrial mass. As shown in Figure 3B and 3C, an increase of FL-1 green fluorescence in axitinib treated compared to untreated glioma cells, resulting by enhanced mitochondrial mass, was observed. This data was also confirmed by NAO staining [27] (Supplementary Figure S1C).

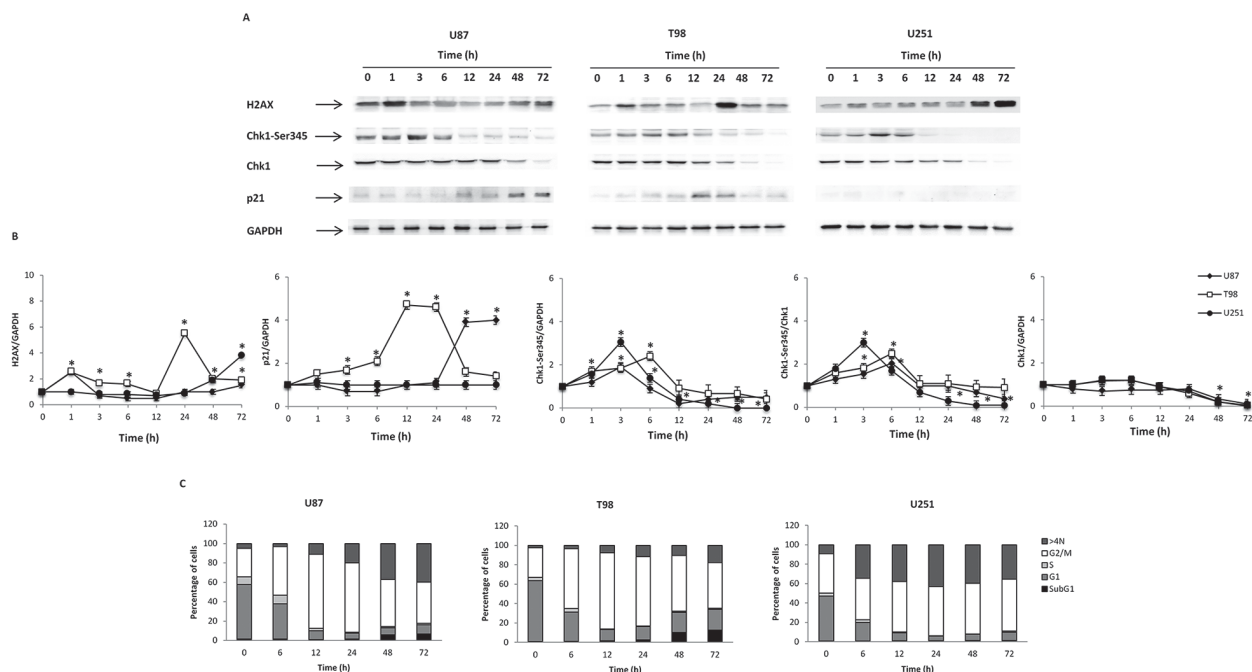


**Figure 2: Axitinib induces DNA damage response and cell cycle arrest.** **A.** Western blot analysis of H2AX, Chk1-Ser345, Chk1 and p21 protein levels in glioma cells after 72 h treatment with 5  $\mu$ M axitinib for U87 and T98 cells, and with 15  $\mu$ M axitinib for U251. Blots are representative of one of three separate experiments. **B.** H2AX, Chk1-Ser345, Chk1 and p21 densitometry values were normalized to GAPDH used as loading control. The Chk1-Ser345 protein levels were also determined with respect to Chk1 levels. Densitometric values shown are the mean  $\pm$  SD of three separate experiments. \* $p$ <0.01 vs untreated cells. **C.** Cell cycle analysis in U87 and T98 cells treated with 5  $\mu$ M axitinib and in U251 cells treated with 15  $\mu$ M axitinib for the indicated times.

### Axitinib triggers senescence-associated cell death and necrosis in U87 and T98 glioma cell lines

Cell cycle arrest in G2/M phase and polyploidy often result in cellular senescence [28]. Thus, a time-dependent accumulation of glioma cells with enlarged and flattened morphology was observed after axitinib treatment by microscopy analysis (Figure 4A). Since these morphological changes are reminiscent of a senescent phenotype, we analyzed the activity of senescence-associated  $\beta$ -galactosidase (SA- $\beta$ -gal), the typical marker of senescent cells, in glioma cells after axitinib treatment [29, 30]. Forty-eight hours after treatment, the increase on SA- $\beta$ -gal activity was detected by flow cytometry using the fluorogenic substrate for SA- $\beta$ -galactosidase, C<sub>12</sub>FDG, and reached the percentage of 51 and 75 in U87 and T98 cells, respectively at 72 h of treatment (Figure 4B). These results were also confirmed by cytochemical assessment of SA- $\beta$ -gal activity that revealed the presence of blue-stained U87 and T98 glioma cells after treatment

with axitinib (Figure 4C). No SA- $\beta$ -gal-positive senescent cells were found in axitinib-treated U251 glioma cells (Figure 4B, 4C).

Recent studies have suggested that reactive oxygen species (ROS) generation triggered by anti-cancer drug can stimulate cellular senescence [31, 32]. Thus, we evaluated the capability of axitinib to trigger ROS generation in glioma cells by flow cytometry using the general redox-sensitive fluorescent dye, DCFDA. As shown in Figure 5A, axitinib stimulated intracellular ROS generation in U87 and T98, but not in U251 glioma cells. It was evident at 24 h after exposure and progressively increased at later time points. This response was reverted by the pre-treatment of glioma cells with the ROS scavenger, N-acetyl-L-cysteine (NAC) (Figure 5B).

Depending whether it is replicative or premature, cellular senescence may also affect cell viability [33, 34]. Thus, we evaluated the effect of axitinib exposure on glioma cell viability by SA- $\beta$ -gal/PI staining and FACS analysis. An increased number of SA- $\beta$ -gal<sup>+</sup>PI<sup>+</sup> and SA-

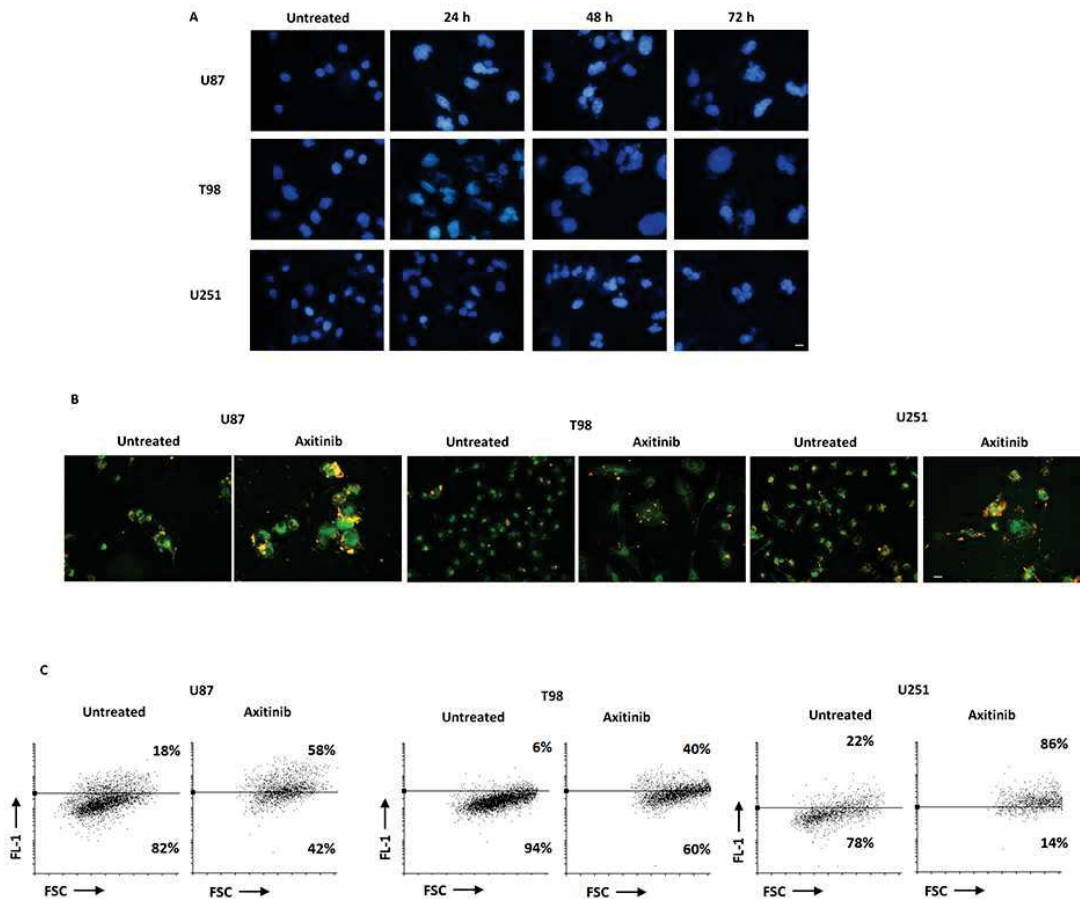


**Figure 3: Axitinib triggers mitotic catastrophe in all glioma cell lines.** **A.** Nuclei of glioma cells untreated or treated with axitinib for the indicated time were stained with Hoechst 33258 and then analyzed on ten random fields. Cells were observed under a fluorescence microscope. Bar: 30  $\mu$ m. **B.** Fluorescence microscope images show increase of green fluorescent signal upon axitinib treatment after 72 h compared to untreated cells. Bar: 30  $\mu$ m. **C.** Change in JC1 green (FL-1) with respect to FSC parameter in cells treated with axitinib for 72 h was detected by flow cytometer.

$\beta$ -gal<sup>+</sup>PI<sup>+</sup> cells, suggestive of premature senescence and necrotic cell death, respectively, was observed in U87 cells after axitinib exposure, whereas axitinib-treated T98 cells showed a SA- $\beta$ -gal<sup>+</sup>PI<sup>+</sup> phenotype (Figure 5C). Neither premature senescence or necrotic cell death were identified in axitinib-treated U251 cells (Figure 5C). Moreover, pre-treatment of axitinib-administered U87 and T98 glioma cells with NAC reduced the percentage  $\beta$ -gal<sup>+</sup>PI<sup>+</sup> in axitinib-treated cells, whereas no changes in NAC-treated cells were observed (Figure 5C).

Altogether, the high percentage of SA- $\beta$ -gal<sup>+</sup>PI<sup>+</sup> U87 and T98 cells suggested that these two cell lines undergo to senescence-associated cell death, and the ROS generation is indispensable for the induction of this process. On the contrary in U251 glioma cells, the inability of axitinib to trigger ROS production results in a failure to induce premature senescence and cell death. Furthermore, the lack of Annexin V<sup>+</sup> cells and caspase-3 activation up to 72 h of axitinib treatment evidenced a necrotic cell death in U87 and T98 cells (Supplementary Figure S1D, 1E).

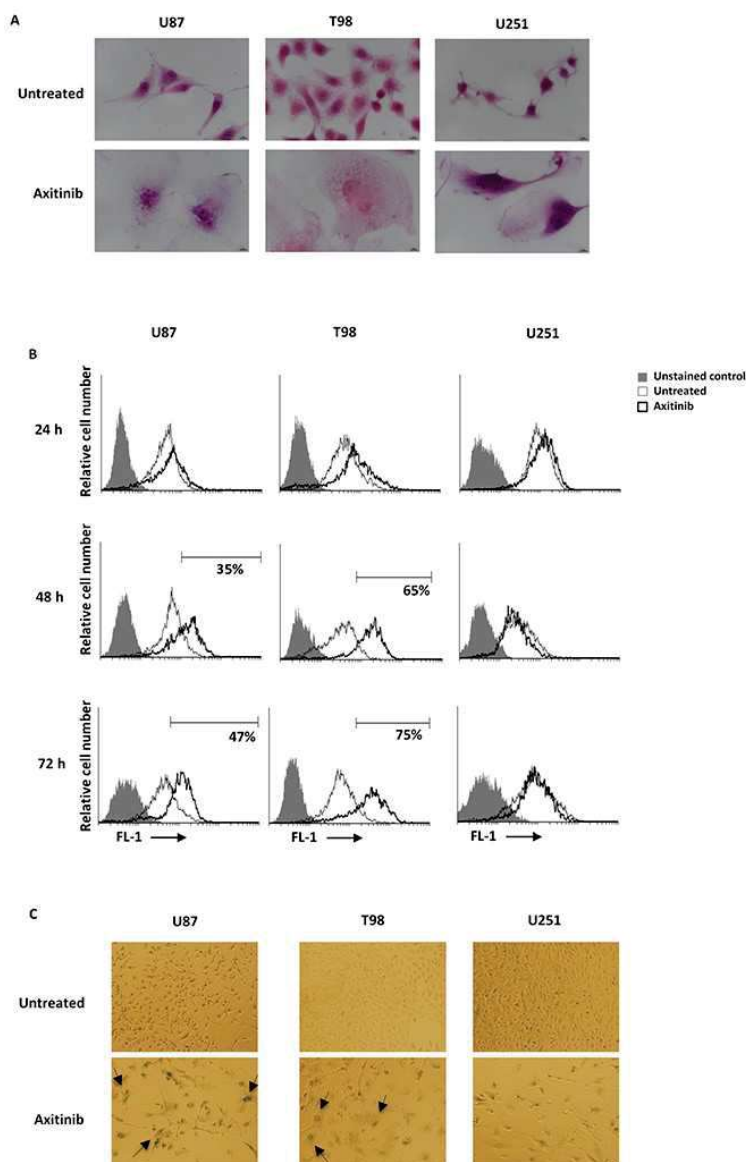


**Figure 4: Axitinib induces cellular senescence in U87 and T98, but not in U251 glioma cell lines.** **A.** Representative image of glioma cells 72 h after treatment with axitinib and then stained with haematoxylin and eosin (H&E). Bar: 10  $\mu$ m. **B.** Representative flow cytometric profiles of glioma cells untreated or treated with axitinib (5  $\mu$ M for U87 and T98 cells and 15  $\mu$ M for U251), then stained with  $C_{12}$ FDG, a fluorogenic substrate for SA- $\beta$ -galactosidase before analysis. Data represent the percentage of positive cells. Grey curve represents unstained cells. **C.** Cellular senescence was assessed in glioma cells after 72 h of axitinib treatment by cytochemistry detection of SA- $\beta$ -galactosidase activity. Bar: 20  $\mu$ m.

To elucidate whether axitinib treatment was able to select resistant glioma cells, the ability to resume proliferation was evaluated. To this purpose U87, T98 and U251 cell lines were incubated with axitinib for 72 h and at the end of the treatment the viable cells remained were washed to remove axitinib, replated and incubated for additional days in fresh media. After axitinib removal, only U251 cells showed the ability to restart to growth although at lower degree respect to untreated cells (Supplementary Figure S2A). Moreover, data obtained

by staining for SA- $\beta$ Gal/PI incorporation showed an increased percentage of SA- $\beta$ Gal<sup>+</sup>/PI<sup>+</sup> and PI<sup>+</sup> cells in U87 and in T98 cells, respectively. In U251 cells the absence of senescence-associated SA- $\beta$ Gal or PI staining respect to untreated cells after culture in fresh media was observed (Supplementary Figure S2B).

Taken together, these results demonstrated that axitinib induces an irreversible senescence and cell death in U87 and T98 cells. On the other hand, U251 cells are confirmed to show a resistant phenotype.

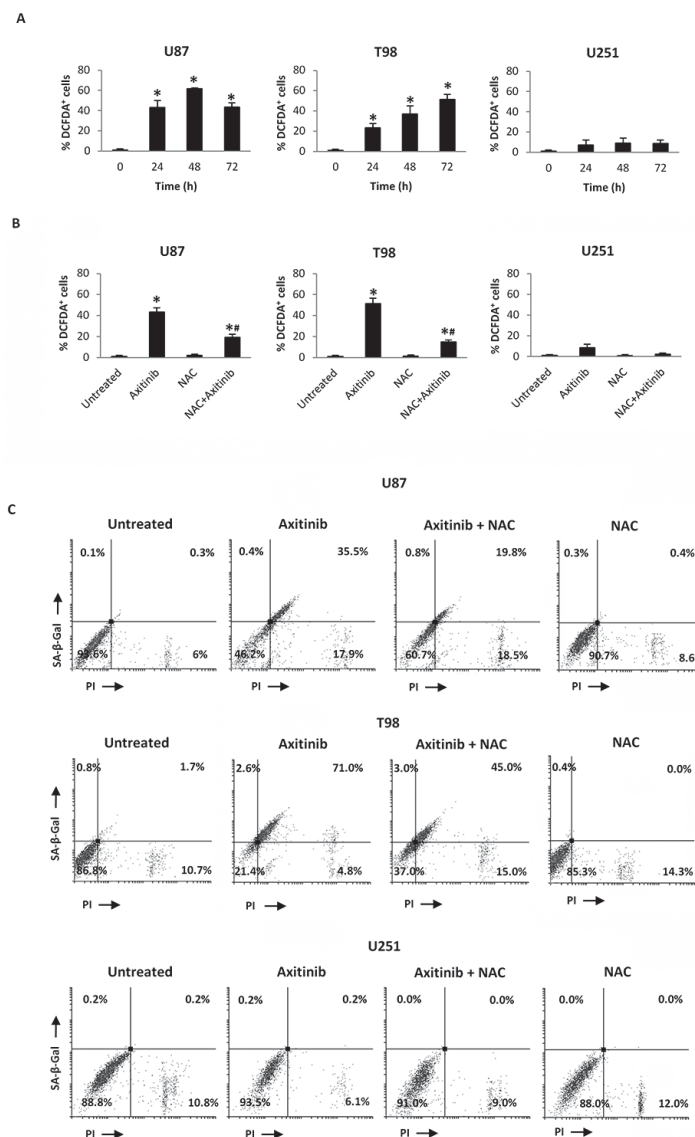


**Figure 5: Axitinib induces ROS-dependent senescence-associated cell death in U87 and T98 cell lines.** **A.** ROS generation in glioma cell lines treated with axitinib (5  $\mu$ M for U87 and T98 cells and 15  $\mu$ M for U251) for the indicated times. Cells were stained with DCFDA before flow cytometric analysis. Data are expressed as percentage of DCFDA positive cells with respect to untreated cells; \* $p < 0.01$  vs untreated cells. **B.** Glioma cells were pretreated with NAC 10 mM for 1 h before the administration of axitinib. After 72 h cells were stained with DCFDA and analyzed as above described. \* $p < 0.01$  vs untreated cells; \*\* $p < 0.01$  vs axitinib or NAC treated cells. **C.** Glioma cells were cultured with axitinib for 72 h, with or without pretreatment with NAC 10 mM for 1 h. Flow cytometric analysis was performed by C<sub>12</sub>FDG and PI double-staining. Data represent the percentage of PI and/or SA- $\beta$ -galactosidase positive cells and are representative of one of three separate experiments.

## Overexpression of p21 sensitizes U251 glioma cells to axitinib treatment

Owing to the potential role of p21 in the senescence pathway, we evaluated whether overexpression of exogenous p21 would sensitize axitinib-resistant U251 cells from axitinib-induced cell death. Therefore, we transfected pCMV vector containing coding sequence for p21 in this cell line, and we investigated the cell viability. Firstly, we evaluated the p21 protein expression in pCMV (transfection control) and pCMV-p21 respect to untransfected U251 glioma cells by western blot analysis. The p21 protein levels were not detectable in untreated and pCMV U251 cells, whereas increased p21 expression was observed in pCMV-p21 U251 transfected glioma cells (Figure 6A). About 40% of growth inhibition was observed upon axitinib treatment in pCMV-p21 U251 glioma cells after 72 h of treatment (Figure 6B). In addition, p21 overexpression increased the percentage of cells in subG1 phase respect to U251 pCMV transfected cells (Figure 6C). Whereas in pCMV transfected cells axitinib treatment increased the percentage of cells in G2/M phase, in pCMV-p21 transfected cells axitinib markedly improved the subG1 phase as compared to untreated cells (Figure 6C). Accordingly, PI staining and cytofluorimetric analysis revealed, an increased percentage (about 50%) of PI<sup>+</sup> cells in axitinib-treated pCMV-p21 U251 cells, as compared to untreated pCMV-p21 U251 cells (Figure 6D). However, axitinib-treated pCMV-p21 U251 cells were not Annexin V positive (Figure 6E). No major differences were found upon axitinib treatment in pCMV U251 cells.

Overall, overexpression of p21 in axitinib-resistant U251 glioma cells overcomes the U251 glioma cell dysfunction, and sensitizes glioma cells to axitinib-induced cytotoxic effects.

## Bortezomib in combination with axitinib stimulates a synergistic cytotoxic effect in glioma cell lines

Bortezomib has been found to induce p21 over expression and apoptotic cell death of glioma cell lines [35]. So, we performed a time course analysis and found that bortezomib reduces the viability in U87, T98 and U251 cells with IC<sub>50</sub> values of 3.5 nM, 4.5 nM and 5.0 nM, respectively (Supplementary Figure S3). Thereafter, to evaluate the potential synergistic effects of axitinib and bortezomib, we performed MTT cell growth assays treating cells with different doses of axitinib (1, 5 and 15 μM) in combination with different doses of bortezomib (1.25, 2.5 and 6.5 nM) for up to 72 h. We evaluated the cell viability on axitinib-sensitive (U87 and T98) and axitinib-resistant U251 glioma cell lines in two different schedules. As shown in Supplementary Figure S4, the synergistic effects between axitinib and bortezomib was present only when drugs were simultaneously administered. In

sequential regimens, axitinib was added for 72 h, then the viable cells were replated and treated with bortezomib for other 72 h. No improvement of cytotoxic effects was observed, rather the axitinib-pretreated cells were more resistant to bortezomib treatment (Supplementary Figure S4A). In simultaneous regimen, both drugs were added on day 0 and the combined effect was evaluated on the basis of the CI (Supplementary Figure S4B). The CI results showed synergism when axitinib and bortezomib are coadministered and the lowest dose of bortezomib displaying a CI<1 (2.5 nM) was selected to study the cytotoxic effects of simultaneous treatment. To ensure that this dose was not cytotoxic, we performed several experiments. Our results demonstrated that bortezomib used at 2.5 nM does not induce mitotic catastrophe as evaluated by nuclear morphology and mitochondrial mass (Supplementary Figure S5A-B), does not alter cell cycle phases (Supplementary Figure S5C), does not induce ROS generation (Supplementary Figure S5D) or cell senescence process (Supplementary Figure S5E), does not exert cytotoxic effects as evaluated by Annexin V-PI double staining (Supplementary Figure S5F) and does not change the VEGFA mRNA levels (Supplementary Figure S5G).

## Effects of the axitinib-bortezomib combination on cell death signaling pathways

Axitinib plus bortezomib coadministration for 72h synergized to increase cytotoxic activity against glioma cells, as compared to axitinib alone, with a 5- and 10-fold reduction of the IC<sub>50</sub> in U87 and T98 glioma cells (IC<sub>50</sub> axitinib = 12.7 and 8.5 vs IC<sub>50</sub> axitinib-bortezomib = 3.4 and 0.9 μM in U87 and T98 glioma cells, respectively) (Figure 7A). Furthermore, axitinib in combination with bortezomib reverted the resistance of U251 glioma cells to axitinib treatment alone and inhibited U251 glioma cell viability with an IC<sub>50</sub> value of 8.8 μM (Figure 7A).

To investigate the synergistic mechanism, we evaluated the effects of bortezomib (2.5 nM) coadministered with the lowest effective dose of axitinib (5 μM in U87 and T98; 15 μM in U251).

After 72 h, all glioma cell lines underwent mitotic catastrophe, as evidenced by nuclear morphology and mitochondrial mass increase (Figure 7B,7C and Supplementary Figure S6). Moreover, the combination of TKI and proteasome inhibitor highly increased the levels of intracellular ROS activity in U87 and T98 cell lines (Figure 7D) whereas lower ROS levels were observed in axitinib-resistant U251 glioma cells compared to cell treated with axitinib alone (Figure 7D). The ROS production effect was attenuated by NAC pretreatment after 72 h of treatment (Figure 7D). Furthermore, axitinib plus bortezomib in combination resulted in an increased percentage of β-gal<sup>+</sup>PI<sup>+</sup> in U87 and T98 cells and β-gal<sup>+</sup>PI<sup>+</sup> U251 cells (Figure 7E), as compared to axitinib (Figure 5C) or bortezomib (Supplementary

Figure S5E,S5F) used alone. Moreover, as described for axitinib monotherapy in T98 and U87, neither Annexin V positive cells, apoptotic DNA fragmentation or caspase-3 activity (Supplementary Figure S7A-S7C) were evidenced in axitinib plus bortezomib treated U251 glioma cells. Since U251 cells resumed proliferation after axitinib removal, we investigated if the coadministration of axitinib plus bortezomib was able to induce an irreversible growth arrest.

Thus, U251 cells were treated with both drugs for 72h, then washed and replated in fresh medium. MTT results showed that the coadministration strongly inhibits the cell growth recovery suggesting that the

drug combination is able to overcome U251 resistant phenotype. Bortezomib alone did not affect the rate of growth (Supplementary Figure S7D).

### Involvement of p21 in cytotoxicity induced by axitinib plus bortezomib

The effects of axitinib plus bortezomib used in combination were associated with an enhanced p21 protein levels in all glioma cell lines with respect to cells treated with bortezomib or axitinib alone. No significant changes of Ser345-Chk1 and H2AX phosphorylation were observed (Figure 8A-8D, Supplementary Figure S8).

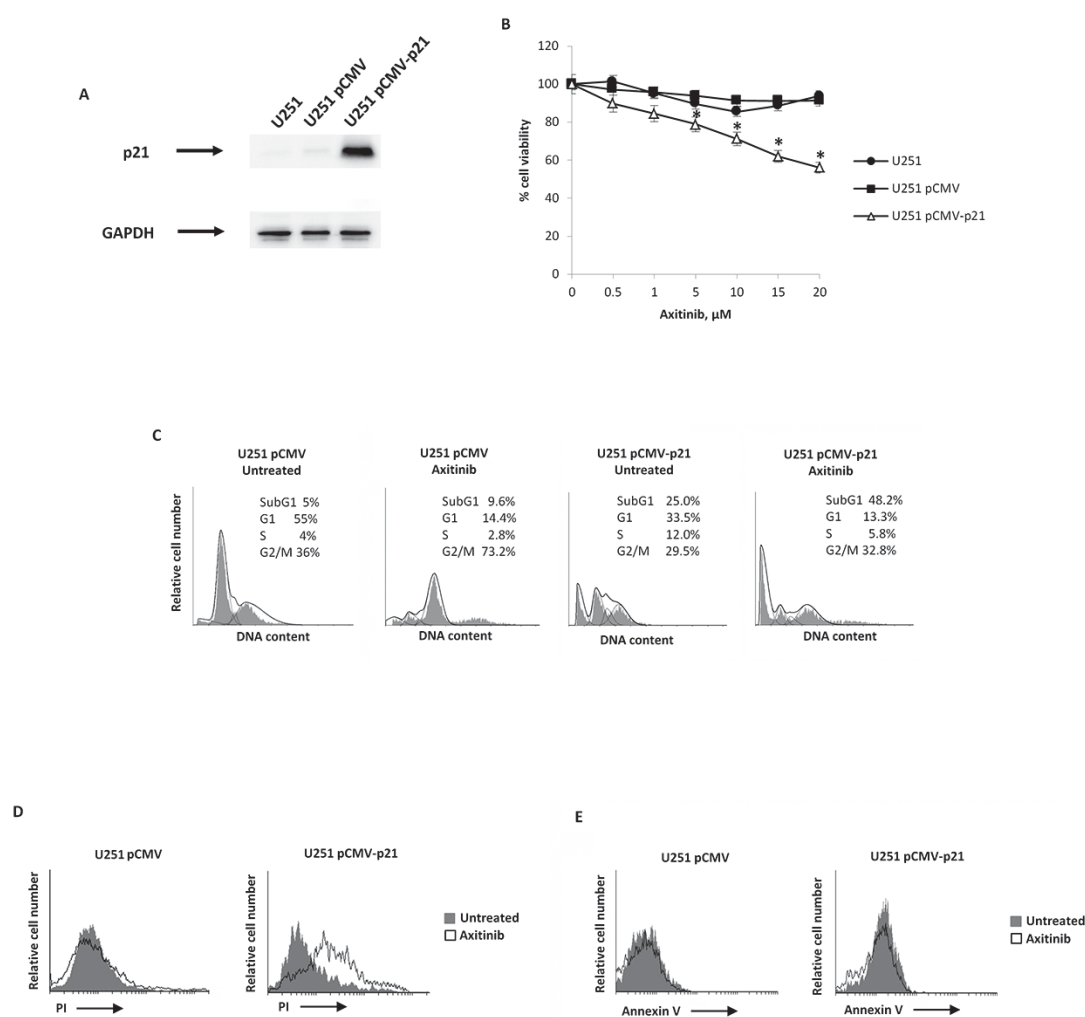


**Figure 6: p21 overexpression decreases cell viability of axitinib-treated U251 glioma cells.** **A.** Lysates from untransfected, pCMV and pCMV-p21 U251 cells were separated on SDS-PAGE and probed with specific rabbit anti-human p21 Ab. GAPDH protein levels were evaluated as loading control. Blots are representative of three separate experiments. **B.** Untransfected, pCMV and pCMV-p21 U251 cell viability was determined by MTT assay after 72 h of transfection. Data shown are the mean  $\pm$  SD of three separate experiments. \* $p < 0.01$  vs untransfected and pCMV U251 cells. **C.** Representative cell cycle distribution in pCMV and pCMV-p21 U251 cells treated for 72 h with axitinib. **D.** U251 cells were treated as above described and then PI incorporation was analyzed by flow cytometry. Histograms are representative of one of three separate experiments. **E.** U251 cells were treated as above described and then Annexin V staining was analyzed by flow cytometry. Histograms are representative of one of three separate experiments.

The fact that p21 was accumulated in all three cell lines cotreated with axitinib and bortezomib, further suggests that p21 may play an essential role in axitinib-induced cell death. Therefore, through RNA silencing (siRNA) technique we analyzed the p21 involvement in T98 cell line. After 72 h of transfection, when p21 expression is impaired by the specific siCDKN1A (Figure 8E), both axitinib- and axitinib-bortezomib-induced

cytotoxicity is reduced in siCDKN1A T98 cells respect to NC1 T98 cells, used as negative transfection control (Figure 8F, 8G).

Overall, bortezomib plus axitinib in combination increase p21 levels and sensitize glioma-sensitive and resistant cells to drug-induced cytotoxic effects by triggering senescence-associated cell death and necrosis, respectively.

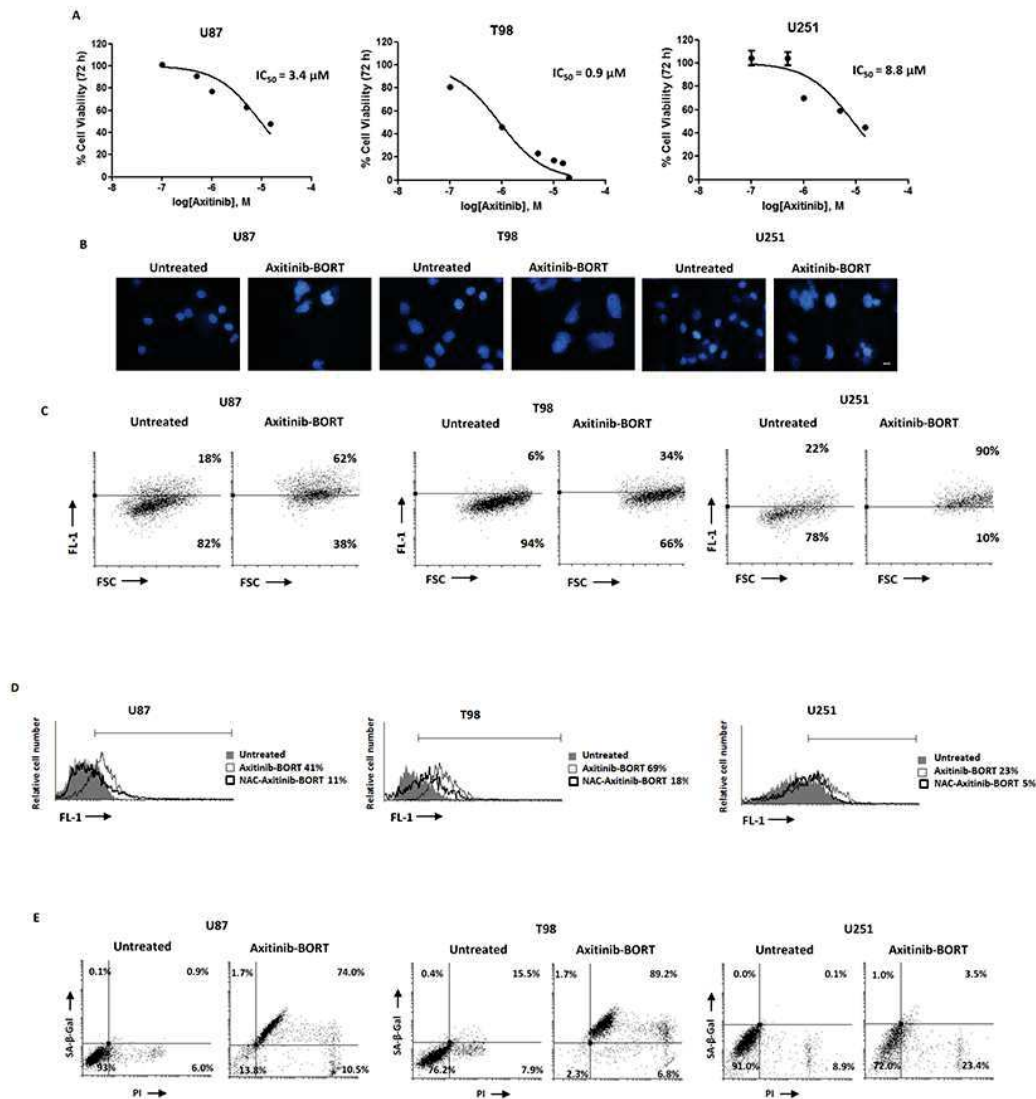


**Figure 7: Cotreatment axitinib-bortezomib induces cell death also in axitinib-resistant U251 glioma cell line.** A. U87, T98 and U251 glioma cell lines were cultured for 72 h with different doses of axitinib administered in combination with 2.5 nM bortezomib. Cell viability was determined by MTT assay. Data shown are expressed as mean ± SE of three separate experiments. B. Glioma cells were cultured for 72 h with the combination axitinib (5 μM for U87 and T98, 15 μM for U251) - bortezomib (2.5 nM). Nuclei of treated cells were then stained with Hoechst 33258 and analyzed on ten random fields. Cells were observed under a fluorescence microscope. Bar: 50 μM. C. Change in JC1 green (FL-1) respect to FSC parameter in cells treated with the combination axitinib-bortezomib as above described was detected by flow cytometer. D. ROS generation in glioma cell lines cotreated for 72 h with axitinib and bortezomib, pretreated or not with NAC 10 mM for 1 h. Cells were stained with DCFDA before flow cytometric analysis. Data are expressed as percentage of DCFDA positive cells with respect to untreated cells. E. Flow cytometric analysis on glioma cells cultured as above described was performed by C<sub>12</sub>FDG and PI double-staining. Data represent the percentage of PI and/or SA-β-galactosidase positive cells and are representative of one of three separate experiments.

## DISCUSSION

In this study, we describe that axitinib treatment affects glioma cell viability inducing the DDR. This response to genotoxic insults involves sensing of DNA damage by a class of protein kinases, including ATM,

ATR, followed by activation of Chk1 and Chk2 kinases that cause temporary cell cycle arrest, as well as promotes assembly of DNA repair complexes at the damaged sites at chromosomes [36]. The checkpoint regulators Chk1 and p21 were found to promote damage-induced mitotic catastrophe and a senescence-like phenotype [37].

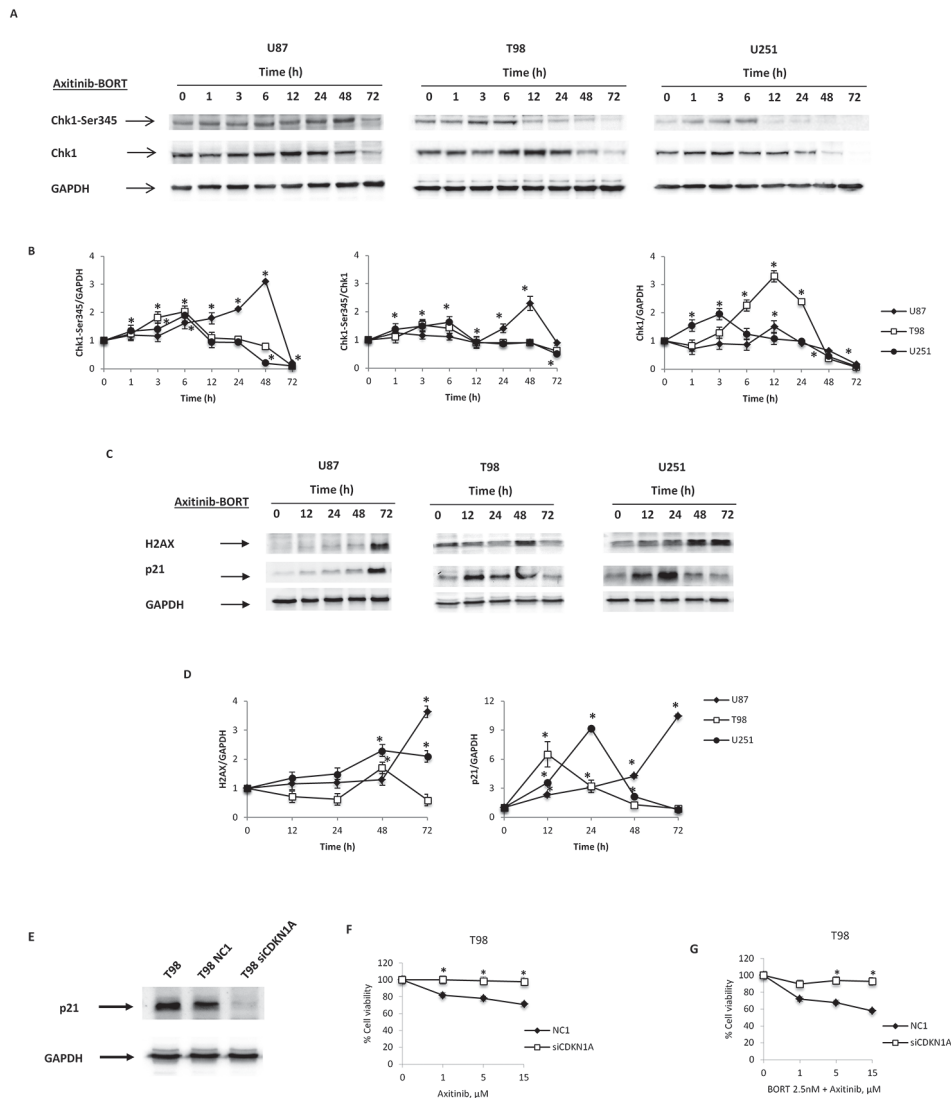


**Figure 8: The role of p21 protein in axitinib-bortezomib induced cytotoxic effects.** **A.** Western blot analysis of Chk1-Ser345 and Chk1 protein levels in glioma cells after treatment with bortezomib (2.5 nM) and axitinib (5  $\mu$ M for U87 and T98, 15  $\mu$ M for U251). Blots are representative of one of three separate experiments. **B.** Chk1-Ser345 and Chk1 densitometry values were normalized to GAPDH used as loading control. The Chk1-Ser345 protein levels were also determined with respect to Chk1 levels. Densitometric values shown are the mean  $\pm$  SD of three separate experiments. \* $p$ <0.01 vs untreated cells. **C.** Western blot analysis of H2AX and p21 protein levels in glioma cells after the axitinib-bortezomib combined treatment. Blots are representative of one of three separate experiments. **D.** Quantitative representation of the experiment reported in panel C. H2AX and p21 densitometry values were normalized to GAPDH used as loading control. Densitometric values shown are the mean  $\pm$  SD of three separate experiments. \* $p$ <0.01 vs untreated cells. **E.** Lysates from untransfected, NC1 (negative control) and siCDKN1A T98 cells were separated on SDS-PAGE and probed with specific rabbit anti-human p21 Ab. GAPDH protein levels were evaluated as loading control. Blots are representative of three separate experiments. **F.** NC1 and siCDKN1A T98 cell viability was determined by MTT assay after 72 h of axitinib treatment. Data shown are the mean  $\pm$  SD of three separate experiments. \* $p$ <0.01 vs NC1 transfected cells. **G.** NC1 and siCDKN1A T98 cell viability was determined by MTT assay after 72 h of axitinib-bortezomib cotreatment. Data shown are the mean  $\pm$  SD of three separate experiments. \* $p$ <0.01 vs NC1 transfected cells.

Here, we found that treatment of glioma cells with axitinib triggers the DDR, evidenced by increased levels of phosphorylated H2AX and Ser345-Chk1, leading to cell cycle arrest at G2/M phase and accumulation of polyploid glioma cells undergoing mitotic catastrophe. Moreover, in U87 and T98 cell lines, at later time points, when Ser345-Chk1 activation declines, the overexpression of the cell cycle inhibitor p21 activates a cell senescent program resulting in senescence-associated cell death and necrosis of treated cells. Conversely, a progressive increase of G2/M phase and an accumulation of polyploidy cells at 72 h after treatment were observed in U251 axitinib-resistant cells.

Numerous anti-tumor drugs, including DNA damaging agents, can induce mitotic catastrophe [25]. In particular, tetraploid tumor cells, intrinsically susceptible to mitotic aberrations, are sensitive to the induction of mitotic catastrophe [24, 25]. To detect the occurrence of mitotic catastrophe, both morphologic characteristics and presence of mitotic defects are used [38]. Originally, mitotic catastrophe was defined as a cell death-related process caused by aberrant mitosis. However, it has been now demonstrated that mitotic catastrophe represents a step preceding apoptosis or necrosis [24, 25]. In this regard, we found that axitinib induces mitotic catastrophe both in drug-sensitive U87 and T98 and -resistant U251 glioma cells. Indeed all glioma cell lines undergoing mitotic catastrophe show multinucleation and increased mitochondrial mass but only U87 and T98 cells die. Overall our findings support the hypothesis that mitotic catastrophe represents a step preceding a senescent-associated cell death.

At present two different types of cellular senescence have been demonstrated *in vivo* and *in vitro*. Replicative senescence represents a stable and long-term loss of proliferative capacity, despite continued viability and metabolic activity, due to telomere loss or dysfunction [33], and premature senescence, a type of DNA-damage senescent-associated cell death that arises at a stage before telomere shortening. This latter senescence program is induced by chemotherapeutic agents, oxidative stress, oncogenic or mitogenic signals [39–41, 34], and results in reduced cell viability and induction of cell death through different cell death modalities despite the p53 status of the different cell lines. Indeed we evidenced an increased number of  $\beta$ -gal<sup>+</sup>PI<sup>+</sup> and  $\beta$ -gal<sup>+</sup>PI<sup>+</sup> cells suggestive of senescent-associated necrosis and necrotic cell death in p53 wild-type U87 cells after axitinib exposure. In p53 mutant T98 cell line, the axitinib-treated cells showed a  $\beta$ -gal<sup>+</sup>PI<sup>+</sup> phenotype, sign of a senescence-associated cell death; no senescent cell death or necrosis were evidenced in axitinib-treated p53 mutant U251 cells.

DNA damage-induced senescent necrosis is caused by an excessive intracellular ROS generation that impairs DNA repair and cell signaling [32]. In this regard, a time-dependent increase of ROS generation

was observed in axitinib-sensitive U87 and T98 cells; pretreatment with the anti-oxidant agent NAC, resulted in a decreased percentage of  $\beta$ -gal<sup>+</sup>PI<sup>+</sup> cells. On the contrary in U251 glioma cells, the inability of axitinib to trigger ROS signals, makes drug-treated cells resistant to premature senescence and cell death. Similarly, treatment of RCC cells and gastric cancer cells with axitinib, results in cell cycle arrest in G2 phase, and induces a ROS-dependent SA- $\beta$ -galactosidase-positive senescent phenotype [7, 42].

Chk1 regulates DNA replication, cell cycle progression, chromatin remodeling and cell death. Here we found that Chk1 activation is associated with cell cycle arrest and mitotic catastrophe in all glioma cell lines tested. However, in axitinib-treated U87 and T98 cells, H2AX phosphorylation and Ser345-Chk1 activation transiently arrested cell cycle in G2/M, accumulated polyploid cells that underwent mitotic catastrophe and induced p21-driven senescent-associated cell death. In U251 cells axitinib treatment stably arrested cell cycle in G2/M and increased polyploid cells that underwent mitotic catastrophe as above described, but the failure to induce p21 overexpression rescued glioma cells to axitinib-induced cell death. Furthermore, we demonstrated that overexpression of p21 in U251 cells restores the sensitivity of glioma cells to axitinib and induces a necrotic cell death as shown by the typical DNA smear and the lack of procaspase-3 activation. These data are in agreement with previous findings demonstrating that p21 is able to bind and inhibit the activity of proteins directly involved in the induction of apoptosis, including procaspase [43]. Further, the overexpression of the cell cycle inhibitor p21, at time of Chk1 activation shutdown, represented a prerequisite to drive glioma cells to death. Similarly, in PC-3 prostate cancer cells, retrovirus-mediated transduction of p21 induces cell death by suppressing Chk1 activation and DDR [42]. On the other hand, the silencing of p21 made T98 cells resistant to axitinib therapy confirming a pivotal role of p21 in the glioma cellular response to this TKI.

Bortezomib and the new proteasome inhibitor, marizomib, have been found to induce increased p21 levels in GBM [44]. The present study demonstrated that the advantageous schedule to treat glioma cells *in vitro* is the axitinib and bortezomib coadministration. We also characterized the molecular mechanisms involved in the synergistic effect between these drugs. We demonstrated that bortezomib when administered at nanomolecular, no toxic doses in combination with suboptimal dose of axitinib, promotes cytotoxic activity both in axitinib-sensitive and -resistant glioma cell lines by increasing p21 protein levels, as supported by the p21 silencing experiments. The axitinib plus bortezomib synergistic effect was associated also with Ser345-Chk1 activation and H2AX phosphorylation mainly in U87 and U251 cell lines, although with different kinetics. This combined treatment induced mitotic catastrophe and ROS-mediated

DNA-damage senescence-associated necrosis in U87 and T98 glioma cells. Interestingly in axitinib-resistant U251 cells, the administration of bortezomib made the cells sensitive to the TKI, by increasing Ser345-Chk1, H2AX phosphorylation and triggering p21 overexpression, with the induction of ROS-dependent necrosis. These results suggest that different levels of ROS and sensitivity of cells to drug-induced oxidative stress, may influence cell death modalities [32, 45]. Overall, these results demonstrated that H2AX, Ser345-Chk1 and p21 phosphorylation levels, as well as ROS generation induced by axitinib alone or in combination with bortezomib, promoted the sensitivity of glioma cells, and overcame the resistance, through the activation of different cell death outcomes.

Finally, although promising results were recently obtained by Duerinck *et al.* (increased 6-month PFS rate and median OS) in a randomized phase II trial [7], a long-term disease control or cures have not been still obtained in glioma patients. On the other hand, bortezomib has been recently demonstrated to sensitize glioma cells to apoptotic cell death *in vitro* [21, 22]. However, also for the ability of high doses of bortezomib to stimulate the angiogenesis of glioma stem-like cells [22], the *in vivo* bortezomib-induced effects are conflicting. The efficacy of bortezomib in combination with chemotherapeutic drugs (e.g., tamoxifen, temozolomide) or radiotherapy is limited [46]. Thus, the need to improve the efficacy of treatment by constructing a rationally directed combination strategy to achieve meaningful anti-glioma activity represents a key point.

Although the extrapolation of *in vitro* data to the clinical setting should be considered with caution, our results obtained administering suboptimal dose of bortezomib demonstrated to not affect cell viability nor VEGFA expression, combined with low doses of the anti-angiogenetic TKI, axitinib may provide a rationale for the ongoing clinical investigation. Moreover, this combinatorial approach could be able to overcome the above-mentioned limitations by enhancing the cytotoxicity against glioblastoma.

## MATERIALS AND METHODS

### Cell line culture

The p53-wild type U87MG glioma cell line was obtained from American Type Culture Collection (LGC Promochem, Teddington, UK). The human p53-mutant T98 and U251 glioma cell lines were obtained from Cell Bank Interlab Cell Line Collection (ICLC, Italy). Glioma cells were grown in Eagle's Minimum Essential Medium (Lonza Bioresearch, Basel, Switzerland) supplemented with 10% (v/v) heat-inactivated fetal bovine serum (FBS), 2mM L-glutamine and 100 IU/ml of penicillin, 100 µg of streptomycin (Lonza), 1 mM sodium pyruvate (Lonza) and non-essential amino acids (Lonza). Cell lines were maintained at 37°C, 5% CO<sub>2</sub> and 95% of humidity.

### Reagents

Axitinib (Inlyta®) was kindly provided by Pfizer (New York, NY). Bortezomib (BORT) was provided by Janssen-Cilag International N.V. (Beerse, Belgium). Mouse monoclonal anti-glyceraldehyde-3-phosphate dehydrogenase (GAPDH) Ab was from Origene (Rockville, MD). Mouse anti-p21 antibody (Ab) was purchased from Santa Cruz Biotechnology (Santa Cruz, CA). Rabbit anti-phospho-histone H2AX (Ser139), anti-Chk1-Ser345, anti-Chk1 and anti-caspase-3 Abs were purchased from Cell Signaling Technology (Danvers, MA). The following secondary antibodies were used: horseradish peroxidase (HRP)-conjugated anti-mouse IgG and HRP-conjugated anti-rabbit IgG (Cell Signaling Technology). Annexin V-fluorescein isothiocyanate (Annexin V-FITC) was purchased from eBioscience (Hatfield, UK). 5-dodecanoylaminofluorescein di-β-D- galactopyranoside (C12FDG) were from Invitrogen (San Diego, CA, USA). Bafilomycin A1, dimethyl sulfoxide (DMSO, used as vehicle), Hoechst 33258, propidium iodide (PI), ribonuclease A, 5-bromo-4-chloro-3-indolyl β-D- galactopyranoside (X-Gal), N-acetyl-L-cysteine (NAC), 10-N-nonyl acridine orange (NAO) and 3-(4,5-dimethylthiazol-2-yl)-2,5-diphenyltetrazolium bromide (MTT) were from Sigma Aldrich (St. Louis, MO). 5,5,6,6-tetrachloro-1,1,3,3-tetraethyl benzimidazolylcarbocyanine iodide (JC-1) was from Invitrogen (Carlsbad, CA).

### MTT assay

The colorimetric MTT assay was used to evaluate cell viability. Three ×10<sup>4</sup> cells/ml were seeded into 96-well plates. After 1 day of incubation, compounds or vehicles were added. To evaluate the single-agent treatment, the cells were exposed to axitinib or bortezomib alone for up to 72 h, and the half maximal inhibitory concentration (IC<sub>50</sub>) was considered as the concentration resulting in 50% cell growth inhibition compared with the untreated control cells. To evaluate the cytotoxic effects of the combined treatment, the cells were treated with two different schedules: pretreated with axitinib for 72 h, washed, replated and treated with bortezomib for 72 h; treated concomitantly with axitinib and bortezomib for up to 72 h. In some experiments cells that were treated with axitinib and/or bortezomib for 72 h, were incubated in drug-free medium for 72 h. Four replicates were used for each treatment. At the indicated time point, cell viability was assessed by adding 0.8 mg/ml of MTT to the media. After 3 h supernatants were discarded and coloured formazan crystals dissolved with 100 µl/well of DMSO, were read by an enzyme-linked immunosorbent assay reader (BioTek Instruments, Winooski, USA). Four replicates were used for each treatment. Vehicle data were omitted since no effects were observed as respect to untreated cells.

Synergistic activity of the axitinib-bortezomib combination was determined by the isobologram and

combination index (CI) methods (CompuSyn Software, ComboSyn, Inc. Paramus, NJ 2007). The CI was used to express synergism (CI < 1), additivity (CI = 1) or antagonism (CI > 1) and was calculated according to the standard isobologram equation [47].

### Cell cycle analysis

Three  $\times 10^4$  glioma cells/ml were treated with the appropriate drugs, collected and fixed in 70% ethanol and then washed with staining buffer (phosphate-buffered saline, PBS, 2% FBS and 0.01%  $\text{NaN}_3$ ). Next, the cells were treated with 100  $\mu\text{g/ml}$  ribonuclease A solution, incubated for 30 min at 37°C, stained for 30 min at room temperature with PI 20  $\mu\text{g/ml}$  and then analysed by flow cytometry using linear amplification.

### Western blot analysis

Cells were lysed in lysis buffer containing protease inhibitor cocktail (Sigma Aldrich). Lysates were separated on 8-14% SDS polyacrylamide gel and transferred onto Hybond-C extra membranes (GE Healthcare). Membrane were incubated overnight at 4°C in primary Abs (anti-phospho-H2AX 1:1000, anti-Chk1-Ser345 1:1000, anti-Chk1 1:1000, anti-p21 1:300, anti-caspase-3 1:1000, anti-GAPDH 1:8000), followed by the incubation (room temperature, 1 h) with HRP-conjugated anti-rabbit or anti-mouse secondary Abs. Peroxidase activity was visualized with the LiteAblot® PLUS and LiteAblot® TURBO (EuroClone, Milan, Italy) kits and densitometric analysis was carried out by a Chemidoc using the Quantity One software (Bio-Rad, Hercules, CA).

### Senescence analysis

We performed the senescence analysis by both microscope and flow cytometry to evaluate the senescence-associated  $\beta$ -galactosidase activity. Treated cells were fixed for 5 min at room temperature in 3% formaldehyde and incubated overnight at 37°C without  $\text{CO}_2$  with fresh SA- $\beta$ -Gal stain solution: 1 mg/mL X-Gal, 150 mM NaCl, 2 mM  $\text{MgCl}_2$ , 40 mM citric acid, 5 mM sodium phosphate (pH 6.0), 5 mM potassium ferrocyanide, and 5 mM potassium ferricyanide. Senescent cells were identified as blue-stained cells by standard light microscopy. Photographs were acquired and analyzed by an Olympus BX51 microscope (Hamburg, Germany) using magnification 40x.

Relatively to flow cytometry, we performed the assay using the fluorogenic substrate  $\text{C}_{12}$ FDG. Drug-treated cells were incubated for 1 h at 37°C and 5%  $\text{CO}_2$  with 100 nM bafilomycin A1 in culture medium to induce lysosomal alkalization at pH 6 and, then, for 1 h with 33  $\mu\text{M}$   $\text{C}_{12}$ FDG. Samples were immediately analyzed using FACScan cytofluorimeter using the CellQuest software. The  $\text{C}_{12}$ -fluorescein signal was measured on

the FL-1 detector, and  $\beta$ -galactosidase activity was estimated as percentage of positive cells. Thereafter, in some experiments, cells were also incubated with 20  $\mu\text{g/ml}$  PI followed by biparametric FACS analysis using the CellQuest software.

### Mitochondria staining

To determine mitochondrial mass mitochondrial staining was performed by 5,5',6,6'-tetrachloro-1,1',3,3'-tetraethylbenzimidazolylcarbocyanineiodide (JC-1) staining [27]. Briefly, treated cells were incubated for 10 min at room temperature with 10  $\mu\text{g/ml}$  of JC-1. Samples were analysed using a FACScan cytofluorimeter with CellQuest software.

To further support the JC1 assay, we used acridine orange 10-nonyl bromide (NAO), a metachromic dye that fluoresces at 533 nm [48]. Treated cells were incubated at 37°C for 30 min with 0.1  $\mu\text{M}$  of NAO, washed and analyzed by flow cytometry.

### Annexin V and PI staining

Cell death was evaluated using Annexin V-FITC and PI staining followed by flow cytometry and FACS analysis. Three  $\times 10^4$  cells/ml were treated with vehicle, axitinib and/or bortezomib for up to 72 h. After treatment, cells were stained with 5  $\mu\text{l}$  of Annexin V-FITC and 20  $\mu\text{g/ml}$  PI for 10 min at room temperature and washed once with binding buffer (10 mM Hepes/NaOH pH 7.4, 140 mM NaCl, 2.5 mM  $\text{CaCl}_2$ ). The percentage of positive cells determined over 10,000 events was analyzed on a FACScan cytofluorimeter using the CellQuest software.

### DNA fragmentation assay

Glioma cells were treated as above described for up to 72 h, and genomic DNA was extracted using the Apoptotic DNA Ladder detection Kit (Life Technologies Italia, Monza, Italia). The purified samples were then subjected to electrophoresis on a 1.25% agarose gel, and DNA was stained with ethidium bromide. Ultraviolet spectroscopy at 302 nm was used to obtain the results.

### ROS production

Cells were cultured for up to 72 h with axitinib or vehicle. In some experiments, cells were preincubated for 3 h with 10 mM NAC. Cells were then washed with PBS, pulsed with DCFDA for 10 min at 37°C, 5%  $\text{CO}_2$ , and analyzed by FACScan cytofluorimeter using the CellQuest software.

### Immunofluorescence and microscopic analysis

Cells cultured for up to 72 h were washed with PBS and fixed in 4% formaldehyde for 10 min at room temperature. For nuclei analysis, cells were stained with

Hoechst 33258 and examined by using the Olympus BX51 microscope. For morphological analysis, cells were stained with haematoxylin for 1 min and washed again before staining with eosin for 30 seconds. Slides were mounted with 50% glycerol, sealed and observed under Olympus BX51 microscope.

### Cell transfection

U251 cells were plated at a density of  $2 \times 10^5$  cells/ml. After overnight incubation, transfections were achieved with 7.5  $\mu$ l/ml of the reagent TransIT-X2 (Mirus MIR-6003, OriGene, Rockville, MD) and 2.5  $\mu$ g/ml of pCMV-p21 or pCMV empty (pCMV) vectors according to the manufacturer's instructions. The cells were harvested at 72 h post-transfection for analysis. The efficiency of transfection was evaluated by western blot analysis.

### p21 silencing

Small interfering RNAs (siRNAs) targeted to p21 (siCDKN1A) and a non-silencing siRNA (NC1) served as control were purchased from Integrated DNA Technologies (Leuven, Belgium). T98 cells were plated at a density of  $2 \times 10^5$  cells/ml. After overnight incubation, transfections were achieved with 7.5  $\mu$ l/ml of the reagent TransIT-X2 and 10 nM of siCDKN1A or NC1 (negative control) according to the manufacturer's instructions. The cells were harvested at 72 h post-transfection for analysis. The efficiency of transfection was evaluated by western blot analysis.

### RT-PCR analysis

Total RNA was extracted with the RNeasy Mini Kit (Qiagen), and cDNA was synthesized using the High-Capacity cDNA Archive Kit (Applied Biosystems, Foster City, PA) according to the manufacturer's instructions. Quantitative real-time polymerase chain reaction (qRT-PCR) for VEGFA was performed using the iQ5 Multicolor Real-Time PCR Detection System (Bio-Rad, Hercules, CA). PCR reaction was performed with RT2SYBRGreen qPCT mastermix (Qiagen) using 1  $\mu$ l of cDNA for reaction, following the amplification protocol described in the manufacture's instruction. RT2 qPCR Primer assays (Qiagen) were used for target gene amplification. All samples were assayed in triplicates in the same plate. Measurement of GAPDH levels was used to normalize mRNA contents, and target gene levels were calculated by the  $2^{-\Delta\Delta C_t}$  method.

### Statistical analysis

The statistical significance was determined by Student's t-test and by one way ANOVA. The statistical analysis of IC<sub>50</sub> levels was performed using Prism 5.0a (Graph Pad).

## ACKNOWLEDGMENTS

A special thanks to Dr. Daniele Tomassoni, School of Biosciences and Veterinary Medicine, University of Camerino, for hematoxylin/eosin staining.

## CONFLICTS OF INTEREST

The authors declare no conflict of interest.

## GRANT SUPPORT

This study was supported by AIRC IG 2014, cod. 15821. We thank Pfizer GmbH for kindly providing Axitinib.

## REFERENCES

1. Mentlein R, Forstreuter F, Mehdorn HM, Held-Feindt J. Functional significance of vascular endothelial growth factor receptor expression on human glioma cells. *J Neurooncol.* 2004; 67: 9-18.
2. Kaur B, Khwaja FW, Severson EA, Matheny SL, Brat DJ, Van Meir EG. Hypoxia and the hypoxia-inducible-factor pathway in glioma growth and angiogenesis. *Neuro Oncol.* 2005; 7: 134-153.
3. Stupp R, Hegi ME, Mason WP, van den Bent MJ, Taphoorn MJ, Janzer RC, Ludwin SK, Allgeier A, Fisher B, Belanger K, Hau P, Brandes AA, Gijtenbeek J, et al. Effects of radiotherapy with concomitant and adjuvant temozolomide versus radiotherapy alone on survival in glioblastoma in a randomized phase III study: 5-year analysis of the EORTC-NCIC trial. *Lancet Oncol.* 2009; 10: 459-466.
4. Cohen MH, Shen YL, Keegan P, Pazdur R. FDA drug approval summary: bevacizumab (Avastin) as treatment of recurrent glioblastoma multiform. *Oncologist.* 2009; 14: 1131-1138.
5. Tzoganis K, Skibeli V, Westgaard I, Dalhus M, Thoresen H, Slot KB, Damkier P, Hofland K, Borregaard J, Ersbøll J, Salmonson T, Pieters R, Sylvester R, et al. The European Medicines Agency approval of axitinib (Inlyta) for the treatment of advanced renal cell carcinoma after failure of prior treatment with sunitinib or a cytokine: summary of the scientific assessment of the committee for medicinal products for human use. *Oncologist.* 2015; 20: 196-201.
6. Wells JC, Stukalin I, Norton C, Srinivas S, Lee JL, Donskov F, Bjarnason GA, Yamamoto H, Beuselinck B, Rini BI, Knox JJ, Agarwal N, Ernst DS, et al. Third-line Targeted Therapy in Metastatic Renal Cell Carcinoma: Results from the International Metastatic Renal Cell Carcinoma Database Consortium. *Eur Urol.* 2016. pii: S0302-2838(16)30258-5.
7. Morelli MB, Amantini C, Santoni M, Soriani A, Nabissi M, Cardinali C, Santoni A, Santoni G. Axitinib induces DNA damage response leading to senescence, mitotic

- catastrophe, and increased NK cell recognition in human renal carcinoma cells. *Oncotarget*. 2015; 6: 36245-36259. doi: 10.18632/oncotarget.5768.
8. Lu L, Saha D, Martuza RL, Rabkin SD, Wakimoto H. Single agent efficacy of the VEGFR kinase inhibitor axitinib in preclinical models of glioblastoma. *J Neurooncol*. 2015; 121: 91-100.
  9. Duerinck J, Du Four S, Vandervorst F, D'Haene N, Le Mercier M, Michotte A, VanBinst AM, Everaert H, Salmon I, Bouttens F, Verschaeve V, Neyns B. Randomized phase II study of axitinib versus physicians best alternative choice of therapy in patients with recurrent glioblastoma. *J Neurooncol*. 2016; 128: 147-155.
  10. Naujokat C, Sezer O, Zinke H, Leclere A, Hauptmann S, Possinger K. Proteasome inhibitors induced caspase-dependent apoptosis and accumulation of p21Waf1/Cip1 in human immature leukemic cells. *Eur J Haematol*. 2000; 65: 221-236.
  11. Goldberg AL. Protein degradation and protection against misfolded or damaged proteins. *Nature*. 2003; 426: 895-899.
  12. Almond JB, Snowden RT, Hunter A, Dinsdale D, Cain K, Cohen GM. Proteasome inhibitor-induced apoptosis of B-chronic lymphocytic leukaemia cells involves cytochrome c release and caspase activation, accompanied by formation of an approximately 700 kDa Apaf-1 containing apoptosome complex. *Leukemia*. 2001; 15: 1388-1397.
  13. Miller CP, Ban K, Dujka ME, McConkey DJ, Munsell M, Palladino M, Chandra J. NPI-0052, a novel proteasome inhibitor, induces caspase-8 and ROS-dependent apoptosis alone and in combination with HDAC inhibitors in leukemia cells. *Blood*. 2007; 110: 267-277.
  14. Hershko A. Roles of ubiquitin-mediated proteolysis in cell cycle control. *Curr Opin Cell Biol*. 1997; 9: 788-799.
  15. Kane RC, Farrell AT, Sridhara R, Pazdur R. United States Food and Drug Administration approval summary: bortezomib for the treatment of progressive multiple myeloma after one prior therapy. *Clin. Cancer Res*. 2006;12: 2955-2960.
  16. Frankland-Searby S, Bhaumik SR. The 26S proteasome complex: an attractive target for cancer therapy. *BBA*. 2012;1825: 64-76.
  17. Caravita T, de Fabritiis P, Palumbo A, Amadori S, Boccadoro M. Bortezomib: efficacy comparisons in solid tumors and hematologic malignancies. *Nat Clin Pract Oncol*. 2006; 3: 374-387.
  18. Asklund T, Kvarnbrink S, Holmlund C, Wibom C, Bergenheim T, Henriksson R, Hedman H. Synergistic killing of glioblastoma stem-like cells by bortezomib and HDAC inhibitors. *Anticancer Res*. 2012; 32: 2407-2413.
  19. Kardosh A, Golden EB, Pyrko P, Uddin J, Hofman FM, Chen TC, Louie SG, Petasis NA, Schönthal AH. Aggravated endoplasmic reticulum stress as a basis for enhanced glioblastoma cell killing by bortezomib in combination with celecoxib or its non-coxib analogue, 2,5-dimethyl-celecoxib. *Cancer Res*. 2008; 68: 843-851.
  20. Lin L, Gaut D, Hu K, Yan H, Yin D, Koeffler HP. Dual targeting of glioblastoma multiforme with a proteasome inhibitor (Velcade) and a phosphatidylinositol 3-kinase inhibitor (ZSTK474). *Int J Oncol*. 2014; 44: 557-562.
  21. Vlachostergios PJ, Papandreou CN. Efficacy of low dose temozolomide in combination with bortezomib in U87 glioma cells: a flow cytometric analysis. *Arch Med Sci*. 2015; 11:307- 310.
  22. Bota DA, Alexandru D, Keir ST, Bigner D, Vredenburg J, Friedman HS. Proteasome inhibition with bortezomib induces cell death in GBM stem-like cells and temozolomide-resistant glioma cell lines, but stimulates GBM stem-like cells VEGF production and angiogenesis. *J Neurosurg*. 2013; 119: 1415-1423.
  23. Rogakou EP, Pilch DR, Orr AH, Ivanova VS, Bonner WM. DNA double-stranded breaks induce histone H2AX phosphorylation on serine 139. *J Biol Chem*. 1998; 273: 5858-5868.
  24. Vakifahmetoglu H, Olsson M, Zhivotovsky B. Death through a tragedy: mitotic catastrophe. *Cell Death Differ*. 2008; 15: 1153-1162.
  25. Denisenko TV, Sorokina IV, Gogvadze V, Zhivotovsky B. Mitotic catastrophe and cancer drug resistance: A link that must to be broken. *Drug Resist Updat*. 2016; 24: 1-12.
  26. Castedo M, Perfettini JL, Roumier T, Andreau K, Medema R, Kroemer G. Cell death by mitotic catastrophe: a molecular definition. *Oncogene*. 2004; 23: 2825-2837.
  27. Jangamreddy JR, Ghavami S, Grabarek J, Kratz G, Wiehce E, Fredriksson BA, Rao Pariti RK, Ciešlar-Pobuda A, Panigrahi S, Los MJ. Salinomycin induces activation of autophagy, mitophagy and affects mitochondrial polarity: differences between primary and cancer cells. *BBA*. 2013; 1833: 2057-2069.
  28. Mao Z, Ke Z, Gorbunova V, Seluanov A. Replicatively senescent cells are arrested in G1 and G2 phases. *Aging (Albany NY)*. 2012; 4: 431-435. doi: 10.18632/aging.100467.
  29. Collado M, Blasco MA, Serrano M. Cellular senescence in cancer and aging. *Cell*. 2007; 130: 223-233.
  30. Roninson IB. Tumor cell senescence in cancer treatment. *Cancer Res*. 2003; 63: 2705-2715.
  31. Ewald JA, Desotelle JA, Wilding G, Jarrard DF. Therapy-induced senescence in cancer. *J Natl Cancer Inst*. 2010; 102: 1536-1546.
  32. Passos JF, Nelson G, Wang C, Richter T, Simillion C, Proctor CJ, Miwa S, Olijslagers S, Hallinan J, Wipat A, Saretzki G, Rudolph KL, Kirkwood TBL, et al. Feedback between p21 and reactive oxygen production is necessary for cell senescence. *Mol Syst Biol*. 2010; 6: 347.
  33. Kuilman T, Michaloglou C, Mooi WJ, Peeper DS. The essence of senescence. *Genes Dev*. 2010; 24: 2463-2479.

34. Ricci MS, Zong WX. Chemotherapeutic approaches for targeting cell death pathways. *Oncologist*. 2006;11: 342-357.
35. Jane EP, Premkumar DR, Pollack IF. Bortezomib sensitizes malignant human glioma cells to TRAIL, mediated by inhibition of the NF- $\kappa$ B signaling pathway. *Mol Cancer Ther*. 2011; 10: 198-208.
36. Maréchal A, Zou L. DNA Damage Sensing by the ATM and ATR Kinases. *Cold Spring Harb Perspect Biol*. 2013; 5: a012716.
37. Bunz F, Dutriaux A, Lengauer C, Waldman T, Zhou S, Brown JP, Sedivy JM, Kinzler KW, Vogelstein B. Requirement for p53 and p21 to sustain G2 arrest after DNA damage. *Science*. 1998; 282: 1497-1501.
38. Gonçalves AP, Máximo V, Lima J, Singh KK, Soares P, Videira A. Involvement of p53 in cell death following cell cycle arrest and mitotic catastrophe induced by rotenone. *BBA*. 2011; 1813: 492-499.
39. Robles SJ, Adami GR. Agents that cause DNA double strand breaks lead to enrichment and the premature senescence of normal fibroblasts. *Oncogene*. 1998; 16: 1113-1123.
40. te Poele, RH, Okorokov AL, Jardine L, Cummings J, Joel SP. DNA damage is able to induce senescence in tumor cells in vitro and in vivo. *Cancer Res*. 2002; 62: 1876-1883.
41. Unterluggauer H, Hampel B, Zwerschke W, Jansen-Durr P. Senescence-associated cell death of human endothelial cells: the role of oxidative stress. *Exp Gerontol*. 2003; 38: 1149-1160.
42. Gabai VL, O'Callaghan-Sunol C, Meng L, Sherman MY, Yaglom J. Triggering senescence programs suppresses Chk1 kinase and sensitizes cells to genotoxic stresses. *Cancer Res*. 2008; 68: 1834-1842.
43. Dotto GP. p21(WAF1/Cip1): more than a break to the cell cycle? *Biochim Biophys Acta*. 2000; 1471: M43-56.
44. Manton CA, Johnson B, Singh M, Bailey CP, Bouchier-Hayes L, Chandra J. Induction of cell death by the novel proteasome inhibitor marizomib in glioblastoma in vitro and in vivo. *Sci Rep*. 2016; 6: 18953.
45. Masgras I, Carrera S, de Verdier PJ, Brennan P, Majid A, Makhtar W, Tulchinsky E, Jones GD, Roninson IB, Macip S. Reactive oxygen species and mitochondrial sensitivity to oxidative stress determine induction of cancer cell death by p21. *J Biol Chem*. 2012; 287: 9845-9854.
46. Kubicek GJ, Werner-Wasik M, Machtay M, Mallon G, Myers T, Ramirez M, Andrews D, Curran WJ Jr, Dicker AP. Phase I trial using proteasome inhibitor bortezomib and concurrent temozolomide and radiotherapy for central nervous system malignancies. *Int J Radiat Oncol Biol Phys*. 2009; 74: 433-439.
47. Chou TC. Theoretical basis, experimental design, and computerized simulation of synergism and antagonism in drug combination studies. *Pharmacol Rev*. 2006; 58: 621-681.
48. Michael E, Widlansky, Jingli Wang, Sherene M, Shenouda, Tory M, Hagen, Anthony R, Smith, Tinoy J, Kizhakekuttu, Matthew A, Kluge, Dorothee Weihrauch, David D, Gutterman, Joseph A. Vita. Altered Mitochondrial Membrane Potential, Mass, and Morphology in the Mononuclear Cells of Humans with Type 2 Diabetes. *Transl Res*. 2010; 156: 15-25.